

Exploring the follicular route for transcutaneous vaccination using nanoparticles

Dissertation

zur Erlangung des Grades

des Doktors der Naturwissenschaften

der Naturwissenschaftlich-Technischen Fakultät III

Chemie, Pharmazie, Bio- und Werkstoffwissenschaften

der Universität des Saarlandes

von

Ankit Mittal

Saarbrücken

2014

Tag des Kolloquiums: 26 May 2014

Dekan: Prof. Dr. Volkhard Helms

Berichterstatter: Prof. Dr. Claus-Michael Lehr

Prof. Dr. Ingolf Bernhardt

Vorsitz: Prof. Dr. Alexandra K. Kiemer

Akad. Mitarbeiter: Dr. Matthias Engel

*“Excellence is a continuous process and not
an accident.”*

Dr. A. P. J. Abdul Kalam

(Former President of India)

To my Family

Table of Contents

Short Summary	1
Kurzzusammenfassung	2
1. Introduction	3
1.1. Transcutaneous vaccination using particle based formulations: State of the art.....	4
1.1.1. <i>Absorption Routes of Nanoparticles Applied to the Skin</i>	6
1.1.2. <i>Nanoparticles for Transfollicular Vaccination</i>	6
1.1.3. <i>Facilitated Absorption Methods</i>	8
1.1.4. <i>Intrinsic Adjuvant Effect— Influence of Particle Properties</i>	11
1.1.5. <i>Coupling of Nanoparticles with Adjuvants</i>	12
1.2. Aim of the thesis.....	16
2. Non-invasive delivery of nanoparticles via hair follicles	18
2.1 Abstract.....	19
2.2. Introduction	20
2.3. Materials and methods.....	22
2.3.1. <i>Material</i>	22
2.3.2. <i>Pig ear skin</i>	23
2.3.3. <i>Mice</i>	23
2.3.4. <i>Nanoparticles preparation</i>	23
2.3.5. <i>Nanoparticle characterization</i>	24
2.3.6. <i>Integrity and Activity of OVA</i>	24
2.3.7. <i>DC activation and stimulation: Preparation and flow cytometric analysis of murine dendritic cells</i>	25
2.3.8. <i>Measurement of cellular proliferation of antigen specific murine CD4+ and CD8+ T cells</i>	26
2.3.9. <i>Adoptive transfer model of TCR transgenic CD4 T cells to characterize OVA specific proliferation</i>	27
2.3.10. <i>Evaluation of follicular uptake on excised pig ears</i>	28
2.3.11. <i>Microscopical evaluation</i>	28

2.3.12. Quantification of follicular uptake: Influence of encapsulating OVA into particles	29
2.3.13. Quantification of follicular uptake: Influence of particle concentration	30
2.3.14. Statistical analysis	30
2.4. Results	30
2.4.1. Characterization of Nanoparticles	30
2.4.2. Integrity and Activity of OVA	32
2.4.3. Activation of dendritic cells	33
2.4.4. Adoptive transfer model of TCR transgenic CD4 T cells to characterize OVA specific proliferation	37
2.4.5. Follicular uptake of Nanoparticles	39
2.5. Discussion	41
2.6. Conclusion	47
3. Efficient nanoparticle-mediated needle-free transcutaneous vaccination via hair follicles requires adjuvantation	48
3.1. Abstract	49
3.2. Introduction	49
3.3. Materials and methods	51
3.3.1. Materials	51
3.3.2. Particle preparation	52
3.3.3. Mice	52
3.3.4. Measurement of transepidermal water loss (TEWL)	53
3.3.5. Immunization protocols	53
3.3.6. In vivo localization of nanoparticles using histology	54
3.3.7. Sample collection	54
3.3.8. Detection of antigen-specific IgG and IgG subtypes	55
3.3.9. Measurement of cellular proliferation	55
3.3.10. Evaluation of cytokine profiles	56
3.3.11. Multifunctional T cells	56
3.3.12. Statistical analysis	57
3.4. Results	57
3.4.1. Characterization of OVA-loaded Chit-PLGA NPs	57

3.4.2. TEWL Measurement	58
3.4.3. <i>In vivo</i> localization of nanoparticles using histology.....	59
3.4.4. Humoral immune response (total IgG, IgG1 and IgG2c).....	61
3.4.5. Measurement of cellular proliferation	63
3.4.6. T cell quality following vaccination	65
3.5. Discussion	68
4. Inverse micellar sugar glass nanoparticles as delivery system: adjuvant co-encapsulation, and administration route have a major impact on immunization outcome	73
4.1. Abstract.....	74
4.2. Introduction	74
4.3. Materials and methods.....	76
4.3.1. Materials.....	76
4.3.2. Pig ear skin	77
4.3.3. Mice.....	77
4.3.4. Nanoparticles preparation	78
4.3.5. Nanoparticle characterization	79
4.3.6. Integrity and Activity of OVA	79
4.3.7. Evaluation and quantification of follicular uptake on excised pig ears: Influence of encapsulating OVA into particles.....	80
4.3.8. Adoptive transfer model of TCR transgenic CD4 T cells to characterize OVA specific proliferation	81
4.3.9. Immunization protocols.....	82
4.3.10. Sample collection	82
4.3.11. Detection of antigen-specific IgG and IgG subtypes.....	83
4.3.12. Evaluation of cellular proliferation and cytokine profiles	84
4.3.13. Multifunctional T cells.....	85
4.3.14. Statistical analysis	86
4.4. Results	86
4.4.1. Characterization of OVA-loaded IMMSG NPs.....	86
4.4.2. Integrity and bio-availability of OVA are not affected by IMMSG NP generation process	87
4.4.3. Follicular uptake of Nanoparticles.....	88

4.4.4. <i>IMSG NPs efficiently deliver OVA to immune cells via TF route.....</i>	89
4.4.5. <i>Adjuvanted IMSG NPs stimulate efficient humoral immune responses following ID immunization</i>	91
4.4.6. <i>Adjuvanted IMSG NPs stimulate efficient cellular immune responses following ID immunization</i>	93
4.4.7. <i>Adjuvanted IMSG NPs fail to stimulate efficient humoral immune responses following IN immunization</i>	96
4.4.8. <i>Adjuvanted IMSG NPs fail to stimulate efficient cellular immune responses following IN immunization</i>	98
4.4.9. <i>Adjuvanted IMSG NPs stimulate efficient humoral immune responses following TF vaccination</i>	100
4.4.10. <i>Adjuvanted IMSG NPs stimulate efficient cellular immune responses following TF vaccination</i>	102
4.5. Discussion	105
4.6. Conclusion.....	110
5. Overall Conclusion and Outlook.....	111
6. List of Abbreviations	117
References.....	119
Curriculum vitae.....	137
List of Publication	138
Acknowledgements.....	141

Short Summary

Transcutaneous vaccination refers to the needle-free delivery of vaccines across the skin. In particular, transfollicular vaccination aims to deliver antigens to the abundant peri-follicular antigen presenting cells. Many of the studies conducted to date to explore this route have been done after pre-treating the skin using techniques such as tape stripping.

The presented work evaluates the potential of the transfollicular route as a perspective for transcutaneous vaccination using nanoparticles (NPs) without compromising the stratum corneum barrier by any pre-treatment. The results presented in this thesis showed that the model antigen ovalbumin can be delivered via the transfollicular route by encapsulating into polymeric NPs (polylactic-co-glycolide (PLGA) and Chitosan-PLGA), and that immunization by this route is able to elicit the same proliferation of antigen-specific CD4⁺ T cells as an intramuscular injection of ovalbumin in an adoptive transfer mouse model. Moreover, immune responses generated by this pathway using a conventional mouse model demonstrated that inclusion of an adjuvant (bis-(3',5')-cyclic adenosine monophosphate, c-di-AMP) in the NP formulation is essential to evoke efficient humoral as well as cellular immune responses. Furthermore, a new particulate carrier system (inverse micelles sugar glass NPs) was prepared, which allowed co-encapsulation of adjuvant and antigen, and showed enhanced stability of encapsulated antigen, better follicular uptake, as well as efficient transfollicular vaccination.

Kurzzusammenfassung

Transkutane Impfungen ermöglichen eine nadelfreie Anwendung von Impfstoffen. Insbesondere die transfollikuläre Vakzinierung erlaubt es, Antigene direkt zu den antigen-präsentierenden Zellen im perifollikulären Bereich zu bringen.

Bei der überwiegenden Zahl bisheriger Studien wurden die Formulierungen auf vorbehandelter Haut (z.B. tape stripping) eingesetzt.

Ziel der vorliegenden Arbeit war es, das Potenzial nanopartikulärer Arzneistoffträgersysteme mittels transkutaner Vakzinierung ohne Vorbehandlung der Haut über die transfollikuläre Route zu untersuchen.

In den vorgestellten Studien wurde das Modell-Antigen Ovalbumin in nanoskalige Trägersysteme, bestehend aus Polylactid-co-Glycolid- (PLGA) bzw. Chitosan-PLGA, verkapselt. Kutane Verabreichung zeigte in einem adoptiven Transfermodell der Maus, dass die Proliferation von antigenspezifischen CD4⁺ T-Zellen im gleichen Maße hervorgerufen wird wie durch eine klassische intramuskuläre Injektion. Zusätzlich konnte in einem Mausmodell gezeigt werden, dass der Zusatz des Adjuvants (bis-(3',5')-cyclo-Adenosin-Monophosphat, c-di-AMP) zur Arzneistoffträgerformulierung notwendig ist, um eine ausreichende humorale und zelluläre Immunstimulierung hervorzurufen.

Neuartige Carriersysteme in Form von glasartigen inversen Mizellen verbesserten die Stabilität des verkapselten Modelantigens, ermöglichten die Co-Verkapselung des Adjuvants, sowie auch die follikuläre Aufnahme und damit eine effiziente transfollikuläre Vakzinierung.

1. Introduction

Parts of this Chapter were published in

Mittal, A. *, Raber, A.S. *, Lehr, C.M., Hansen, S. (2013). **Particle based vaccine formulations for transcutaneous immunization.** *Human vaccines and immunotherapeutics*. 9 (9), pp. 1950-1955.

**These authors contributed equally to this work*

The author of the thesis made the following contribution to the publication:

- Planned and designed the manuscript
- Interpreted and wrote sections of the manuscript concerning particle based adjuvant effects and coupling of adjuvants in nanoparticles along with introduction and conclusion.

1.1. Transcutaneous vaccination using particle based formulations:

State of the art

Infectious diseases impose a serious threat to public health worldwide. Among the strategies to fight infections only vaccination has the potential to eradicate the disease (the World Health Organization, WHO, certified the eradication of smallpox in 1979). New, safe, efficient, and cheap vaccination strategies are desperately needed to meet the needs of a growing population in developing countries as well as the challenges of fast spreading infectious diseases due to global traffic (e.g. 2009 swine flu pandemics).

Particle based vaccine formulations for TCI address several key issues in vaccination today. First of all TCI has been shown to induce superior immune responses as compared to systemic vaccines and to hold the potential to convey mucosal immunity. This is highly desirable to prevent microbial pathogens from entering the body through mucosal surfaces and thus block disease at a very early stage. This will also help to reduce the risk of horizontal transmission from infected individuals to susceptible hosts.

Many of the current strategies for TCI (e.g. micro-needles, Gene gun, PowderJect, skin abrasion), reduce the protective SC barrier for a significant time to facilitate the absorption of the vaccine. This makes them suboptimal for mass vaccination campaigns under critical hygienic conditions. Particle based formulations are an interesting alternative to this. Needle free strategies are at the forefront to combat vaccination related transmitted diseases due to sharing of needles or needle stick accidents.

Over the past decade, particulate carriers have emerged as an attractive delivery strategy for antigens and adjuvants. Particle based formulations combine several

desirable aspects which make them very attractive for antigen encapsulation. Vaccine antigens are often difficult biological entities, including DNA, peptides, proteins, attenuated viruses, microorganism fragments. (Nano)encapsulation can improve the stability, facilitate absorption and also increase antigenicity by mimicking the size of microorganisms.

The co-delivery of adjuvants is tantamount to increase the immunogenicity of the antigen and may allow a reduction of the antigen dose. In the context of vaccination so-called dose sparing allows reaching more people when limited amount of vaccine antigen is available such as in global pandemics. Furthermore, vaccines with higher efficiency are also needed to enable protection of immunosuppressed and elderly patients. Importantly, by choosing the right adjuvant it is possible to polarize the immune response in a predetermined direction and convey mucosal immunity.

However, until now TCI using particle based vaccine formulations has made no impact on medical practice. One of the main difficulties is that NPs cannot penetrate the skin to an extent that would allow the application of the required dose of antigen. This is due to the formidable stratum corneum (SC) barrier, the limited amount of antigen in the formulation and often an insufficient immunogenicity. A multitude of strategies are currently under investigation to overcome these issues.

We highlight selected methods presenting a spectrum of solutions ranging from transfollicular delivery, to devices disrupting the SC barrier and the combination of particle based vaccines with adjuvants discussing their advantages and shortcomings. Some of these are currently at an experimental state while others are already in clinical testing. All methods have been shown to be capable of transcutaneous antigen delivery.

1.1.1. Absorption Routes of Nanoparticles Applied to the Skin

One of the main challenges in TCI is that the vaccine antigens need to overcome the SC barrier in order to reach the Langerhans cells (LCs) in the epidermis which act as antigen presenting cells (APCs). Intact human skin is widely impermeable to solid NPs and MPs. Ultra-flexible liposomes are an exception to this rule. Due to the addition of edge activators such as surfactants and/or ethanol they are able to change shape and squeeze through the lipid channels of the SC, supposedly following an osmotic gradient [1, 2]. Ultra-flexible liposomes have been used foremost for encapsulating protein antigens [3, 4]. By including positively charged lipids in the formulation they become amenable to complexing nucleotide based drugs and thus may be an alternative for DNA vaccination [5-7]. For a more extensive overview the reader is referred to some recent reviews [8, 9]. Furthermore, ultra-small NPs with sizes less than 10 nm can enter the SC to a low and highly variable extent [10]. The toxicity and lack of biodegradability of quantum dots, metal or metal oxide NPs notwithstanding, ultra-small NPs are not suitable for drug delivery and vaccination purposes due to the extremely small amount of drug or antigen which can be loaded onto these particles. Also due to their low and variable degree of penetration such formulations would probably require some active means of penetration enhancement to enable delivery of a suitable dose.

1.1.2. Nanoparticles for Transfollicular Vaccination

Polymeric NPs as well as lipid carriers which are often in the size range of a few 100 nm are especially interesting delivery systems for the purpose of TCI. Nonflexible NPs which are applied onto the skin migrate into the hair follicle openings by a size-selective mechanism (Fig. 1A) [11]. The hair follicle is a

promising target for TCI without compromising the skin barrier [12]. Interestingly, the transfollicular route is a common pathway for the invasion of allergens such as pollen grains [13]. First evidence for the importance of the transfollicular route for transcutaneous vaccine delivery came from differences observed between hairy and nude mice [14]. At least for DNA vaccines the hair cycle state also seems to determine the successful transfection [15]. Inside the hair follicles antigen uptake by the rich pool of peri-follicular antigen presenting cells (APCs) is facilitated due to the absence of a SC barrier in the lower follicular orifice [16]. Therefore this delivery strategy does not require application of any further measures which would reduce the skin barrier. It seems that transfollicular delivery elicits a CD8+ biased response which is recommendable for combating intracellular microbes and developing vaccines against cancer and virus infections [17]. We showed that transfollicular delivery of the nano-encapsulated model antigen ovalbumin (OVA) elicited similar proliferation of OVA specific CD4+ T cells as an intra-muscular (i.m.) injection of the same dose of soluble antigen in an adoptive transfer model [12]. Nano-encapsulation into polymeric NPs improved the delivery of OVA into the hair follicles on excised pig ears by a factor of 2.5–3 compared with OVA in solution and protected OVA from cleavage or aggregation so that it maintained its biological activity to a high degree during storage and shipping [12]. As an important outcome of the study we observed in vitro as well as in vivo an intrinsic adjuvanticity of the NPs which was also influenced by the polymer material used [12]. The effect can probably be enhanced and directed by the combination or co-encapsulation of adjuvants into the formulation. As hair follicles cover only 0.1% of the skin surface trans-follicular delivery has long been discussed to be negligible. It was demonstrated however that the capacity of hair follicles is similar to that of the SC [18]. Lademann et al. showed that NPs penetrated more efficient into the

hair follicles than solutions and form a depot in the follicle that persists for more than one week [19]. Still a big issue with transfollicular application is the loss of formulation on the skin surface. Consequently a higher amount of vaccine would be required to achieve delivery of the required dose, which will need to be optimized in the future to make transfollicular vaccination a real alternative.

1.1.3. Facilitated Absorption Methods

Particle based vaccines benefit from any form of skin pre-treatment which reduces or removes the SC or any mechanical or electrical application method which transfers them into the epidermis by force (for review see also ref. [20]). Occlusion or chemical penetration enhancers, while enhancing permeation of molecules by several folds due to influencing molecular partition and/or diffusion coefficients, have very little effect on the permeability of particles [21]. Apart from facilitating invasion the barrier disruption additionally causes a non-specific immunostimulation [22]. Often these facilitating methods require special devices. Important points to consider in this context include (1) cost for devices, (2) ease and reproducibility of use also by non-trained personnel (e.g., in a pandemic or for mass vaccination in developmental countries lacking medical infrastructure), (3) severity and area of barrier disruption, time scale of barrier recovery which are connected to the risk of invasion of pathogens through the superficial wound. The severity of these issues varies depending on the type of vaccination which is aspired. Naturally the tendency to tolerate risk is higher with therapeutic vaccines than with prophylactic immunizations.

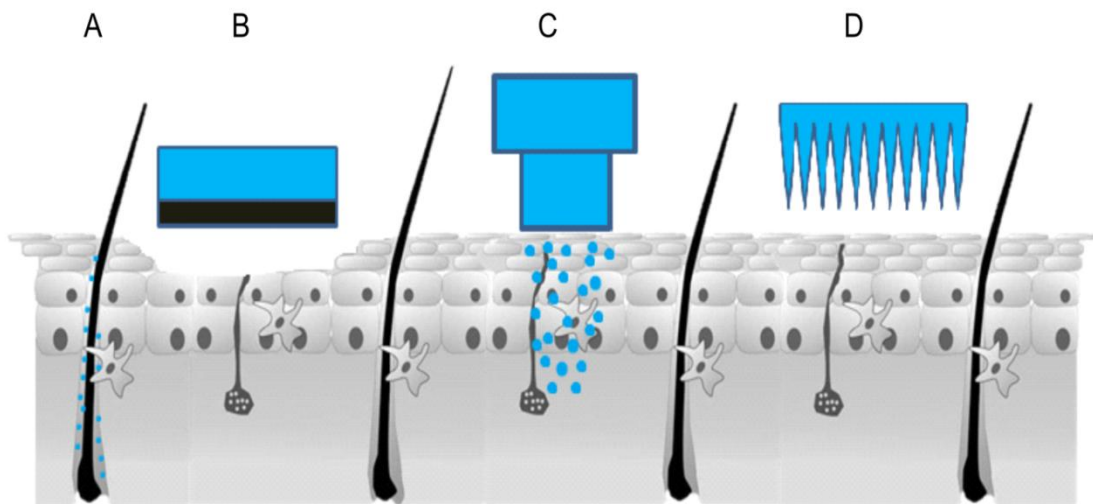


Figure 1. Schematic representation of methods to enable or facilitate TCI: (A) transfollicular delivery, (B) mechanical dermabrasion, (C) jet injection of liquids or powders, (D) microneedles (Images are not drawn to scale)

For example mechanical abrasion of the SC across a large area may be acceptable to improve the permeability of an HIV vaccine. In the DermaVir patch plasmid DNA encoding for 15 HIV antigens is complexed with mannosylated positively charged polyethylene imine to form particles with sizes of 80–400 nm [23]. Mannosylation in this case facilitates the uptake of the particles by APCs. The patch is applied onto skin sites (2–8 areas 80 cm² each on the back and the thighs) which are previously being abraded with a DermaPrep medical sponge (Fig. 1B) [24, 25]. In phase II clinical trials the patch was applied to HIV infected individuals on combination antiretroviral therapy (cART) [24, 25]. The treatment was well tolerated also in a dose escalation study; mostly side effects were limited to mild local irritation [24, 25]. The vaccination increased CD-8+ cell counts and may enable intermission of cART [24].

Devices such as jet-injectors (Fig. 1C) or gene guns may relatively easily be compatible with particle based vaccine formulations. The principle relies on the

generation of a jet of liquid or powder formulation which is propelled into the skin with great force. Dry formulations have considerable stability advantages. Depending on volume and injection depth a small amount of pain or bleeding and a relatively strong local inflammation may occur [26]. Immunogenicity is reported to be higher or equal to classic vaccine application [26, 27]. The history of using jet-injectors for vaccination goes back to the 1950s [28]. Problems with cases of hepatitis B which were transmitted person-to-person by multi-dose injectors were overcome by next generation devices which may either be prefilled for single use or come with exchangeable cartridges [29].

As a third technology with great potential to facilitate the absorption of NPs microneedles (Fig. 1D), either solid, hollow, or biodegradable, should be mentioned. They can be used for pretreatment (e.g., Derma Roller) or as a leave on patch which also delivers the formulation. Although not needle-free they reduce sharps associated issues. In contrast to intradermal injections (including the prefilled syringe system BD Soluvia which is approved in Europe for influenza vaccination) microneedles only reach the epidermis, stay above the dermal nerve endings and avoid pain. The particles can indeed be integrated in the microneedle arrays. DeMuth et al. constructed a system made from biodegradable antigen loaded MPs [30]. MPs made of poly(lactide-co-glycolide) (PLGA) were embedded in water soluble poly(acrylic acid) (PAA) which actually forms the microneedles [30]. Upon insertion into the skin, PAA dissolves; the microneedles themselves disintegrate and leave a depot of MPs providing controlled release of the antigen [30]. This design may enable separate delivery of a fast (from the matrix) and a slowly available dose (from the MPs, in mice MP-associated fluorescence was demonstrated up to 10 d after microneedle insertion at the site of injection) [30].

Likewise the system could be advanced to deliver initial and booster doses of the vaccine in a single application.

1.1.4. Intrinsic Adjuvant Effect— Influence of Particle Properties

While for most applications NPs should be inert, that means that complement activation is not desirable, an immunostimulatory effect of the nano-formulation may be a benefit for vaccination purposes. Various properties such as size, surface charge and material properties play a vital role in shaping an immune response. A wide variety of particulate systems, including liposomes, virosomes, nanocomplexes and polymer based carriers are being investigated, all showing a different immunological outcome. For example, a particle based vaccine formulation may be capable of provoking a strong humoral response but fail to generate cellular responses. This might be due to different particle properties.

It is widely accepted that particle based vaccine delivery systems are more immunogenic than soluble antigen as particulate system mimic the size and structure of a pathogen. Among others this is due to the enhanced uptake by APCs. Carrier size also plays an important role in determining the type of response induced [31]. Recently, Mottram et al. showed that small differences in particle size (20–200 nm) influence the cytokine balance after a single immunization, showing that particle size in the range of 40–49 nm induces type 1 (cellular) responses and larger particles with 93–123 nm inducing type 2 (humoral) responses [32]. These findings are especially noteworthy while considering strategies of immunization against viruses where cellular responses are required. Surface charge of the particles is another vital property which not only determines the stability of particles but plays an important role in contributing the immuno-regulatory effect of the particulate systems. With respect to TCI, Rancan et al.

showed that positively charged particulate systems seem to be taken up better by LCs due to electrostatic interactions with cell membrane eventually favoring their internalization [33]. Moreover, Ma et al. showed even the appropriate surface charge density is crucial to have an effective and efficacious immune-regulatory effect [34].

Finally, particle material may influence immunogenicity. The main function of a material is to stabilize the antigen by protecting it from the surrounding biological conditions, to slow down the clearance of antigens and to enhance delivery to APCs with design constraints such as biodegradability and biocompatibility. One strategy is to use materials extracted from microbial (e.g., total polar lipid extract from archae bacteria, or poly- γ -glutamic acid [35, 36] to formulate particulate carriers. Interestingly, the materials themselves do not show adjuvant properties when delivered as solution but when formulated as particulate carrier they upregulated cytokine responses and MHC molecules, suggesting that particulate formation is necessary for the interaction between materials and certain surface molecule on APCs [35, 36].

1.1.5. Coupling of Nanoparticles with Adjuvants

Adjuvants are commonly added to vaccine formulations to enhance immunogenicity of poorly immunogenic antigens such as subunit vaccines or to shape the type of immune response, e.g., to increase cellular responses. For the same reasons particulate vaccine formulations may be combined with adjuvants. A variety of adjuvants with different mode of actions are being used in clinical testing, marketed formulations as well as in research settings. An important consideration is the risk of side effects by adjuvants. This is especially true for prophylactic vaccines which are given to healthy people and therefore have to

fulfill the strongest safety criteria. For example cholera toxin and E. coli heat labile toxin (LT) are both very effective adjuvants for TCI and are very effective in humans [37].

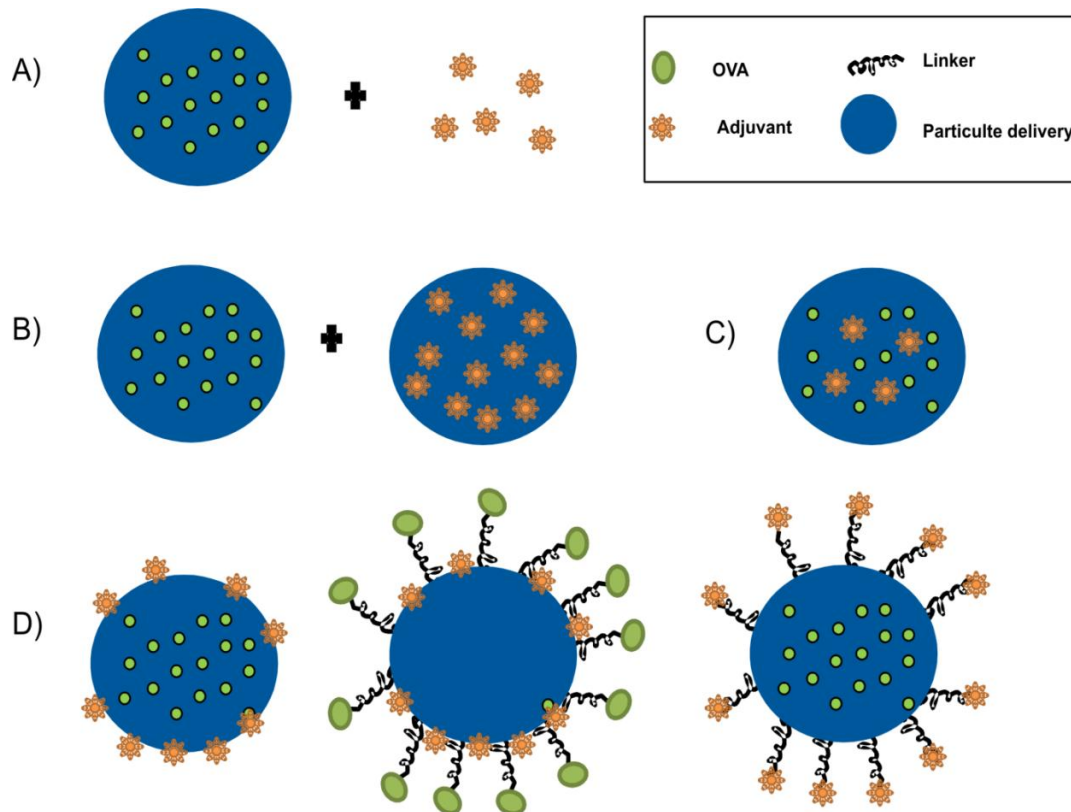


Figure 2. Combinations of antigen and adjuvant in a particulate carrier: (A) adjuvants are co-administered with the encapsulated antigen, (B) antigen and adjuvant are encapsulated in separate particles, (C) antigen and adjuvant are co-encapsulated in same particle, (D) the particle surface is decorated with the antigen and/or the adjuvant by physical or chemical association.

Nonetheless considering the application of LT as patch against travelers' diarrhea even the appearance of skin rashes and discoloration at the patch site may lead to the termination in a late clinical phase. At present, the choice of adjuvant is a compromise between necessity for adjuvanticity and minimal level of side effects [38]. Nevertheless, combination of adjuvant, antigen and particulate carrier may reduce the dose of antigen as well as adjuvant required in the formulation and consequently minimize the risk of side effects of novel adjuvant candidates for

prophylactic vaccines [39, 40]. Adjuvants may either be (1) simply co-administered with encapsulated antigen, (2) encapsulated in separate particles or (3) co-encapsulated with the antigen in the same particle. Alternatively the particle surface may be decorated with the adjuvant by physical or chemical association (Fig. 2). Recently, Bershteyn et al. showed that co-delivery of antigen with an adjuvant decorated on the surface of a particle generates humoral as well as cellular immune responses at ultra-low doses (at nanogram levels) of antigen and adjuvant [41]. In the same study, the authors have shown that co-loading of antigen and adjuvant in the same particle after a single immunization was significantly advantageous compared with antigen and adjuvant delivered on separate particles. But this advantage was lost after a boost immunization, suggesting that after boosting it does no longer matter whether antigen and adjuvant were on the same or separate particles. However, conflicting results exist in literature, whether it is beneficial to co-encapsulate adjuvant and antigen in the same particles or admix the adjuvant just prior to immunization (either in solution or separately encapsulated) in order to generate long lasting immune responses [42, 43].

Future studies also need to clarify which type of association between adjuvant and particle should be preferred. Conceivably this may depend on the type of adjuvant used. For example, an adjuvant which has receptors expressed on the surface of APCs (e.g., some sugars such as mannose) will probably benefit from being displayed on the particle surface. In contrast, encapsulation of intracellularly processed adjuvants will possibly generate a more robust immune response due to enhanced uptake by APCs and intracellular delivery compared with administration as solution [44]. Overall, combining adjuvant and antigen in

particulate carriers either by (co-)encapsulation or admixing is an attractive approach to improve the efficacy of vaccines and reduce the cost of vaccination.

1.2. Aim of the thesis

From the introduction section of the thesis and literature survey, it can be easily concluded that transcutaneous vaccination promises superior immunogenicity in comparison to intra-muscular injection. However, many of the current strategies for transcutaneous vaccination (e.g. micro-needles, Gene gun, PowderJect, skin abrasion), reduce the protective stratum corneum barrier in order to facilitate the absorption of the vaccine, making them suboptimal for certain applications, such as mass vaccination campaigns in countries having critical hygienic conditions.

In contrast, transfollicular vaccination aims to reach the peri-follicular antigen presenting cells without impairing the SC barrier. Nonetheless, transfollicular vaccination is usually performed after pre-treating the skin area by plucking the hairs, waxing, or cyanoacrylate (superglue) stripping.

Thus, the aim of this thesis was to evaluate the potential of transfollicular vaccination using nanoparticles without applying SC barrier-reducing measures. The following strategy was used to achieve this aim. Firstly, proof of concept studies were conducted to answer whether immune responses could be generated via the transfollicular route without skin pre-treatment, with the help of an adoptive transfer mouse model using ovalbumin as model antigen and encapsulating it inside polymeric nanoparticles (chapter 4). Extensive characterization of immune responses triggered by transfollicular vaccination using ovalbumin-loaded nanoparticles without skin pre-treatment was then carried out using normal C57BL/6 mice (chapter 5). Moreover, side-by-side comparisons of different formulations on tape stripped and intact skin were conducted to determine the necessity of different components of nano-formulations to generate immune responses via this pathway (chapter 5). Furthermore, a new nanoparticulate

delivery system was fabricated to apply learning from the above mentioned studies and to formulate a better delivery system (alleviating observed shortcomings of polymeric nanoparticles) for generation of better immune responses via the transfollicular route as well as via other routes of vaccination.

The work in this thesis has been divided into the following chapters, under which the above points are explored in more detail:

Chapter 2: Non-invasive delivery of nanoparticles via hair follicles

Chapter 3: Efficient nanoparticle-mediated needle-free transcutaneous vaccination via hair follicles requires adjuvantation

Chapter 4: Inverse micellar sugar glass nanoparticles as delivery system: adjuvant co-encapsulation and administration route have a major impact on immunization outcome

2. Non-invasive delivery of nanoparticles via hair follicles

Parts of this Chapter were published in

Mittal, A. *, Raber, A.S. *, Schaefer, U.F., Weissmann, S., Ebensen, T., Schulze, K., Guzmán, C.A., Lehr, C.M., Hansen, S. (2013). **Non-invasive delivery of nanoparticles to hair follicles: A perspective for transcutaneous immunization.** *Vaccine*, 31 (34), pp. 3442-3451.

**These authors contributed equally to this work*

The author of the thesis made the following contribution to the publication:

- Planned and designed all experiments.
- Performed experiments related to particle preparation and characterization, and quantitative studies related to follicular uptake of particles.
- Analysed data from the above mentioned studies and interpreted all experimental data.
- Wrote the manuscript.

2.1 Abstract

Transfollicular vaccination aims to reach the peri-follicular antigen presenting cells without impairing the stratum corneum (SC) barrier. This would be an optimal vaccination strategy under critical hygienic conditions. Nanoparticles (NPs) are the ideal vehicles for transfollicular delivery of vaccines as they are able to (i) penetrate deeper into the hair follicles than molecules in solution, (ii) can help to stabilize protein based antigen and (iii) improve and modulate the immune response.

This study investigates the potential of transfollicular delivery of polymeric NPs using ovalbumin (OVA) as a model antigen. The NPs were prepared by a double emulsion method from pharmaceutically well characterized biocompatible and biodegradable polymers poly(lactide-co-glycolide) (PLGA) or chitosan-coated PLGA (Chit-PLGA) using polyvinyl alcohol as stabilizer. The NP formulations are available as freeze dried product which can be re-constituted with water or cell culture medium before use to yield any desired OVA/NP concentration. OVA was protected from cleavage or aggregation inside the NPs and retained its biological activity to 74% (PLGA) and 64% (Chit-PLGA). Thus, when applying a typical dose of 8.5 μ l NP formulation per cm^2 (50 mg NPs/ml, 54.3 ± 0.047 and 66.5 ± 0.044 μ g OVA/mg NPs for PLGA and Chit-PLGA NPs respectively) an effective dose of 17 μ g/ cm^2 (PLGA) or 18 μ g/ cm^2 (Chit-PLGA) of active OVA is administered. In a cell culture assay encapsulated OVA stimulated the proliferation of CD4⁺ (PLGA and Chit-PLGA) and CD8⁺T-cells (only Chit-PLGA) to a larger extent than OVA in solution. Both NP formulations improved the delivery efficiency of OVA into the hair follicles on excised pig ears by a factor of 2-3 compared to OVA solution. This

delivery efficiency could further be increased by increasing the number of NPs applied per skin area by a factor of ≈ 2 -2.4.

Consequently formulation of OVA into PLGA and Chit-PLGA NPs may offer to reduce the dose which needs to be applied for transfollicular immunization.

2.2. Introduction

Transcutaneous immunization (TCI) refers to the needle-free application of vaccines across the skin [45]. Major benefits include the possibility of self-administration, improved patient compliance, no requirement of “sharps” waste removal, and reduced storage and transport issues. The skin is a superior organ for eliciting an immune response compared to the muscle due to the abundance of professional antigen presenting cells (APCs) such as dendritic cells (DCs) and Langerhans cells (LCs) in different layers of the skin [8, 46]. In addition, TCI can generate both a humoral as well as a cellular response at the site of administration and also at distant mucosal sites [22]. Hence, TCI may allow reducing the antigen dose, as well as eliciting an improved immune response in persons with a disease- or age-compromised immune system [47].

The major challenge for TCI is to enhance the transport of antigens across the stratum corneum (SC) barrier. To this end often barrier disrupting measures are applied, such as chemical permeation enhancers, abrasion, electroporation, micro-needles, PowderJect, gene gun, etc. In contrast, transfollicular vaccination aims to deliver antigens to the abundant perifollicular APCs [14, 48]. Any additional barrier disrupting measures should be expendable as the SC only extends into the upper third of the follicle. Solid NPs are the ideal vehicles for transfollicular delivery as they accumulate in hair follicles and skin folds and penetrate deeper into hair follicles than molecules in solution [19]. Transfollicular delivery has been widely

investigated for DNA vaccines, and lately also for non-nucleotide based antigens such as a seasonal flu vaccine as well as nanoparticle (NP) based formulations. Nonetheless, transfollicular vaccination is usually performed after pretreating the skin area by plucking the hairs, waxing, or cyanoacrylate (superglue) stripping. This pretreatment induces the hair cycle into anagen (proliferation) state and markedly increases the transfection efficiency of follicular keratinocytes [15, 49]. The pretreatment is therefore helpful for DNA vaccines, however, it may be expendable for protein or peptide based antigens. At the same time the SC is (at least partially) removed so that it is not clear to which extent the antigen penetrates via the hair follicles or across the permeabilized SC. This is especially critical as the reduced barrier increases the risk of pathogen entry which is of particular importance for transfollicular vaccination in (i) countries with critical hygienic conditions, and (ii) immuno-compromised individuals, such as elderly people with poor wound healing and young children.

This study investigates the potential of transfollicular delivery of ovalbumin (OVA) using polymeric nanoparticles (NPs) without compromising the SC barrier by any pretreatment for the purpose of non-invasive TCI. NPs were prepared by a double emulsion method from poly(lactide-co-glycolide) (PLGA) or chitosan-coated PLGA (Chit-PLGA) and polyvinyl alcohol (PVA) as stabilizer. These are biocompatible and biodegradable polymers which are widely used for biomedical applications. The NPs were characterized physico-chemically in terms of size, surface charge, OVA encapsulation/loading and morphology. The integrity and biological activity of the encapsulated OVA was monitored by SDS page, *in vitro* proliferation of OVA-specific lymphocytes, and ELISA. The follicular delivery efficiency was measured in intact pig skin based on the differential stripping technique and compared to OVA solution [19, 50]. An adoptive transfer experiment was performed as a proof

of concept study, to analyze the usefulness of the non-invasive transfollicular immunization route.

To our knowledge this is the first study to evaluate the potential of transfollicular vaccination using NPs without applying SC barrier reducing measures.

2.3. Materials and methods

2.3.1. Material

EndoGrade® Ovalbumin (OVA) was obtained from Hyglos GmbH (Bernried, Germany); poly(d,l-lactide-co-glycolide) (PLGA) (Resomer RG 50:50 H; inherent viscosity 0.31 dL/g) was kindly provided by Boehringer Ingelheim (Boehringer Ingelheim GmbH & Co. KG, Ingelheim, Germany); polyvinyl alcohol (PVA) Mowiol® 4-88 was obtained from Kuraray Specialties Europe GmbH (Frankfurt, Germany); ultrapure chitosan chloride salt (Protasan® UP CL113) was purchased from FMC BioPolymer AS (Oslo, Norway); trehalose was obtained from Sigma-Aldrich (St. Louis, MO, USA); fluorescein isothiocyanate conjugated ovalbumin (FITC-OVA) was obtained from Invitrogen (Molecular Probes Inc., Germany). Superglue was kindly provided by Uhu GmbH & Co.KG, (Bühl, Germany). Tesa film was obtained from TESA SE, Hamburg, Germany. The OVA specific ELISA kit was purchased from USCN life science Inc. (Hölzel Diganostik, Germany). All other solvents and chemicals used were of the highest grade commercially available. Deionized water (Milli Q Plus system, Millipore, Bedford, MA, USA) was used throughout the investigation.

2.3.2. Pig ear skin

Ears from freshly slaughtered pigs were removed before scalding. The ears were washed with water, blotted dry and the hairs were shortened with scissors. The ears were stored at 4-8 °C for a maximum period of 3 days.

2.3.3. Mice

Female BALB/c (H-2d) or C57BL/6 (H-2b) mice at the age 6-8 weeks were purchased from Harlan (Germany). OVA-TCR transgenic mice OT-I (C57BL/6-Tg(TcraTcrb)1100Mjb/J) and OT-II (C57BL/6-Tg(TcraTcrb)425Cbn) were bred at the animal facilities of Helmholtz Centre for Infection Research under specific pathogen-free conditions.

2.3.4. Nanoparticles preparation

PLGA NPs were prepared by a modified double emulsion method [51]. Briefly, 50 mg of PLGA were dissolved in 2 ml of ethyl acetate at room temperature. Then 400 µl of (1.875% wt/V) OVA solution in water was added to form a primary water-in-oil (w/o) emulsion. After sonicating at 20 % amplitude (A) for 15 s, 4 ml of 2% (wt/V) PVA solution was added to the primary emulsion and again sonicated at 20 A for 20 s. Water was added drop-wise to the resulting w/o/w emulsion under constant stirring to allow diffusion and evaporation of the organic solvent. The particles were collected by centrifugation at 10,000 g for 15 min, washed once with distilled water to remove excess surfactant and free drug and freeze dried using trehalose (0.2% wt/V) as cryoprotectant.

Chit-PLGA NPs were prepared in a similar manner as described above with the difference that Protasan® UP CL113 (0.2% wt/V) was added to the PVA solution.

FITC labeled OVA loaded NPs and FITC labeled blank NPs were prepared by replacing OVA or the PLGA polymer with their fluorescent counterparts, respectively.

2.3.5. Nanoparticle characterization

Size and ζ -potential of the NPs were analyzed by photon correlation spectroscopy (PCS) using a Nano-ZS (Malvern Instruments, Malvern, UK). The morphology of the NPs was characterized using scanning electron microscopy (SEM) (JSM 7001F Field Emission SEM (Jeol, Japan)) and atomic force microscopy (AFM) (Multimode V (Veeco, USA)). For SEM, prior to scanning, NPs were sputtered with gold (layer thickness approximately 10 nm). The accelerating voltage was 10 kV with a focal distance of 10 mm. For AFM imaging, NPs were scanned using tapping mode and scan rates of 0.6 Hz. A standard non-contact mode cantilever was used for imaging (OMCL-AC160TS, Olympus, Essex, Great Britain).

The entrapment efficiency (% EE = wt OVA encapsulated/wt OVA added initially) and loading efficiency (% L = wt OVA encapsulated/wt polymer) of OVA in PLGA and Chit-PLGA NPs were determined using a QuantiPro bicinchoninic acid (BCA) assay (Pierce, Rockford, IL, USA) according to the manufacturer's instructions for 96 micro-well plates. Briefly, 5 mg of the lyophilized particles were hydrolyzed in 0.1 N NaOH for 6 h and then neutralized with 0.1 N HCl [51]. Blank NPs were used as a control.

2.3.6. Integrity and Activity of OVA

The integrity of OVA was determined by SDS PAGE analysis. Briefly, OVA was extracted from freeze-fried NPs under alkaline conditions (0.1 N NaOH). The total amount of protein was quantified using a QuantiPro BCA assay. A dose of 1 μ g of OVA was loaded onto a 12% (wt/V) polyacrylamide gel under reducing conditions

[52]. Detection of protein was performed by staining with colloidal Coomassie blue (Fermentas, St. Leonrot, Germany).

To determine the activity of OVA encapsulated in NPs 1 ml of each NP dispersion (1 mg/ml) was incubated for 24 h in phosphate buffer (pH 5.5) at 32 °C under continuous stirring at 100 rpm. The dispersion was centrifuged for 20 min at 24,000 g and the total amount of protein in the supernatant was quantified using a QuantiPro BCA assay. Subsequently, the active OVA fraction was quantified using an ELISA assay which was performed according to the instructions provided by the manufacturer. The ELISA was calibrated using standards provided by the manufacturer in the range of 0.156 – 10 ng/ml (lower limit of detection, LLOD = 0.053 ng/ml). Supernatant obtained from blank NPs were used as negative control.

2.3.7. DC activation and stimulation: Preparation and flow cytometric analysis of murine dendritic cells

Bone marrow-derived primary dendritic cells (conventional DCs) from C57BL/6 mice were generated by flushing femur and tibia of mice with media. Erythrocytes were lysed by adding ACK buffer (0.15 M NH_4Cl , 1.0 M KHCO_3 , 0.1 mM EDTA, pH 7.2). Cells were washed and incubated on cell culture dishes for up to 2 h. Then non-adherent DC precursors in the supernatant were transferred to 12-well plates (2×10^6 /well) and differentiated for 5 days in media supplemented with 50 ng/ml GM-CSF. On day 5, DCs were co-incubated with PLGA OVA [10 $\mu\text{g/ml}$], Chit-PLGA OVA and different controls, such as PLGA alone for 24 h at 37°C. Control cells were treated with OVA LPS free [10 $\mu\text{g/ml}$] and OVA co-administered with LPS derived from *Salmonella enterica* Serovar Typhimurium (Invivogene) at a final concentration of 1 $\mu\text{g/ml}$. For flow cytometry, cells were pre-blocked using anti-

mouse CD16/32 antibody for 15 min. Then, DCs were stained with several differentiation and maturation markers conjugated with different fluorochromes, such as CD40 (HM40-3), CD54 (YN1/1.7.4), CD80 (16-10A1), CD86 (GL1), MHC-II M5/114.15.2), and MHC-I (34-1-2S) antibodies (eBioscience, USA). The FACS analysis of 20,000 events was performed using a LSR-II and the FACSDiva software (BD Bioscience, USA), gating on CD11c positive cells. Results are expressed as histograms and correspond to one representative experiment out of three independent tests.

2.3.8. Measurement of cellular proliferation of antigen specific murine CD4⁺ and CD8⁺ T cells

Differentiated murine DCs were incubated with 10 µg/ml of LPS-free OVA (EndoGrade® OVAalbumin, #321001, Hyglos, Germany), PLGA or PLGA-OVA and Chitosan-PLGA or Chitosan-PLGA-OVA. After 24h CD8⁺ T cells derived from spleens of OT-I mice, which have a transgenic T cell receptor specific for the OVA immune-dominant peptide (aa 257-264, SIINFEKL) presented in the context of the MHC class I H-2K^b, or CD4⁺ T cells derived from spleen of OT-II mice expressing the TCR specific for OVA (aa 323–339, ISQAVHAAHAEINEAGR) presented in the MHC class II molecule I-A^b were isolated. Afterwards, the spleen cells were stained with 10 µM carboxy fluorescein succinimidyl ester (CFSE; Molecular Probes, USA) in PBS for 5 min and co-cultured with antigen stimulated murine DCs for 4 days. The loss of CFSE⁺ labelling of CD8⁺ and CD4⁺ T cells in response to stimulation with PLGA-OVA or Chitosan-PLGA-OVA were determined by flow cytometry on a BD LSR-II and analysed using the FACSDiva software.

2.3.9. Adoptive transfer model of TCR transgenic CD4 T cells to characterize OVA specific proliferation

Naïve non-activated CD4 T-cells ($CD4^{+} CD62L^{hi} CD44^{lo} CD25^{-}$) were isolated from pooled lymph nodes and spleens of OTII x Thy1.1 mice by FACS with an ARIA II sorter (purity $\geq 98\%$). These cells express an OVA-peptide AA323-339 specific T cell receptor (TCR) and the congenic marker Thy1.1 (CD90.1, while wild type mice express Thy1.2 (CD90.2)). The congenic marker, which slightly differs in structure but not in function, allows the identification of the transferred cells *ex vivo* by non-cross-reactive monoclonal antibodies. The sorted cells were labeled with CFSE to track their proliferation later on.

Immunization was carried on the flank part of the mice. Flank part of mice were shaved (under anesthetic) at least 2 d before immunization. Shaved areas were carefully inspected for cuts or skin irritation in which case these mice were excluded from the experiment. A day prior to immunization the CFSE labeled cells were transferred to OVA naïve C57BL/6 mice by tail vein injection (1.5×10^6 per mouse). On the day of immunization, the mice were immunized either i.m. or via the transfollicular route.

The animals were assorted to the following treatment groups (4 animals per group): (1) negative control, received Chit-PLGA + 5 μ g c-di-AMP as adjuvant dispersed in physiological buffer via i.m. injection; (2) positive control, received 200 μ g / 50 μ l LPS-free OVA dissolved in physiological buffer via i.m. injection; (3) received 200 μ g LPS-free OVA in Chit-PLGA NPs + 5 μ g c-di-AMP as adjuvant via transfollicular application. After another 4 days the animals were sacrificed and spleens and draining lymph nodes (iliac and axillary LNs pooled) were isolated separately for each animal. Cells were stained for live/dead, CD3+, CD4+ and

Thy1.1+ and analyzed with a LSRII flow cytometer. Cells were gated for viability, CD3+ CD4+ Thy1.1+ and the proliferation (CFSE dilution) was analyzed.

2.3.10. Evaluation of follicular uptake on excised pig ears

Incubation sites of 1.767 cm² were marked on the outer auricle of the pig ears with a permanent marker. A dose of 15 µl of either an aqueous solution of FITC-OVA, an aqueous dispersion of FITC-OVA in PLGA NPs, or FITC-OVA in Chit-PLGA NPs (8.5 µg OVA/cm², 0.42 and 0.36 mg NPs/cm² for PLGA NPs and Chit-PLGA NPs, respectively) were applied and massaged manually with a gloved forefinger for 3 min. The ears were incubated for 1 h at 32°C under non-occlusive conditions.

2.3.11. Microscopical evaluation

Cross-sections of 12 µm thickness were performed on a cryomicrotome (Cryostat Type MEV, Slee, Mainz, Germany). The biopsy was placed in a vertical direction relative to the blade to prevent the spreading of NPs from the skin surface to deeper skin layers. The sections were collected on objective slides, embedded in FluorSave™ embedding medium (Calbiochem®, USA) and sealed with a cover slip.

For the top view image, a skin biopsy was mounted on an objective slide with distance holders and sealed with a cover slip, which immediately touched the skin as well as the distance holders to prevent any skin movement during the imaging process.

Cyanoacrylate biopsies were obtained as described below and fixed on an objective slide.

All samples were imaged under the confocal microscope (Zeiss LSM 510 META system, Carl Zeiss, Jena, Germany). An Argon laser at 458 nm was used to excite the fluorescence signal. As objective a water immersion lens 25X was used. The

high auto fluorescence of the skin was excluded by choosing appropriate filters and gain settings. In addition, for the cross-sections and cyanoacrylate biopsies transmission light images were superimposed with the fluorescence images. For top-view and cyanoacrylate biopsy images optical stacks (z-stacks) were performed. Image processing was performed using Volocity® 3D Imaging Analysis Software (Perkin Elmer Inc. USA).

2.3.12. Quantification of follicular uptake: Influence of encapsulating OVA into particles

After the incubation the skin surface was cleaned from remaining formulation by removing 10 tape strips (Tesa kristallklar, Tesa SE, Germany). A roller was used to enhance the contact between tape strip and skin surface [53]. Subsequently, 2 cyanoacrylate biopsies were performed to collect the amount of OVA penetrated into the hair follicles. The cyanoacrylate biopsies were extracted in acetonitrile:0.1 N NaOH (70:30) for 3 h on a horizontal shaker and the fluorescence intensity of all samples was measured using a Tecan platereader (Excitation 490 nm, Emission 525 nm). The amount of FITC-OVA extracted from the cyanoacrylate biopsies was calculated with the help of standards prepared from FITC-OVA / FITC-OVA in PLGA NPs / FITC-OVA in Chit-PLGA NPs dissolved in acetonitrile : 0.1 N NaOH (70:30) in the range of 0.1-10 µg/ml. The results for the NPs were expressed relatively to FITC-OVA solution.

Blank samples were taken from an incubation site of the same pig ear, double distilled water was applied instead of NPs. The blank values were subtracted from the fluorescence intensity of the samples.

2.3.13. Quantification of follicular uptake: Influence of particle concentration

Follicular uptake was quantified using particle concentrations of 0.22/0.42/0.85 mg NPs/cm². Briefly, 15 µl of each NP dispersion at a concentration of 25/50/100 mg NPs/ml were applied to an area of 1.767 cm² and processed exactly as described above. The NPs used in these experiments were prepared using FITC-PLGA to enable detection and did not contain any OVA. FITC-labeling of PLGA was performed as described in [54]. Standards were prepared from blank FITC-PLGA or Chit-FITC-PLGA NPS in the range of 5-380 µg/ml dispersed in acetonitrile:0.1 N NaOH (70:30). Blank samples were taken from an incubation site of the same pig ear, double distilled water was applied instead of NPs. The blank values were subtracted from the fluorescence intensity of the samples.

2.3.14. Statistical analysis

Statistical analysis was performed by a one-way ANOVA. A p value of ≤ 0.05 was considered significant.

2.4. Results

2.4.1. Characterization of Nanoparticles

The SEM and AFM images in Fig.1 show smooth, spherical particles. The characteristics of the NPs are summarized in Table 1. The mean size of OVA loaded PLGA and Chit-PLGA NPs was ca. 170 nm and 180 nm, respectively, with a monodisperse size distribution (PDI < 0.2).

Table 1

Physico-chemical characterization of the optimized PLGA and Chit-PLGA NPs

Nanoparticle	Size (nm)	PDI	Z.P. (mV)	% EE	% L	%A
Blank PLGA	162.8 ±	0.056 ±	-31.5 ±	-	-	
	1.66	0.005	1.03			
OVA loaded PLGA	168.5 ±	0.063 ±	-24.8 ±	27.61 ±	5.43 ±	73.59 ±
	1.45	0.008	0.89	1.03	0.19	2.91
Blank Chit-PLGA	171.5 ±	0.123 ±	24.1 ±	-	-	
	1.36	0.012	0.78			
OVA loaded Chit-PLGA	183.6 ±	0.171 ±	20.2 ±	36.54 ±	6.65 ±	63.57 ±
	2.71	0.012	1.05	1.08	0.18	2.68

Values represent mean ± standard error of the mean (SEM) of n = 6 independently prepared batches, except for %A where n = 3. Z.P. zeta potential, %EE encapsulation efficiency (wt OVA encapsulated/wt OVA added initially), %L loading (wt OVA encapsulated/wt polymer), %A activity (wt OVA active/OVA encapsulated)

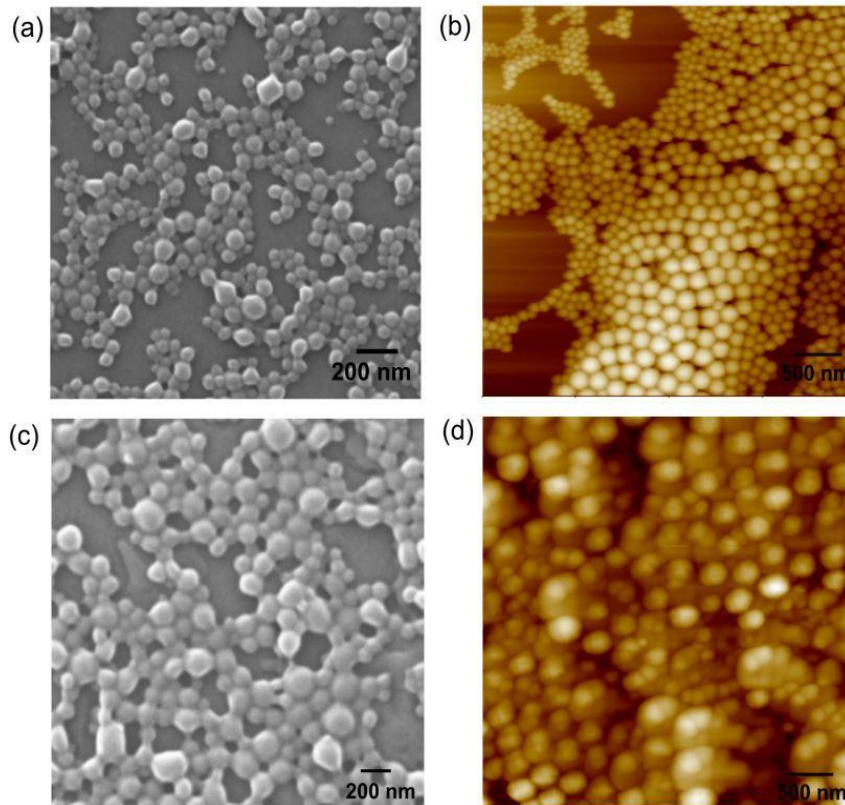


Figure 1. Top: (a) & (b) SEM and AFM images of OVA loaded PLGA NPs; bottom: (c) & (d) SEM and AFM images of OVA loaded Chit-PLGA NPs

PLGA NPs have a negative surface charge whereas Chit-PLGA NPs have a positive surface charge. Antigen incorporation into PLGA and Chit-PLGA NPs

slightly increased the particle size and reduced the overall surface charge compared to blank NPs. For both particle types similar %EE of $27.61 \pm 2.52\%$ and $36.54 \pm 2.44\%$ and %L of $5.43 \pm 0.47\%$ and $6.65 \pm 0.44\%$ were obtained (for PLGA and Chit-PLGA NPs respectively).

2.4.2. Integrity and Activity of OVA

To investigate the formation of fragments or aggregates of OVA during NP preparation, an SDS PAGE was performed. Weak differences in the migration pattern of OVA extracted from NPs compared to control (OVA in aqueous solution) were observed as shown in Fig. 2. While no fragments were obtained, low amounts of higher molecular weight adducts, probably dimers and trimers (ca. 95 and 135 kDa), were observed in the case of OVA extracted from NPs. Lanes 3 and 5 (blank NPs) show that no interference from the NP formulations is to be expected.

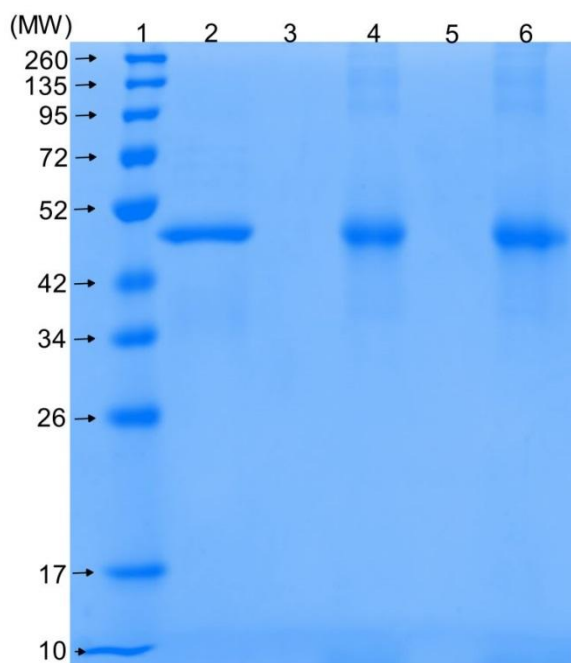


Figure 2. Integrity of OVA extracted from NPs by 0.1 N NaOH and analyzed by SDS PAGE, Lane 1: MW standards, Lane 2: OVA control, Lane 3: Blank PLGA, Lane 4: OVA extracted from PLGA NPs, Lane 5: Blank Chit-PLGA, Lane 6: OVA extracted from Chit-PLGA NPs

In addition, ELISA was performed using the OVA which had been extracted from the NPs. By relating the result to the total amount of protein in the sample the activity of the encapsulated OVA was determined as 74% and 64% in PLGA and Chit-PLGA NPs, respectively.

2.4.3. Activation of dendritic cells

We analyzed the effect of PLGA-OVA and Chit-PLGA-OVA on the activation and maturation of bone marrow-derived murine DCs. Both, PLGA-OVA and Chit-PLGA-OVA were able to promote an efficient activation and maturation of DCs *in vitro* when used at a final OVA concentration of 10 µg/ml. Changes in the activation markers (% of CD11c+ DCs indicates the number of activated DCs; MFI indicates the expression level of a certain marker per cell) were modest but except for CD54 an increase compared to negative control was detected for all NP groups as well as for OVA alone (Fig. 3). Interestingly, no significant differences in the expression levels of activation markers per cell have been observed comparing values of DCs stimulated with OVA alone with those of DCs incubated in the presence of any NP formulation (Fig. 3). In general incubation of DCs in the presence of OVA alone and in combination with LPS stimulated similar changes in activation markers except for CD40 and CD80 where the addition of LPS increased the marker expression per cell (Fig. 3).

However, we next evaluated the capacity of APCs loaded with antigen in presence of PLGA-OVA and Chit-PLGA-OVA to stimulate the proliferation of antigen-specific CD8+ and CD4+ T cells. DCs stimulated with OVA loaded Chit-PLGA NPs were able to induce a strong antigen-specific proliferation of CD8+ T cells (67.5%) from OT-I mice, as shown by the loss of CFSE+ stained cells (Fig. 4, left column).

Furthermore, these DCs were also able to stimulate the proliferation of CD4⁺ T cells (95.6%) derived from OT-II mice (Fig. 4, right column). Nevertheless, weaker T cell proliferation was also observed when DCs were stimulated with OVA LPS-free alone (21 and 68%, respectively). DCs stimulated with OVA loaded PLGA NPs were also able to stimulate the proliferation of OT-I and OT-II cells although to a lesser extent compared with OVA alone and the OVA loaded Chit-PLGA NPs (10 and 95.1%, respectively). OVA free NPs promote only very marginal DC activation/ T-cell proliferation if any at all (Fig. 4). Interestingly, LPS induced only weak CD4⁺ T cell proliferation compared to OVA and PLGA-OVA and Chit-PLGA-OVA (Fig. 4).

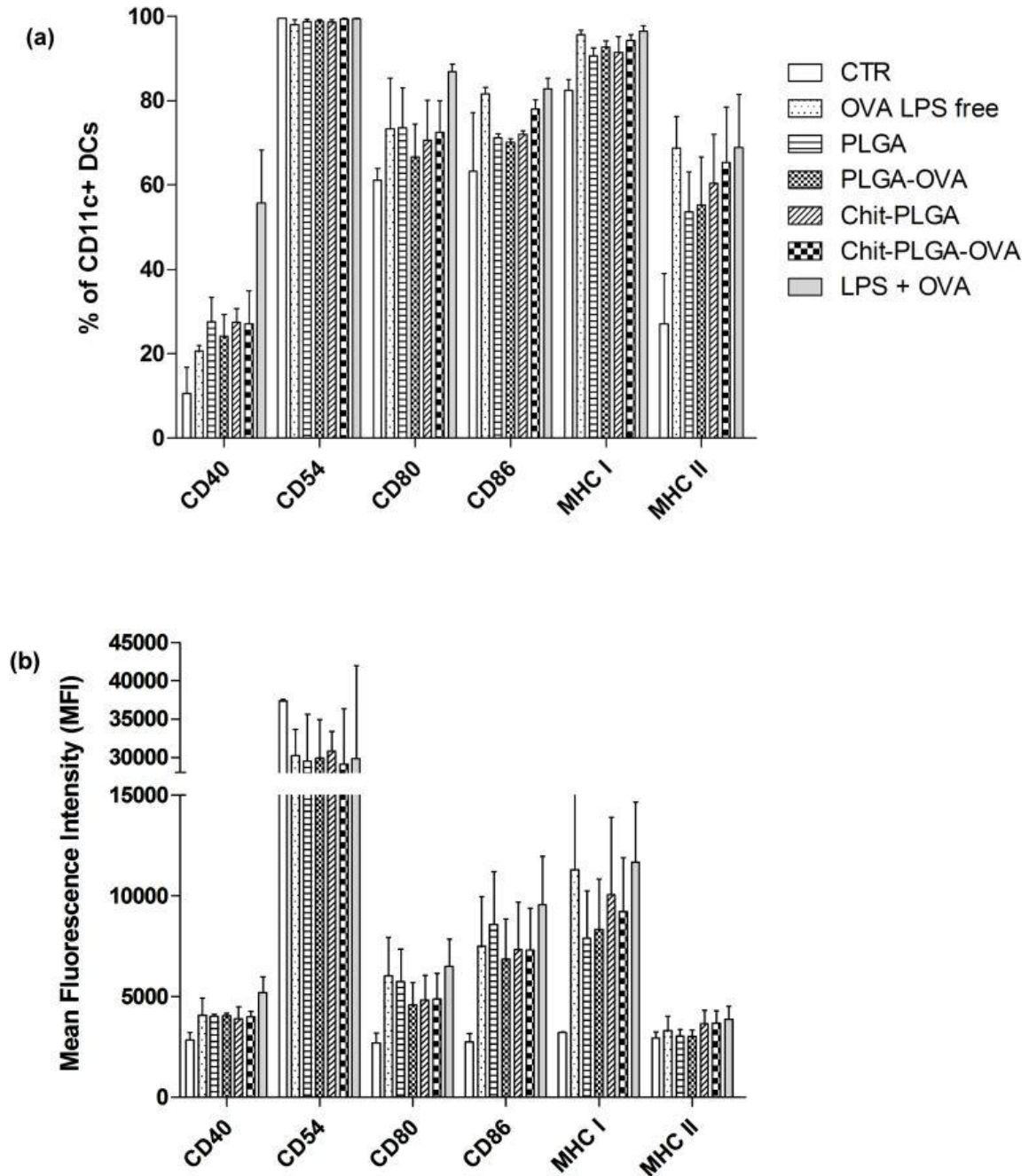


Figure 3. Expression of activation marker by murine DCs after stimulation with PLGA-OVA and Chit-PLGA-OVA. The expression of surface markers on CD11c⁺-gated bone marrow-derived murine DCs following stimulation with OVA LPS free [10 µg/ml], PLGA, PLGA-OVA [10 µg/ml], Chit-PLGA and Chit-PLGA-OVA [10 µg/ml], respectively, was investigated by flow cytometry. After 24 h of incubation DCs were stained with Abs specific for CD40, CD54, CD80, CD86, MHC-I and MHC-II molecules and analyzed by flow cytometry (BD LSR-II). Results are mean \pm SEM of three independent experiments and expressed as percentage (a) and mean fluorescence intensity (MFI) (b), respectively, of CD11c⁺ cells.

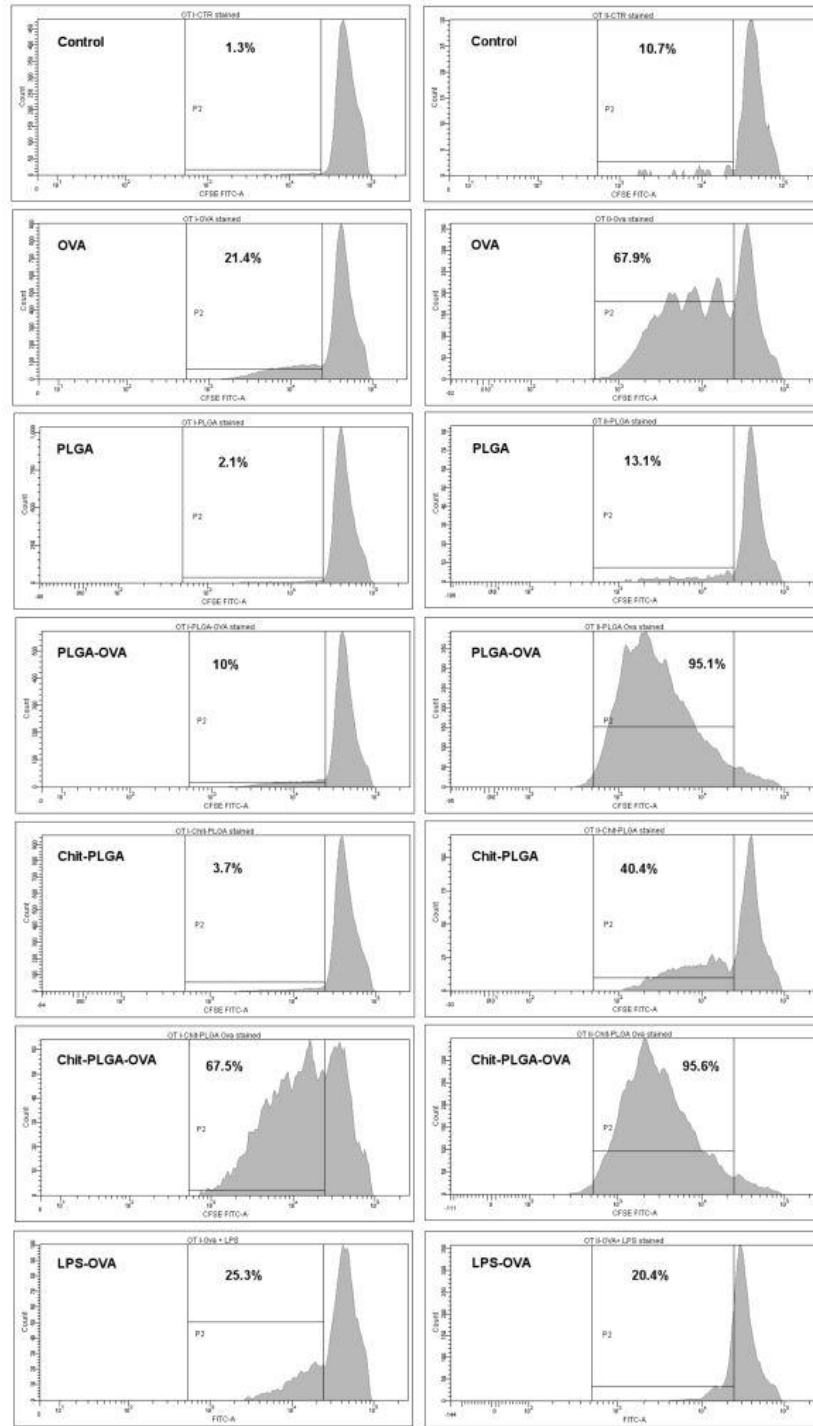


Figure 4. Ova-specific proliferation of OT-I (left panel) and OT-II lymphocytes (right panel) stimulated by NP-OVA pulsed DCs. Bone marrow-derived DCs were incubated for 24 h in the presence of OVA LPS free [10 µg/ml], PLGA, PLGA-OVA [10 µg/ml], Chit-PLGA and Chit-PLGA-OVA [10 µg/ml], respectively. Non-stimulated pulsed DCs were used as negative control. Then, the loaded DCs were co-cultured with either CFSE labeled naïve CD8⁺ or CD4⁺ T cells derived from OT-I and OT-II mice, respectively, for 4 days and further analyzed by flow cytometry. The results are representative out of two experiments and are expressed as histograms showing the percentage of proliferating OVA-specific T cells of all CD8⁺ (OT-I) and CD4⁺ (OT-II) T cells, respectively.

2.4.4. Adoptive transfer model of TCR transgenic CD4 T cells to characterize OVA specific proliferation

In order to verify the feasibility of transfollicular immunization as alternative vaccination strategy, an adoptive transfer model was established. Proliferation of adoptively transferred OVA specific CD4 T cells was measured by CFSE dilution in the draining lymph nodes and secondary lymphatic organ.

The number of divided OVA specific CD4 T cells is shown in Fig. 5 (one representative animal of 4 animals per group). As expected no proliferation of transferred cells isolated from draining lymph nodes have been observed in the negative control (Fig. 5a), whereas animals of group 2 (immunized i.m. with OVA protein as positive control) showed a strong proliferation (95.9% of the transferred cells proliferated, Fig. 5b). Mice immunized by transfollicular application of Chit-PLGA-OVA co-administered with c-di-AMP as adjuvant showed a comparable proliferation potential (96.2%, Fig. 5c).

Fig. 6 shows the percentage of divided transferred cells for each experimental group. The four animals of each group were analyzed separately. While no proliferation was observed in the negative control (group 1), full proliferation of the transferred cells was observed in animals of the positive control group (group 2) and in animals immunized transfollicularly with Chit-PLGA-OVA and c-di-AMP as adjuvant (group 3). This experiment demonstrates that the model antigen OVA can be delivered via the transfollicular route and that the immunization by this route is able to elicit the same proliferation OVA specific CD4⁺ T cells as the i.m. injection of OVA.

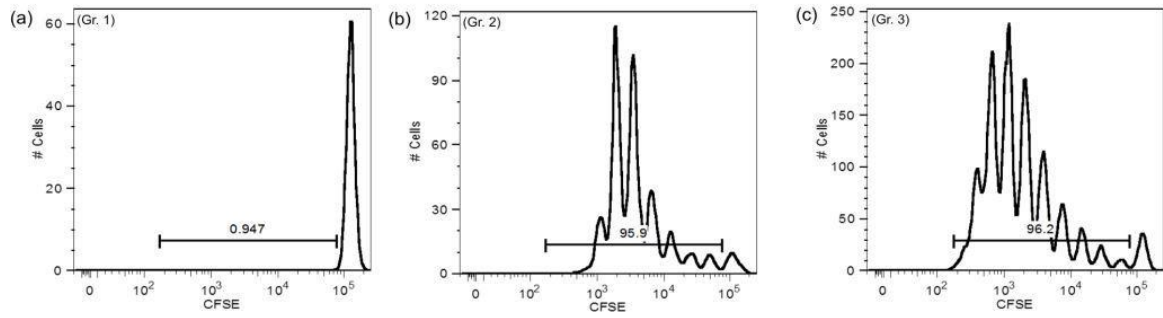


Figure 5. Animals of group 1 were immunized with empty Chit-PLGA NPs and the adjuvant c-di-AMP i.m.. As expected no proliferation of transferred cells was observed in this negative control (A). Animals of group 2 were immunized i.m. with OVA protein as positive control. More than 95% of the transferred cells proliferated after this stimulation (B). The mice of group 3 were immunized by transfollicular application of OVA loaded Chit-PLGA NPs and c-di-AMP as adjuvant which led to proliferation comparable to the positive control (C). Shown is the proliferation of cells isolated from draining lymph nodes of one representative animal per group.

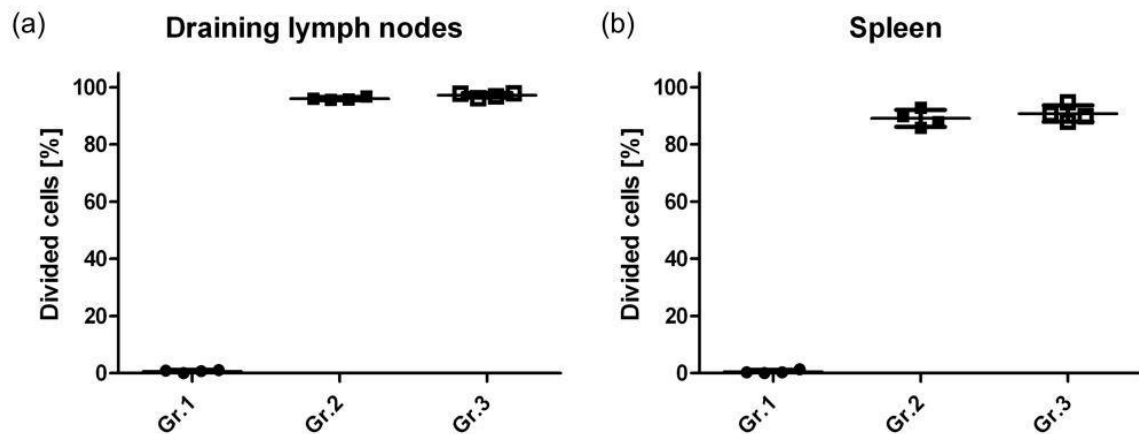


Figure 6. The percentage of divided transferred cells in the draining lymph nodes (a) and the spleen (b) for each experimental group is shown. The four animals of each group were analyzed separately. While no proliferation was observed in the negative control (Gr.1), full proliferation of the transferred cells was observed in animals of the positive control group (Gr.2) and in animals immunized transfollicularly with Chit-PLGA-OVA and c-di-AMP as adjuvant (Gr.3.). This experiment demonstrates that the model antigen OVA can be delivered via the transfollicular route and that the immunization by this route is able to elicit the same proliferation of OVA specific CD4⁺ T cells as the i.m. injection of OVA.

2.4.5. Follicular uptake of Nanoparticles

Fig. 7 shows representative images illustrating the distribution of fluorescently labeled NPs on the skin surface and in the hair follicle after application to excised pig ears. From both the cross-section as well as the top-view it is apparent that the NPs accumulated in the follicle openings, cover the hair and invade into the follicular duct (Fig. 7(a,b)). Fig. 7c shows a cyanoacrylate biopsy of the follicular content, which further confirms the presence of NPs inside the hair follicles.

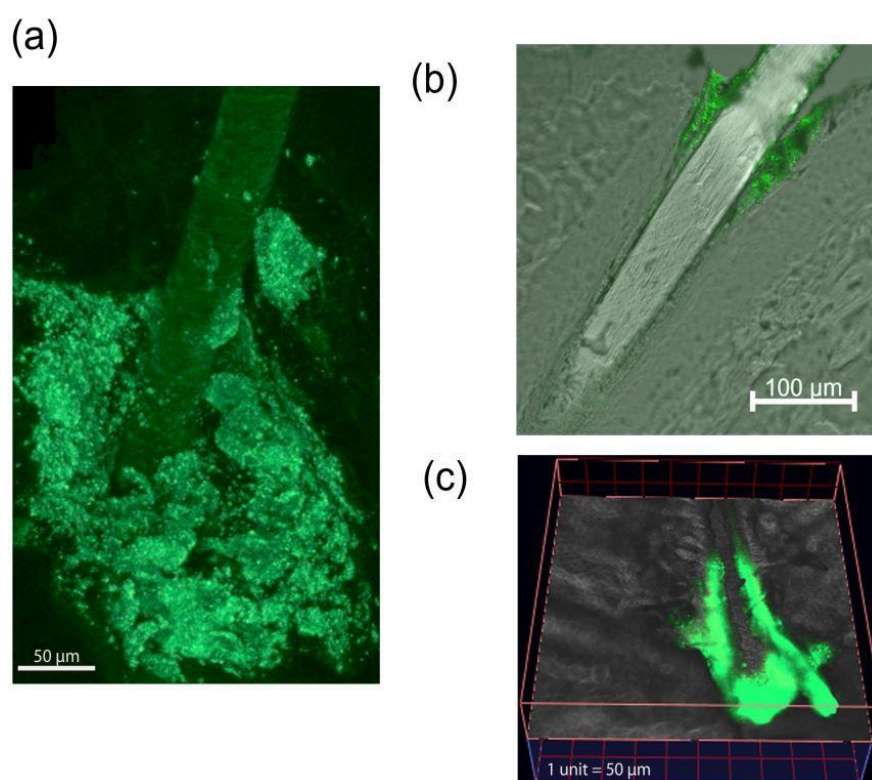


Figure 7. Distribution of fluorescently labeled NPs in hair follicles after application to excised pig ears. (LSM 510 Meta, Carl Zeiss GmbH, Jena Germany; excitation wavelength 458 nm)

(a) Top view onto the skin surface – image reconstituted after optical sectioning (41 individual frames of 3 μm thickness); NPs accumulate in the follicle opening. The hair is visible as a negative image due to NPs on the hair surface.

(b) Transversal cryo section (thickness 12 μm); overlay of fluorescence and transmission light images: NPs are visible on the skin surface and inside the follicle.

(c) Cyanoacrylate biopsy – one plane selected from optical sectioning (section thickness 0.5 μm); the position of the plane relative to the entire optical stack can be estimated from the height of the box; overlay of fluorescence and transmission light images; the skin surface is oriented towards the bottom of the image: NPs are visible deep inside the cyanoacrylate biopsy which was performed to extract the follicular content.

By extracting cyanoacrylate biopsies with organic solvents and quantifying the fluorescence in the extract the uptake into the follicles was quantified (Fig. 8). Encapsulation of OVA into NPs significantly enhanced follicular uptake of OVA by a factor of 2.85 ± 0.6 (FITC-OVA in PLGA NPs) and 2.33 ± 0.52 (FITC-OVA in Chit-PLGA NPs) compared to OVA solution (Fig. 8a). Follicular uptake of OVA was slightly lower for Chit-PLGA compared to PLGA NPs; however, this difference was not significant (Fig. 8a).

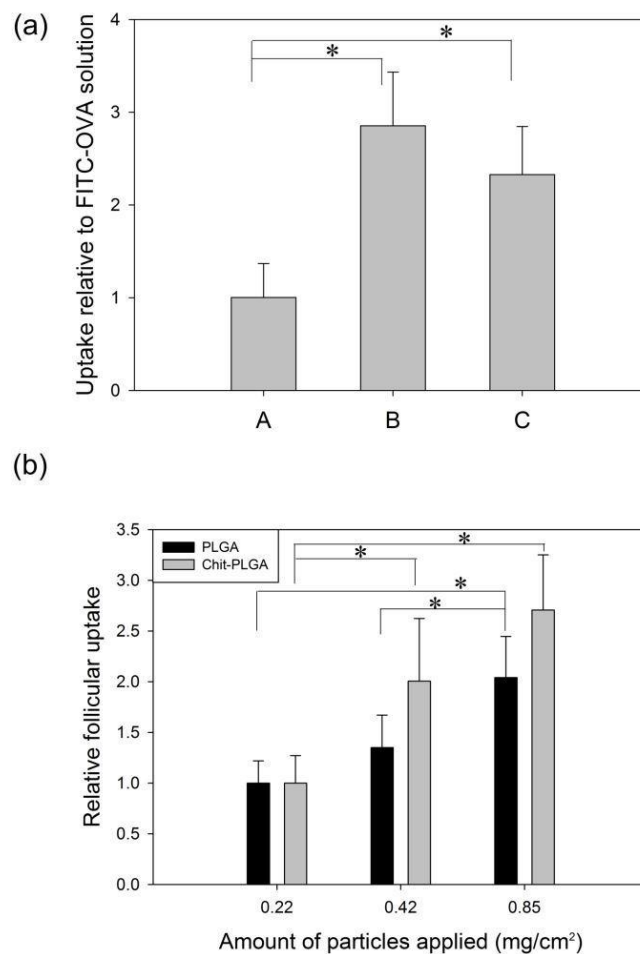


Figure 8. (a) Uptake of FITC-labeled OVA encapsulated in NPs relative to FITC-OVA solution A: FITC-Ova solution, B: FITC-OVA in PLGA NPs, C: FITC-OVA in Chit-PLGA NP. (applied dose: $8.5 \mu\text{g OVA}/\text{cm}^2$, $0.42 \text{ mg NPs}/\text{cm}^2$; $n = 6$, mean \pm SEM; * indicates significant differences compared to A with $p < 0.05$)

(b) Effect of NP concentration on follicular uptake. The results are expressed relatively to the lowest NP concentration. ($n = 3$ except for the highest conc. measured with Chit-PLGA NPs where $n = 2$, mean \pm SEM; * indicates significant differences compared to the lowest NP concentration with $p < 0.05$)

Furthermore, using FITC-labeled PLGA it turned out that follicular uptake of particles is a function of the NP dose/area relation. Thus the uptake can further be enhanced by increasing the NP concentration in the formulation (Fig. 8b).

2.5. Discussion

Transfollicular delivery of antigen by using NPs holds the potential for TCI without the need to weaken the protective SC barrier. So far, studies demonstrating transfollicular antigen delivery used additional barrier disrupting methods such as tape stripping, plucking or intense skin hydration [15, 55, 56]. We hypothesize that by encapsulating the antigen into NPs transfollicular vaccination can be optimized benefiting from the unique properties of such formulations which should finally allow the application without any barrier disrupting measures. Most NPs cannot overcome the intact SC except for ultrafine particles (<10 nm, consequently suffering from an extremely low loading capacity) and ultra-flexible liposomes [8]. However, once the particles are located deep inside the hair follicles the SC is no longer an obstacle towards penetration. It has already been demonstrated (although only in mice) that 200 nm particles can be taken up by perifollicular APCs [55, 56]. In fact, transfollicular vaccination by using NPs to encapsulate the vaccine antigen imitates the natural route of delivery observed for pollen allergens in patients suffering from atopic dermatitis. Pollen grains are micron-sized particles which accumulate in the follicle openings and release the allergen after getting into contact with sweat [13, 57]. Also, upon depletion LCs quickly re-populate the epidermis within a period of 24 h, the primary source for LCs being the hair follicles [58, 59].

In this study we prepared polymeric NPs from PLGA and/or chitosan. Both polymers are widely used for drug delivery purposes, especially for preparing depot formulations with a sustained bioavailability of protein and peptide drugs [60-62]. Chitosan and its derivatives are widely used as non-viral vectors for nucleotide based drugs as these are easily complexed by the positively charged polymer [63, 64]. Both polymers are “generally regarded as safe” (GRAS), biocompatible and biodegradable. Chitosan furthermore has mucoadhesive properties, facilitates permeation, and has intrinsic adjuvant properties [65, 66].

Encapsulation into NPs can help to stabilize protein based antigen, modify the release, and improve uptake by APCs [67-69]. At the same time the NP preparation process itself threatens protein integrity and bioactivity due to exposure to organic solvents, interfacial tension, and high shear forces [70]. Liquid/liquid and solid/liquid interfaces occur during all steps of protein encapsulation, protein release and storage and may cause conformational changes and/or aggregation. Apart from losing therapeutic activity aggregates may cause unpredictable side effects and lead to immunogenicity or toxicity [62]. During storage these issues may be minimized by freeze-drying. However, upon reconstituting the lyophilisate and during drug release degradation of PLGA will create an acidic microenvironment which leads to acidic hydrolysis of protein antigens [71, 72]. For comparison, commercially available preparations of BSA usually contain 5–20% of covalent multimeric water soluble aggregates [73]. We could show that 74% and 64% of OVA released from PLGA and Chit-PLGA NPs respectively bind to a monoclonal antibody. This allows a conservative estimate of the activity of the released OVA as at least the epitope recognized by the primary antibody in the ELISA has to be intact. Our results show that despite the formation of aggregates during particle preparation the activity of OVA was largely retained.

In other words, by applying a usual dose of 8.5 μl NP suspension per cm^2 (50 mg NPs/ml, 54.3 ± 0.047 and 66.5 ± 0.044 μg OVA/mg NPs, 74% and 64% activity, for PLGA and Chit-PLGA NPs respectively) an effective dose of 17 $\mu\text{g}/\text{cm}^2$ (PLGA) or 18 $\mu\text{g}/\text{cm}^2$ (Chit-PLGA) of active OVA is administered considering the measured loading efficiency and activity of the encapsulated OVA.

Using OVA loaded PLGA and Chit-PLGA NPs for the stimulation of DCs demonstrated that these particles exhibit the capacity to activate murine DCs in vitro (Fig. 3). This is a critical step for the development of immune interventions based on NPs, since activation and maturation of DCs is recognized as a key event in the stimulation of adaptive immune responses [74]. Only marginal differences have been observed comparing the expression levels of activation markers by DCs stimulated with OVA alone and OVA loaded NPs (Fig. 3). Only the number of MHC class II molecules seems to be slightly increased on DCs stimulated with Chit-PLGA formulations compared to those stimulated with OVA alone. This may be due to the influence of regulatory T cells present in the OT splenocyte preparation which was used to for the co-culture with DCs [75].

Interestingly, following co-incubation of bone marrow derived DCs with OVA and LPS only CD40 expression was increased compared to DCs stimulated with OVA alone, whereas in case of all other investigated markers only marginal differences have been observed (Fig. 3). In addition, also the capacity of LPS stimulated DCs to promote T cell proliferation was marginal (Fig. 4). One possible explanation might be a contamination of the assay with IL-10 which was shown to inhibit the expression of TLR4 by DCs which subsequently prevents their activation by the TLR4 agonist LPS [76]. The source of IL-10 could be bone marrow-derived macrophages which were left in the DC population prepared from murine bone marrow and which were shown to produce IL-10 by stimulation with LPS [77].

Nevertheless, DCs stimulated with OVA loaded NPs were able to stimulate a strongly enhanced clonal expansion of OVA-specific CD4⁺ OT-II cells compared to those stimulated with OVA protein alone. However, only Chit-PLGA NPs were able to also promote an enhanced proliferation of OVA-specific CD8⁺ OT-I cells (Fig. 4). An obvious difference between PLGA and Chit-PLGA NPs which both have similar size/shape/OVA loading/Ova stability is their opposing surface charge (Table 1). This leads to conclude that the positive particle charge, which generally improves cellular adhesion, internalization, and endosomal escape, may be a reason for the superiority of the Chit-PLGA NPs to promote CD4⁺ and CD8⁺ proliferation [78]. A preferred stimulation of CD8⁺ T cells may further be expected upon transfollicular application [17, 55]. Antigen uptake by DCs and induction of DC maturation by Chit and PLGA NPs has been investigated by other groups as well but shows inconclusive results, unfortunately also concerning the absence [79] or presence of an effect of particle surface charge [80]. This indicates that in addition to the surface charge also the composition of the NPs may play a role [81, 82]. The composition (e.g. degree of substitution, chain length) of the biopolymer chitosan depends on the source of manufacturer as well as varies from batch to batch which makes it difficult to compare between studies.

The adoptive transfer model is a well-established tool to characterize T cell activation in vivo, since TCR-transgenic mice are tolerogenic to their TCR specific Ag (reviewed in [83]). In the present study adoptive transfer experiments were performed to analyze the transfollicular vaccination route in comparison with the i.m. route in an in vivo setting. Transfollicular immunization and subsequent analysis of the triggered immune responses in the draining lymph nodes and secondary lymphatic organ four days after immunization appeared as the most suitable technique to assess proliferation of the transferred cells. Indeed,

transfollicular administered OVA in Chit-PLGA NPs+ c-di-AMP as adjuvant elicited strong OT-II cell proliferation. The fact that more cell divisions were observed after transfollicular administration of Chit-PLGA-OVA NPs compared to those observed following i.m. administration of OVA alone provides evidence that combination of OVA with NPs activated the OVA-specific cells more efficiently which resulted in enhanced proliferation. Future immunization studies with disease relevant antigens need to show whether a potent immune response can be elicited by transfollicular vaccination without the use of barrier disrupting methods. It should be kept in mind that secondary to permeabilizing the skin, tape stripping or other barrier disrupting methods activate the innate immune response and thus work as an unspecific adjuvant. This includes the secretion of the proinflammatory cytokines TNF- α , IL-1 α , IL-1 β , and GM-CSF by keratinocytes. TNF- α and IL-1 β trigger the upregulation of the expression of $\alpha 6$ integrins, intercellular adhesion molecule 1 (ICAM.1), CD86 and MHC class II molecules which then promote the dissociation of LCs from keratinocytes, their subsequent maturation and migration, and improves the antigen-specific immune responses [22, 59, 84]. The use of immune-stimulating molecules or adjuvants in the formulation is an alternative to further optimize the elicited immune responses. This may become important to overcome the tolerogenic potential of the perifollicular LCs and dermal DCs. Mattheolabakis et al. showed that TCI with OVA encapsulated in poly(lactic acid) NPs was less immunogenic than soluble OVA, however by the addition of the adjuvant cholera toxin boosted the immunogenicity of the NP formulation over that of soluble antigen [85].

While the immunological response towards vaccines is foremost evaluated in different mouse models, rodent skin is not appropriate for testing transdermal

delivery and especially transfollicular penetration. Mouse SC has a different corneocyte architecture as well as lipid composition and arrangements, leading mouse skin to be more leaky and therefore an inappropriate surrogate for transdermal delivery in man [86]. With special regards to their hairs, mice have a higher follicular density than man while pig and man resemble each other more closely (mouse: $>5000 \text{ cm}^2$, pig: ca. 22 cm^2 , human ca. 25 cm^2 on the forearm) [87, 88]. Due to the limitations the mouse model represents, we also investigated the delivery of nano-encapsulated OVA to terminal follicles on the porcine ear. Pig skin is an appropriate substitute for human skin, pig ears are the gold standard model for investigating follicular penetration [89]. The ear cartilage prevents tensile fibres from irreversibly closing the follicle openings which drastically reduces follicular uptake in excised human skin [90].

For transfollicular vaccination it will be essential that the delivery efficiency into the hair follicle is high, i.e. that major parts of the dose are delivered to the perifollicular APCs. We observed the distribution of the NPs on the skin surface and within the follicular duct (Fig. 7). The real invasion depth into the follicle remains elusive from these images as only the upper part of the follicle is visible in the cross-section. It requires an extensive number of consecutive cuts to obtain reliable measurements due to the angular orientation of the hairs inside the skin [11, 91]. We observed 2–3 times higher drug amounts in the hair follicles if OVA was encapsulated in NPs compared to solution. The follicular uptake efficiency could further be increased by increasing the NP dose/area. No significant differences were observed in the follicular uptake of PLGA and Chit-PLGA NPs (Fig. 8a). Both NPs have a similar size and size distribution but opposite surface charges. These results are in line with the study by Patzelt et al. who suggested that the invasion depth into the follicles depends foremost on NP size and less on

particle surface properties [11]. In general, follicular uptake of microparticles is preferred [92]. For terminal hairs in pigs the optimum particle size for deep penetration was found to be 650 nm [11, 91]. The data presented in this work further underline the great potential of NPs to improve transfollicular vaccination as compared to administering the “naked” antigen across the intact SC.

2.6. Conclusion

In conclusion OVA protein could be incorporated with only moderate loss of biological activity into NPs made from PLGA and Chit-PLGA. Encapsulation increases the delivery of OVA to the follicle by a factor of 2 to 3 and can be further increased by increasing the dose of particles applied by area. No pretreatment such as plucking the hairs, waxing or superglue stripping was required to achieve a follicular uptake so that the SC barrier was left intact. Deep penetration into the follicles by the help of NPs delivers the antigen into the vicinity of the perifollicular APCs. OVA loaded PLGA and Chit-PLGA NPs were able to stimulate efficiently murine DCs and subsequently antigen-specific CD4⁺ and CD8⁺ T-cells. An adoptive transfer experiment demonstrated that the model antigen OVA can be delivered via the transfollicular route and that the immunization by this route is able to elicit the same proliferation of OVA specific CD4⁺ T cells as the i.m. injection of OVA. Thus, transfollicular delivery seems a promising opportunity vaccination strategy under critical hygienic conditions, for example in individuals with impaired immune system or the elderly.

3. Efficient nanoparticle-mediated needle-free transcutaneous vaccination via hair follicles requires adjuvantation

Parts of this Chapter were submitted to a peer reviewed journal:

Mittal, A.*; Schulze, K.*; Ebensen, T., Weissmann, S., Hansen, S., Lehr, C.M., Guzmán, C.A., **Efficient nanoparticle-mediated needle-free transcutaneous vaccination via hair follicles requires adjuvantation.**

**These authors contributed equally to this work*

The author of the thesis made the following contribution to the publication:

- Planned and designed all experiments.
- Performed experiments related to particle preparation and characterization, skin integrity studies, histology studies and *in vivo* formulation application.
- Analysed data from the above mentioned studies and interpreted all the experimental data.
- Wrote the manuscript.

3.1. Abstract

Trans-follicular (TF) vaccination has recently been studied as a unique route for non-invasive transcutaneous vaccination. The present study aims to extensively characterize the immune responses triggered by TF vaccination using ovalbumin loaded chitosan-PLGA nanoparticles without skin pre-treatment to preserve skin integrity. The impact of formulation composition i.e. antigenic solution or antigen-loaded nanoparticles with or without adjuvant (bis-(3',5')-cyclic dimeric adenosine monophosphate) on immune response quality following TF immunization was analysed and compared with immune responses obtained after tape-stripping the skin. The results presented in this study confirm the potency of nanoparticle based vaccine formulations to deliver antigen across the intact skin via the follicular route, but at the same time demonstrate the necessity to include adjuvants to generate efficient antigen-specific humoral and cellular immune responses.

3.2. Introduction

Vaccination is one of the most promising strategies to prevent infectious diseases. Its potential therapeutic use against communicable and non-communicable (e.g. cancer) diseases is also attracting considerable interest. However, to meet the current challenges of vaccine delivery an easy-to-use, needle-free and non-invasive delivery system is needed [22]. In this perspective, transcutaneous immunization (TCI) offers an attractive approach for the development of highly accepted and needle-free vaccines, which are not only safe but also effective due to the presence of abundant professional antigen presenting cells (APCs), such as dendritic cells (DCs) and Langerhans cells (LCs), in different layers of the skin.

However, the main challenge for TCI is to enhance the transport of antigens across the stratum corneum (SC) barrier. To this end, reversible barrier disruption

methods are often applied, such as chemical permeation enhancers, abrasion, electroporation, micro-needles, PowderJect and gene gun [93]. In contrast, TF vaccination aims to deliver antigens to the abundant peri-follicular APCs without compromising the SC barrier function [14]. Nanoparticles (NPs) have been shown to be ideal vehicles for TF delivery, since they preferentially accumulate and penetrate deeper into hair follicles than conventional formulations [19]. In our previous studies, we have shown that this holds also true in case of delivery of antigenic molecules encapsulated into NPs not only in terms of penetration of antigen in hair follicles but also quantitatively. We observed 2–3 times higher antigen amounts in the hair follicles of excised pig ear skin, when the antigen had been encapsulated in NPs as compared to antigen applied as solution [12].

However, TF vaccination is usually performed after pre-treating the skin area by plucking hairs, waxing or cyanoacrylate (superglue) stripping [15, 56, 94]. Pre-treatment not only permeabilizes the skin by removing the upper layers of the SC, but also activates the innate immune system [22]. Both factors probably improve the immunogenicity of a topically applied vaccine. On the downside also pathogens can possibly overcome the permeabilized SC, which makes these strategies suboptimal for various purposes, for example mass vaccination campaigns or vaccination of immune-compromised individuals, elderly, people with poor wound healing or young children.

Our previous studies investigated the potential of the TF route for the delivery of antigen using NPs without pre-treating the skin for the purpose of non-invasive TCI. As a proof of concept, we showed the successful delivery of antigen via the TF route using antigen-loaded NPs in an adoptive transfer mouse model by measuring the proliferation of antigen-specific CD4⁺ T cells [12]. Although the adoptive transfer model demonstrated the viability of this vaccination route, the

experimental setting does not resemble a true vaccination. The proliferation of ovalbumin (OVA)-specific CD4⁺ T cells provides a hint on the feasibility of this approach. However, while in a normal mouse antigen-specific T cells are supposed to be in a ratio of 1 in 100,000, this ratio is artificially elevated to at least 1 in 100 by the adoptive transfer method.

Here, we extended our in vivo mouse studies in a normal vaccination setting to confirm the viability of the TF route, as well as to obtain deeper insights in the immune responses generated using NPs without pre-treatment of the skin. To this end, vaccination experiments were performed in conventional mice in which i) skin integrity and maintenance of the skin barrier function was monitored throughout the experiment, ii) immune responses generated by applying different formulations on tape stripped and intact skin were compared, and iii) immune responses generated by applying antigen-loaded NPs on skin without compromising the SC barrier in the presence or absence of an adjuvant were extensively characterized. The obtained results should assist in the rational designing of particulate formulations for prophylactic or therapeutic vaccination via the TF route.

3.3. Materials and methods

3.3.1. Materials

EndoGrade® OVA was obtained from Hyglos GmbH (Bernried, Germany); poly(d,l-lactide-co-glycolide) (PLGA) (Resomer RG 50:50 H; inherent viscosity 0.31 dl/g) was kindly provided by Boehringer Ingelheim (Boehringer Ingelheim GmbH & Co., KG, Ingelheim, Germany). c-di-AMP (C₂₀H₂₄N₁₀O₁₂P₂) was synthesized by cyclization, according to established protocols [95]. Polyvinyl alcohol (PVA) Mowiol® 4–88 was obtained from Kuraray Specialties Europe

GmbH (Frankfurt, Germany); ultrapure chitosan chloride salt (Protasan® UP CL113) was purchased from FMC BioPolymer AS (Oslo, Norway); trehalose was obtained from Sigma–Aldrich (St. Louis, MO, USA); Vybrant DiD cell-labeling solution was obtained from Invitrogen (Molecular Probes Inc., Germany). Tesa film was obtained from TESA SE, Hamburg, Germany. All other solvents and chemicals used were of the highest grade commercially available. Deionized water (Milli Q Plus system, Millipore, Bedford, MA, USA) was used throughout the investigation.

3.3.2. Particle preparation

OVA-loaded Chit-PLGA NPs were prepared by modified double emulsion method [12]. Briefly, 50 mg of PLGA were dissolved in 2 ml of ethyl acetate at room temperature (RT). Then, 400 µl of (1.875% wt/V) OVA solution in PBS was added to form a primary water-in-oil (w/o) emulsion. After sonication at 6 W for 15 s, 4 ml of 2% (wt/V) PVA and Protasan® UP CL113 (0.2% wt/V) solution was added to the primary emulsion which was again sonicated at 8 W for 20 s. Water was added drop-wise to the resulting w/o/w emulsion under constant stirring to allow diffusion and evaporation of the organic solvent. The particles were collected by centrifugation at 10,000 × g for 15 min, washed once with distilled water to remove excess surfactant and free drug and freeze dried using trehalose (0.2% wt/V) as cryoprotectant.

3.3.3. Mice

Female C57BL/6 (H-2b) mice 6–8 weeks old were purchased from Harlan Germany. All animal experiments in this study have been performed with ethical agreement by the local government of Lower Saxony (Germany) with the No. 33.11.42502-04-017/08.

3.3.4. Measurement of transepidermal water loss (TEWL)

TEWL was assessed on the dorsal side of flank part of four C57BL/6 mice skin using an AquaFlux AF200 which operates with a closed measurement chamber (Biox Systems Ltd., London, UK). Measurements of TEWL were taken on day 0 (of untreated skin, serving as control reading, and again after performing depilation), on day 1 and day 2, according to the manufacturer's instructions.

3.3.5. Immunization protocols

Immunization was carried out on the flanks of the mice. In brief, 2 days before the immunization mice were anesthetized and hair was removed using clippers and a depilatory cream. Depilated areas were carefully inspected for cuts or skin irritation, in which case these mice were excluded from the experiment.

Female C57BL/6 mice (n = 5) were immunized on day 0, 14, 28 and 42 by applying 60 µl of different formulations containing 200 µg of LPS-free OVA topically to an area of 2.25 cm² of either intact or tape stripped skin (Table 1).

Tape stripping was performed as follows: 5 successive adhesive tapes (TesaFilm kristallklar, Tesa SE, Germany) were removed from the application area. For each stripping, a fresh piece of tape was lightly pressed onto the skin and subsequently pulled off. Directly after stripping, control or vaccine formulations were applied and allowed to dry completely. During this procedure the mice remained anesthetized to secure optimal uptake of the formulations.

Table 1.
Immunization groups

S.no.	Group	Skin condition	Dose (OVA ± c-di AMP / µl)
1	Blank NPs + c-di AMP	Intact skin	Equivalent to OVA-loaded NPs
2	OVA	Intact skin	200 µg/ 60 µl
3	OVA	Tape stripped skin	200 µg/ 60 µl
4	OVA + c-di AMP	Intact skin	200 µg + 20 µg / 60 µl
5	OVA-NPs	Intact skin	200 µg/ 60 µl
6	OVA-NPs	Tape stripped skin	200 µg/ 60 µl
7	OVA-NPs+ c-di AMP	Intact skin	200 µg + 20 µg / 60 µl

3.3.6. *In vivo* localization of nanoparticles using histology

Histo-pathologic studies were performed on skin sites 4 h after topical application of DiD loaded Chit-PLGA NPs. Skin sites were removed and immediately embedded in O.C.T™ (Tissue-Tek®, Sakura Finetek Germany GmbH, Germany) for cryopreservation. Frozen tissues were sequentially sectioned into 6 µm slices with a Microm HM 560 cryostat (MICROM International GmbH, Walldorf, Germany). Subsequently, sections were stained with DAPI (4',6-Diamidine-2-phenylindole dihydrochloride, Roche) and analyzed with a fluorescence microscope.

3.3.7. Sample collection

Blood samples from immunized mice were taken from the retro-orbital complex on day -1, 13, 27, 41 and 56. In order to gain sera from the blood samples were incubated for 1 h at 37 °C followed by 30 min incubation at 4 °C. Afterwards, samples were centrifuged for 10 min at 3000 × g and sera were stored at -20 °C prior to determination of OVA-specific antibodies.

On day 56, mice were sacrificed, lymph nodes and spleens were collected and single cells were obtained by homogenization of the organs mechanically using a

sieve pooled within groups and collectively analysed for the presence of antigen-specific cells, as previously described [95].

3.3.8. Detection of antigen-specific IgG and IgG subtypes

OVA-specific antibodies in sera of individual animals were determined by ELISA, using microtitre plates coated with 100 µl/ well of the antigen (2 µg/ml in 0.05 M carbonate buffer, pH 9.6), as previously described [95]. After overnight incubation at 4 °C, unspecific binding sites were blocked incubating the plates with 3% bovine serum albumin (BSA) in PBS for 1 h at 37 °C. Afterwards, plates were washed with 1% BSA/PBS/0.05% Tween 20 and serial 2-fold dilutions of sera in 3% BSA/PBS were added (100µl/well). After 1 h incubation at 37 °C plates were again washed six times with 1% BSA/PBS/0.05% Tween 20 before the secondary antibodies were added: biotinylated γ chain-specific goat anti-mouse IgG or for determination of different IgG subclasses, biotinylated goat anti-mouse IgG1 and IgG2c (Sigma, USA), respectively,. Subsequently, samples were incubated at 37 °C for 1 h. After six washing steps, 100 µl of peroxidase-conjugated streptavidine (BD Pharmingen, USA) was added to each well and the plates were incubated at RT for 1 h. Finally, after another six washes, reactions were developed using ABTS [2, 20-azino-bis(3- ethylbenzthiazoline-6-sulfonic acid)] in 0.1 M citrate-phosphate buffer (pH 4.35) containing 0.01% H₂O₂. Endpoint titres were expressed as absolute values of the last dilution that gave an optical density at 405 nm that was 2 times higher than the negative control values after a 15 and 30 min incubation.

3.3.9. Measurement of cellular proliferation

Spleen and Lymph node cells of vaccinated mice were obtained by mashing the organs and subsequently lysing erythrocytes for 1 min with ammonium chloride

(ACK) buffer. After several washes with complete medium (RPMI supplemented with 10% fetal calf serum, 100 U/ml penicillin and 100 µg/ml streptomycin), cell suspensions were adjusted to 5×10^6 cells/ml and seeded at 100 µl/well in flat-bottomed 96-well microtiter plates (Nunc, Roskilde, Denmark), which were incubated in quadruplicates for 4 days in the presence of different concentrations of EndoGrade® Ovalbumin (Hyglos, Germany), 5 µg/ml Concanavalin A or medium alone [95]. During the final 18 h of culture, 1 µCi of (³H)thymidine (Amersham International, Freiburg, Germany) was added to each well. Then, cells were harvested on paper filters (Filtermat A; Wallac, Freiburg, Germany) by using a cell harvester (Inotech, Wohlen, Switzerland) and the relative amount of proliferating cells was determined by measuring the beta radiation of (³H)thymidine incorporated into the DNA of the cells (Wallac 1450 β-scintillation counter Micro-Trilux). The obtained results are expressed as stimulation index (SI).

3.3.10. Evaluation of cytokine profiles

To quantify the cytokines and chemokines secreted by antigen-specific immune cells, lymphocytes and splenocytes were re-stimulated *in vitro* with different concentrations of EndoGrade® OVA (Hyglos, Germany). After 96 h of incubation supernatants were collected and stored at -80 °C until processing. Then, the amounts of IL-2, IL-4, IL-5, IL-6, IL-10, IL-13, IL-17, TNFα and IFNγ were determined using the Mouse Th1/Th2 FlowCytomix cytokine array according to the manufacturer's instructions (eBioscience, Bender MedSystems®, USA).

3.3.11. Multifunctional T cells

In order to evaluate the capacity of the different vaccine formulations to stimulate OVA-specific multifunctional T cells, splenocytes from immunized mice were taken and their capacity to produce different cytokines was evaluated by flow cytometry.

In brief, splenocytes (2×10^7 cells per well) of immunized mice were incubated (37 °C, 5 % CO₂) in 2 ml RPMI containing OVA protein [1µg/ml]. After 16-20 hours 5 µg/ml BrefeldinA and 6 µg/ml Monensin (Sigma-Chemie, Germany) were added and cells were incubated for additional 6 hours. Subsequently, cells were stained for dead cells (Fixable Dead Cell Stain, Invitrogen, USA) and surface markers (CD3 and CD8, BD, USA; CD4, eBioscience, Germany). Then, cells were fixed with 2 %PFA, permeabilized for 45-60 min with 0.5 % BSA and 0.5 % Saponin in PBS and stained for intracellular cytokines (IL-2 and IFN γ , BD, USA; TNF α , IL-17 and IL-4, eBioscience, Germany). Finally, cells were resuspended in PBS and light emission measured using BD LSRII. After spectral overlap compensation with the BD FACS Diva Software, the data were analyzed using FlowJo (Tree Star, USA)

3.3.12. Statistical analysis

The statistical significance of the differences between experimental groups was analysed using one way ANOVA. Differences were considered significant at $p < 0.05$ (*) and highly significant at $p < 0.001$ (***)

3.4. Results

3.4.1. Characterization of OVA-loaded Chit-PLGA NPs

The characteristics of the NPs are summarized in Table 2. The mean size of OVA-loaded Chit-PLGA NPs was ca. 180 nm and a monodisperse size distribution (PDI < 0.2). The particles carried a positive surface charge and had an entrapment efficiency (wt OVA encapsulated/wt OVA added initially) of $30.85\% \pm 1.08\%$ and % loading (wt OVA encapsulated/wt polymer) $6.65\% \pm 0.18\%$. Admixing the

adjuvant to the OVA-loaded NPs did not change the particle characteristics in terms of size and charge.

Table 2
Physico-chemical characterization of the optimized Chit-PLGA NPs

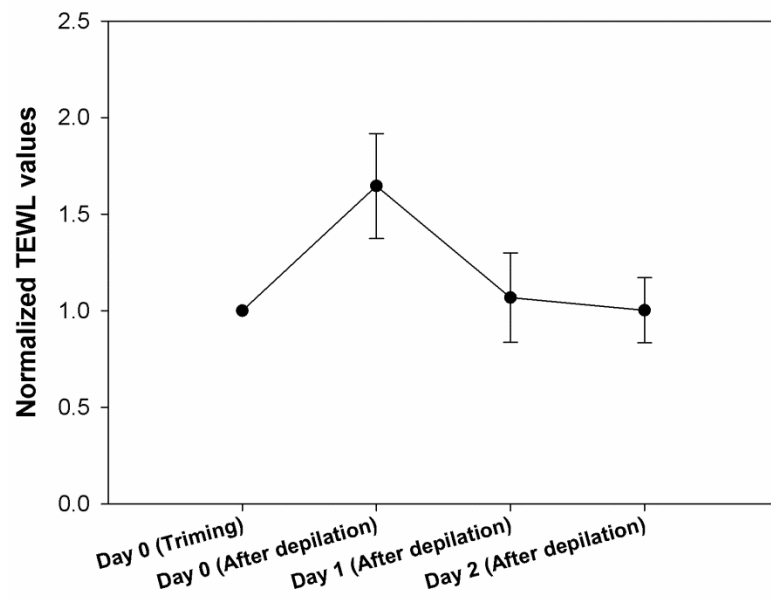
Nanoparticle	Size (nm)	PDI	Z.P. (mV)	% EE	% L
Blank Chit-PLGA	163.8 ± 3.36	0.093 ± 0.012	33.1 ± 1.02	-	-
OVA-loaded Chit-PLGA	168.2 ± 4.71	0.135 ± 0.023	27.7 ± 1.05	28.54 ± 1.08	6.65 ± 0.18

Values represent mean ± standard error of the mean (SEM) of n = 4 independently prepared batches, Z.P. zeta potential, %EE encapsulation efficiency (wt OVA encapsulated/wt OVA added initially), %L loading (wt OVA encapsulated/wt polymer)

3.4.2. TEWL Measurement

TEWL measures the skin barrier towards water and is a well-established non-invasive tool in dermatology to assess the integrity of the skin barrier in vivo and for testing skin irritancy [96]. Its high sensitivity allows detecting clinically invisible damage to the skin induced by various physical and chemical injuries. When skin is damaged, its barrier function is impaired resulting in higher trans-epidermal water loss. To evaluate if the skin barrier was intact on the day of immunization, i.e. 2 days after depilation, TEWL was measured before treatment, directly after depilation and on two subsequent days. Just 30 min after depilation, the TEWL measurement of the depilated area was twice that of normal untreated skin, thereby showing the barrier disruption via this procedure even in the absence of any visible cut or irritation of the skin. As shown in Fig. 1, the skin barrier recovered to its normal value within 2 days of the depilation procedure.

A



B

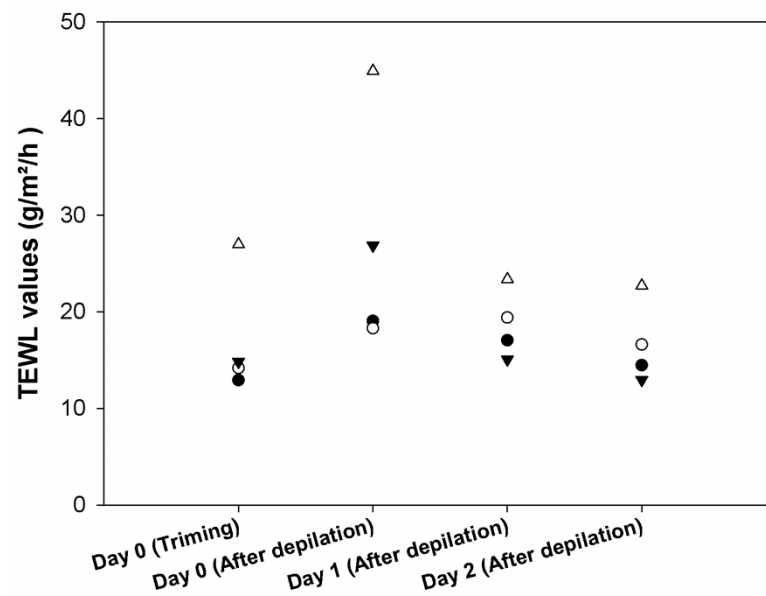


Figure 1. Determination of the integrity of the skin at different time points according to TEWL measurements. A) Normalized TEWL measurement at different time points. B) Individual TEWL measurement at different time points (n=4). Standard deviation (STD) is indicated by vertical lines

3.4.3. In vivo localization of nanoparticles using histology

Applying antigenic solutions onto intact skin usually does not result in the stimulation of immune responses as the SC forms a barrier towards penetration of foreign substances. However, NPs are preferentially taken up into hair follicles and

accumulate in the upper duct (infundibulum). Fig. 2 shows a representative image illustrating the distribution of DiD (fluorescently dye) loaded Chit-PLGA NPs on the skin surface and in the hair follicle after application to mice skin. It is apparent that the NPs accumulated in the follicle openings, cover the hair and invade into the follicular duct.

LCs, which are natural residents of the epidermal sheath surround the hair follicle [97], get in contact with the antigen-loaded NPs resulting in stimulation of immune responses [55]. In line with these observations, NPs incorporated in our vaccine formulations also reached the upper hair-follicular duct and thus, most likely can be taken up by local LCs (Fig. 2).

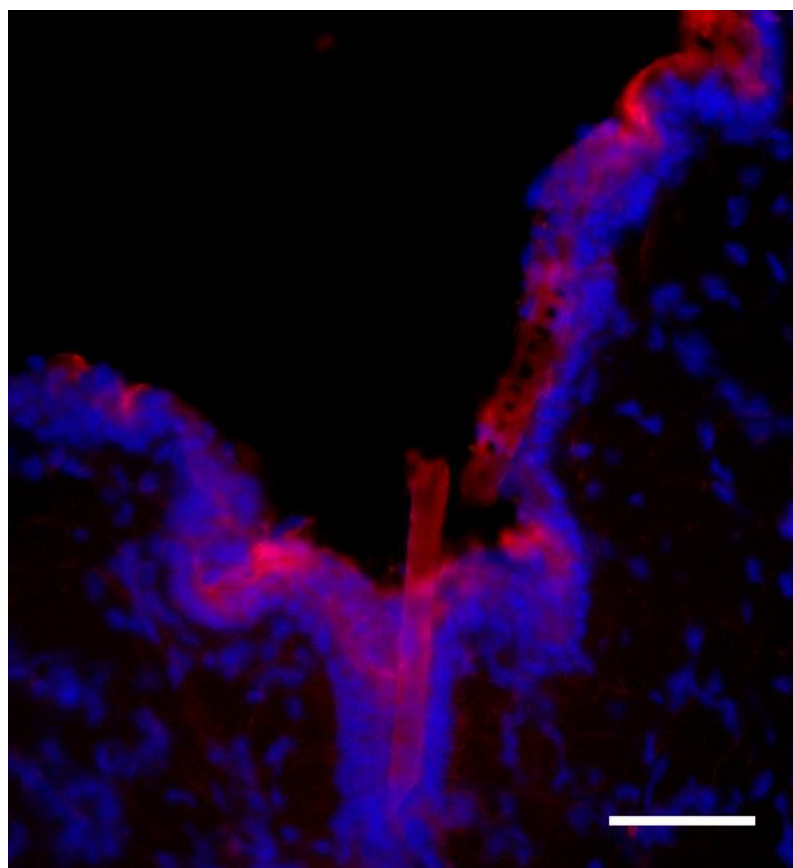


Figure 2. Localization of DiD loaded Chit-PLGA NPs 4 h after topical application on the skin of the flank of mice. The analysis of cryosections (6 μm) showed NPs (red) which are visible on the skin surface and penetrate inside the hair follicles. Scale bar: 50 μm . Cell nuclei were stained with DAPI (blue)

3.4.4. Humoral immune response (total IgG, IgG1 and IgG2c)

Serum anti-OVA IgG antibody levels obtained after TF vaccination with OVA and OVA-loaded NPs with or without co-administration of bis-(3',5')-cyclic dimeric adenosine monophosphate (c-di-AMP) as adjuvant on intact or tape stripped skin are shown in Fig. 3A. OVA alone applied onto the intact skin or tape stripped skin promotes very low IgG titres. However, stripping the skin results in significantly ($p < 0.5$) increased IgG titres for OVA-loaded NPs as compared to OVA-loaded NPs applied on intact skin. OVA + c-di-AMP applied on intact skin also promoted low IgG titres. Interestingly, OVA-loaded NPs + c-di-AMP applied on intact skin stimulated significantly increased ($p < 0.5$) OVA-specific IgG titres in comparison to all tested formulations, except OVA NPs applied onto the tape stripped skin. For mice immunized with OVA loaded NPs + c-di-AMP, the difference in OVA-specific IgG titres after priming and the 1st boost were less distinct. However, after the 2nd and 3rd boost significantly increased titres ($p < 0.001$) were obtained in comparison to all tested groups, except OVA NPs applied on tape stripped skin after 2nd boost ($p < 0.05$) (Fig. 3B).

The ratio of IgG1:IgG2c is an indication on whether the cellular immune response is Th1 or Th2 biased. All groups receiving OVA alone or OVA-loaded NPs applied either on intact skin or tape stripped skin mainly showed anti-OVA IgG1 but not IgG2c (i.e. Th2 biased responses). However, admixing the adjuvant with the NPs resulted in significantly increased levels of the IgG2c subclass (i.e. Th1) when applied on intact skin (Fig. 3C).

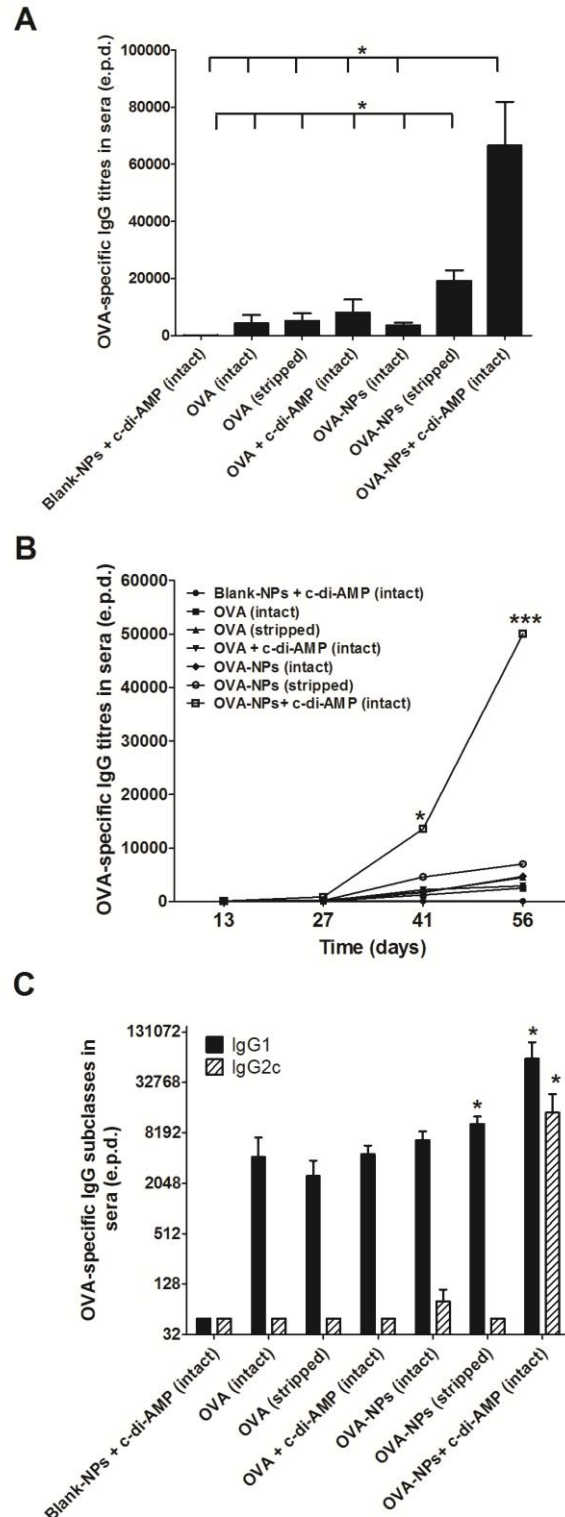


Figure 3. Systemic humoral immune responses stimulated in C57BL/6 mice ($n = 5$) after four vaccinations with different OVA-containing formulations via intact and tape stripped skin. (A) OVA-specific IgG titres in sera after immunization ($n = 5$). (B) Kinetic analysis of OVA-specific IgG titres in sera of immunized mice on day 10, 30, 50 and 68. (C) Analysis of OVA-specific IgG subclasses stimulated in mice following immunization with different OVA-containing vaccine formulations. Results are expressed as log₂ of the last dilution giving the double value (OD_{450 nm}) of the

background value (negative control). Standard error of mean (SEM) is indicated by vertical lines. Differences were considered significant at $p < 0.05$ (*) and $p < 0.001$ (***), respectively.

3.4.5. Measurement of cellular proliferation

The stimulation of cellular immune responses in mice after immunizing them with different OVA formulations on intact and tape stripped skin was then analysed. To this end, lymph node cells and splenocytes were re-stimulated in vitro with different concentrations of OVA for 96 h and cellular proliferation was determined by measuring the incorporation of [3H] thymidine.

The strongest proliferative capacity was observed for lymphocytes derived from mice immunized with OVA-loaded NPs co-administered with c-di-AMP, as demonstrated by the Stimulation Index (Fig. 4). In contrast, lymphocytes of mice immunized with OVA alone or OVA-loaded NPs showed no proliferative capacity when re-stimulated with OVA. A similar pattern was observed with splenocytes.

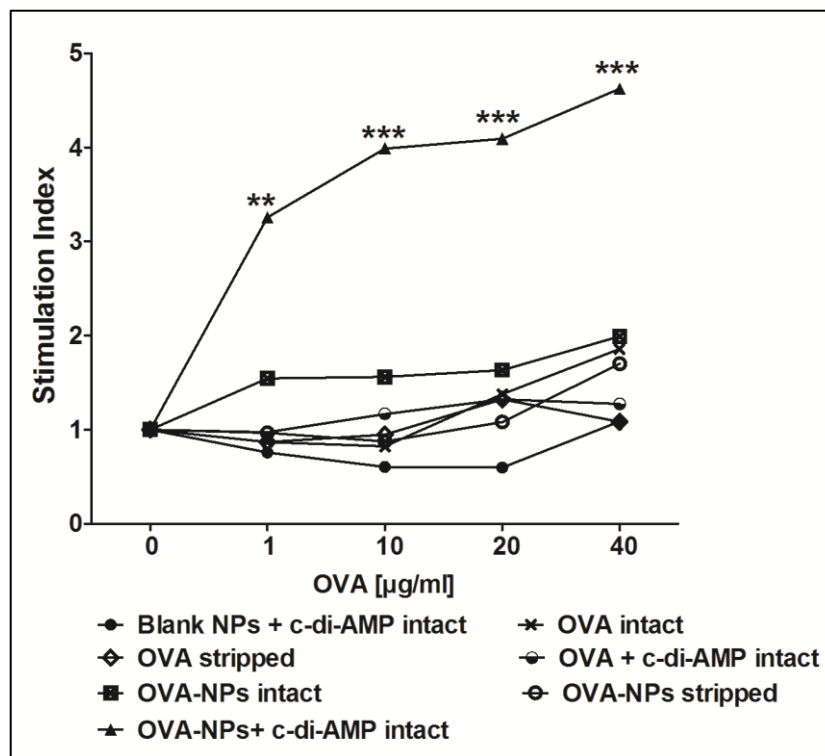


Figure 4. Evaluation of the cellular responses stimulated in mice after four vaccinations with different OVA-containing formulations via intact and tape stripped skin. Lymph node cells from

vaccinated animals were restimulated with different concentrations of OVA for 96 h. Cellular proliferation was then assessed by determination of the [3H] thymidine incorporated into the DNA of replicating cells. Results are averages of quadruplicates and they are expressed as stimulation index (SI). The differences were considered significant at $p < 0.01$ (**) and $p < 0.001$ (***), respectively.

The cytokine secretion profiles of lymphocytes from vaccinated mice was then analysed by cytometric bead arrays (Fig. 5). Again, the strongest cytokine production was observed in mice immunized with OVA-NPs co-administered with c-di-AMP (Fig. 5). No differences were observed in the cytokine profiles of groups receiving OVA protein via the TF route with highest levels of IL-13 followed by IL-5, and IL-10. Thus, indicating a Th2-dominated immune response. When OVA protein was co-administered with c-di-AMP production of IL-17, IL-4 and $\text{IFN}\gamma$ was also stimulated, indicating a mixed Th1/Th2/Th17 response (Fig. 5). Interestingly, the same was true when analysing the profiles stimulated by OVA-NPs applied either via intact or tape stripped skin. Strong $\text{IFN}\gamma$ production (Th1 response) was only achieved by tape stripping the mouse skin prior to immunization with OVA-NPs. The necessity of breaching the skin barrier in order to elicit efficient immune response can be overcome by co-administration of OVA-NPs with c-di-AMP (Fig. 5).

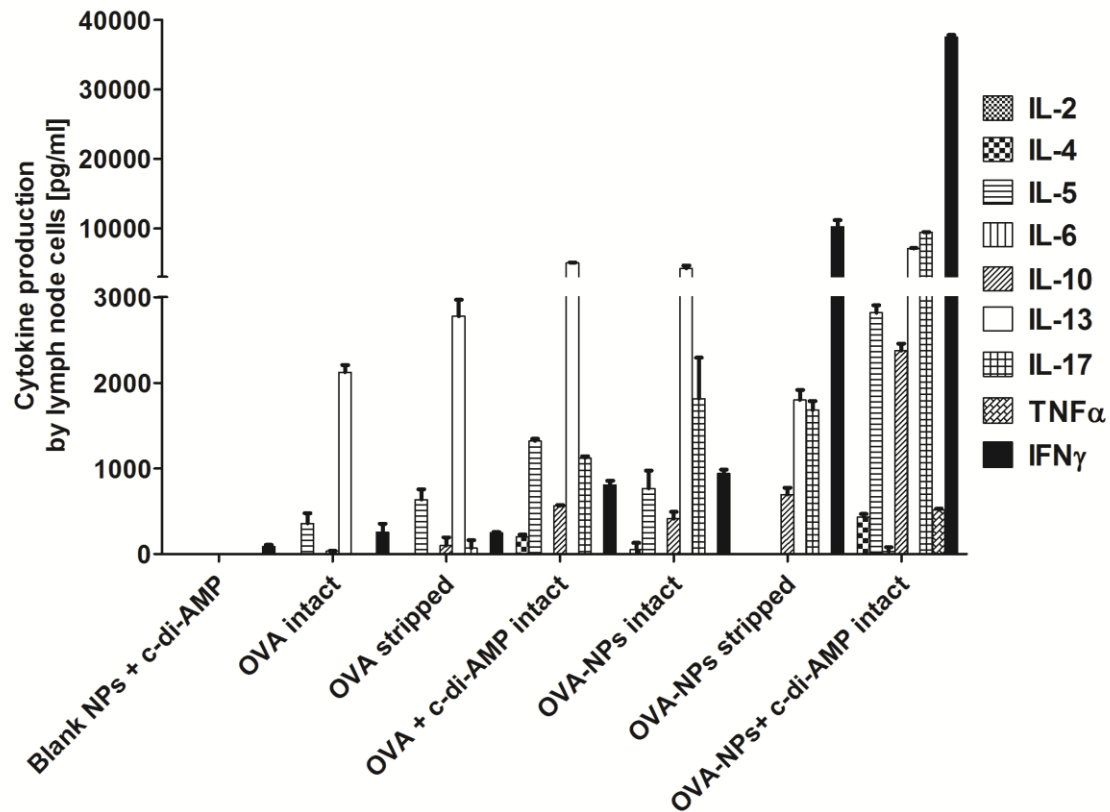


Figure 5. Analysis of cytokines secreted by immune cells of vaccinated mice. Cells were re-stimulated in triplicates with different concentrations of OVA for 96 h. Results are expressed in pg/ml. Standard error of mean (SEM) is indicated by vertical lines.

3.4.6. T cell quality following vaccination

Beside the magnitude of cellular responses, vaccine efficacy also depends on the quality of the stimulated antigen-specific T cell responses. There is consensus that multifunctional T cells are associated with enhanced protection against infection, likely based on a broader functional spectrum [98].

Thus, the quality of the T cell responses stimulated by different vaccination regimes was investigated. Immunization via the TF route stimulated only single (IFN γ +) and double positive (IFN γ +/TNF α +, IFN γ +/IL-2+) antigen-specific CD8+ T cells (Fig. 6A).

Interestingly, only in mice tape stripped prior to vaccination increased numbers were observed whereby IFN γ ⁺/TNF α ⁺ double positive CD8⁺ T cells constitute the predominant subset. However, as shown for the stimulated cytokine profiles, co-administration of c-di-AMP with OVA-NPs not only elicits strong Th1/Th2 response, but also resulted in the strongest stimulation of antigen-specific CD8⁺ responses (Fig. 6A). When analysing the quality of the stimulated CD4⁺ responses, it is even more obvious that only incorporation of c-di-AMP results in efficient cellular responses (Fig. 6B). Furthermore, co-administration of OVA-NPs with c-di-AMP efficiently stimulated multifunctional double (IFN γ ⁺/TNF α ⁺, IFN γ ⁺/IL-2⁺) and triple positive (IFN γ ⁺/TNF α ⁺/IL-2⁺) CD4⁺ cells (Fig. 6B). In accordance with the results obtained analysing the IgG subclasses as well as the cytokine profiles and proliferative capacity of antigen-specific cells, vaccination via the TF route seems to favour the stimulation of multifunctional CD4⁺ rather than CD8⁺ T cell responses.

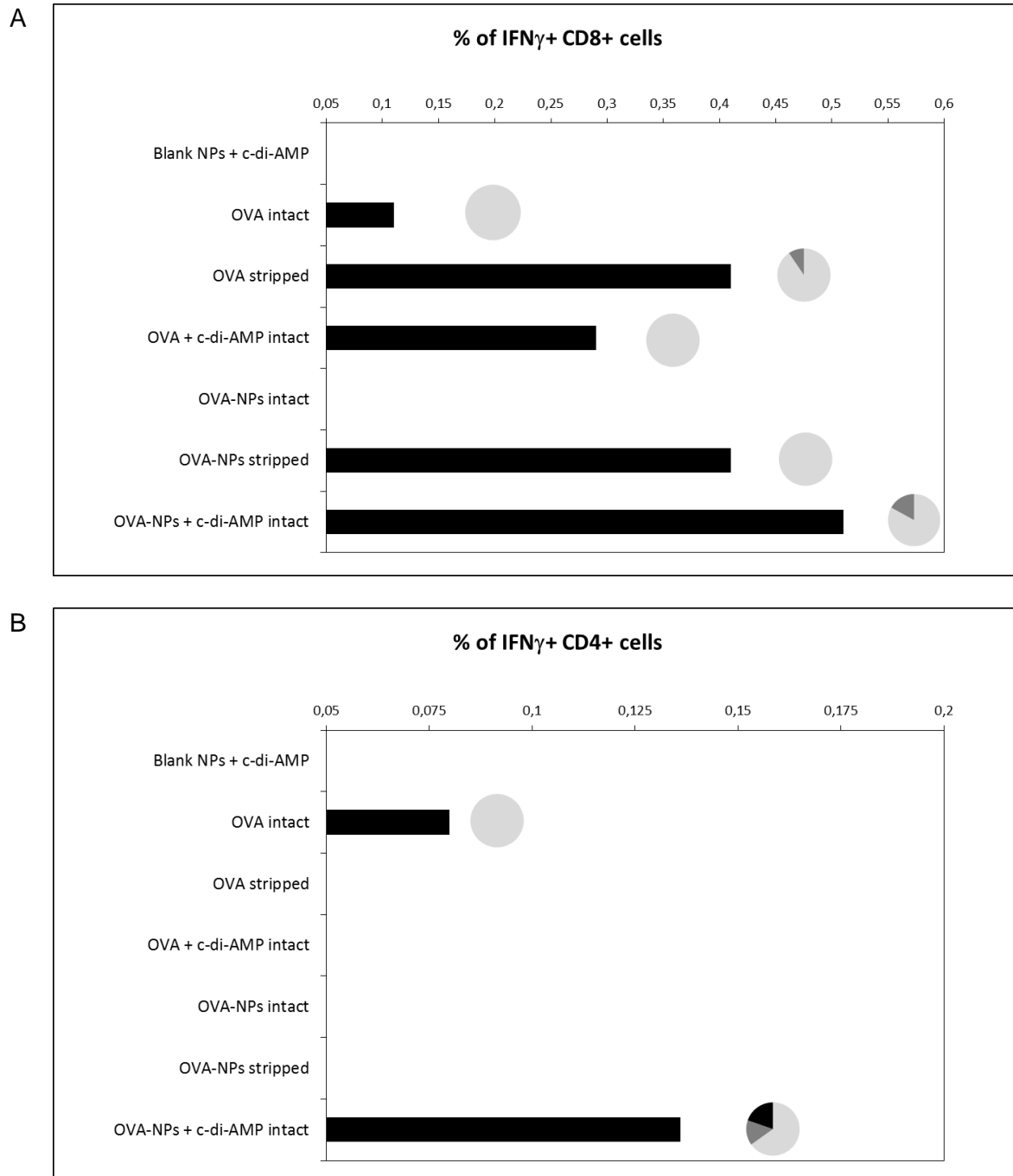


Figure 6. T cell responses stimulated following vaccination via TF route. Cells were collected at day 14 after the last immunization and subsequently incubated for 24 h in the presence and absence of OVA. Results are expressed as difference between re- and non-restimulated % of all CD8+ and CD4+ cells, respectively, expressing IFN γ . Living cells were gated for CD3+ CD8+ and CD3+ CD4+ double positive cells, respectively. These subpopulations were further divided into monofunctional expressing only IFN γ , bifunctional expressing two cytokines (IFN γ / IL-2 or IFN γ / TNF α) and trifunctional expressing IFN γ , IL-2 and TNF α . Pie charts represent the proportion of tri- (black), bi- (dark gray) and mono-functional (light gray) cells.

3.5. Discussion

It is quite evident in literature that skin is an attractive organ for immunization that can be easily manipulated for vaccination purposes. Recently, the topical delivery of antigens formulated into particulate delivery systems has evoked considerable interest. NPs have been shown to be promising carriers for TCI and for modulating the immune response depending on the site of delivery [55]. In particular, TF vaccination using NPs holds potential for non-invasive and needle-free vaccine delivery without disrupting the barrier properties of the skin. It has been shown that NPs of a size of approx. 200 nm were taken up by the LCs lying around the hair follicles [56].

TCI with antigen (gp100 protein) loaded chitosan NPs was shown to improve the survival of tumour bearing mice in comparison to antigen solution [99]. However, it was unclear from these studies, if the particles were applied on intact or tape stripped skin [99]. Stripping results not only in mild to moderate skin disruption, but also activates the innate immune system [12, 22, 100]. Mattheolabakis et al. showed the efficacy of TCI following a prime-boost protocol using OVA-loaded poly-lactic acid NPs [85]. Mice received a priming and a 1st boost immunization via the topical route, whereas the 2nd boost was administered via the subcutaneous route [85]. However, whether the outcome after immunization using NPs reflects superiority compared to antigen solution, the true potential of TF immunization in terms of overall magnitude of antibody response and its subclasses, kinetics, cytokines release profiles, cellular response, and many other factors still remained ambiguous. In the present study an in depth characterisation of the immune responses stimulated after TF immunization using NPs as a needle-free vaccination strategy without any barrier disrupting measure is

described. This is crucial, since even modest barrier disruption is immunostimulatory and may confound the effects resulting from antigen or antigen loaded delivery systems.

For this purpose it is essential to demonstrate skin integrity and the maintenance of skin barrier function throughout the experiment. A critical step is the hair trimming and depilation procedure which is necessary in order to provide an even field onto which the formulation can be applied homogeneously. We tested the integrity of skin using TEWL measurement before and after depilation and for the following 2 days. Interestingly, we found that TEWL measurements doubled those of the normal untreated skin after 30 min of depilation. This shows the barrier disruption caused by this procedure, even without any visible cuts or redness which could indicate skin damage or irritation. This demonstrates the sensitivity of TEWL measurement for testing the barrier function of the skin towards water, which makes it suitable to detect also transient damage to the skin barrier. The skin seemed to recover fully within 2 days of depilation, as TEWL values returned to the baseline levels observed before depilation. Therefore, this study revealed that careful analysis of the skin barrier integrity is mandatory before applying the formulation on depilated skin. This is particularly important considering that, according to the literature, formulations are often applied immediately or within 30 min of depilation [85, 99].

Humoral immune responses observed after applying different vaccine formulations on intact and tape stripped skin were compared. OVA-loaded NPs applied on tape stripped skin promoted significantly higher anti-OVA IgG titres in comparison to OVA-loaded NPs applied on intact skin. This result is in agreement with the studies done by Li et al. showing an increase of IgG response after stripping the skin which might be due to mild barrier disruption or immunostimulation caused by

tape stripping [101]. However, co-administering an adjuvant (c-di-AMP) along with OVA-loaded NPs applied on intact skin promoted the highest IgG titres among all tested formulations. In contrast, only low IgG titres were observed for OVA + c-di-AMP when applied on intact skin, thereby indicating that the capacity to induce strong humoral immune responses depends on the synergistic effect of combining NPs and adjuvant in the formulation. This potentiated immune response may be explained by: i) enhanced delivery of antigen to hair follicles when encapsulated into NPs, as shown in our previous work,⁵ and ii) activation of the LCs lying near to hair follicles by the adjuvant present in the formulation which acts as a danger signal, thereby promoting LCs activation, motility and dendritic probing, and directed migration and entry into lymphatic vessels [102].

In line with previous reports showing that OVA alone applied onto intact or tape stripped skin generates predominantly the production of IgG1 [103] similar results were obtained in case of OVA-loaded NPs, which also stimulated mainly the production of IgG1. In order to evaluate the impact of adjuvant not only to strengthen the OVA-specific immune responses but also to modify them in terms of cellular and humoral direction, we co-administered c-di-AMP along with OVA solution and OVA loaded NPs onto intact skin. This adjuvant is known to stimulate balanced Th1/Th2 responses when applied via the mucosal or systemic route resulting in the generation of cytotoxic responses as well [95]. Interestingly, when OVA protein was applied together with c-di-AMP on the intact skin, no modification of the T helper cell response was stimulated as indicated by the observed IgG1 dominated response (Th2). In contrast, when mice received OVA-NPs + c-di-AMP a balanced IgG1/IgG2c response (Th1/Th2) was stimulated, indicating a synergistic effect by combining NPs and adjuvant in the formulation via this route. This synergistic can be explained by the improved efficiency in delivery of antigen

and adjuvant to the perifollicular antigen presenting cells in comparison to solutions. This is in line with reports by Mahe et al. showing improved uptake and translocation of nano-encapsulated antigen via the hair follicles [56]. Similarly Kahlon et al. observed that modification of the immune response stimulated in mice following TCI with OVA using cholera toxin as adjuvant was achieved only when animals were tape stripped prior to vaccination, i.e. only after damaging the skin barrier and thus enabling transcutaneous OVA/adjuvant delivery [104].

These results were confirmed by the analysis of the cytokines produced by lymphocytes of immunized mice. Only cells derived from mice immunized with OVA-NPs + c-di-AMP secreted significant amounts of both the Th1 cytokine IFN γ and Th2 cytokines IL-4, IL-5 and IL-13, thereby reflecting a mixed Th1/Th2 response. In contrast, cells derived from all other groups secreted mainly IL-13 followed by IL-5 and IL-17, and showed only marginal levels of IFN γ . The observed cytokine profiles also correlate with findings showing that Th2 biased immune responses recruit eosinophils from bone marrow and blood to the sites of inflammation [105]. Eosinophils were shown to act as antigen-presenting cells which interact with CD4 $^{+}$ T cells resulting in the production of IL-4, IL-5 and IL-13 by the latter [106-108]. Furthermore, Roth et al. have shown that the shape of T helper responses stimulated in skin diseases do not depend on the eosinophil-specific IL-5, but on the levels of IL-13 and IFN γ , respectively [109]. This would further explain the mixed Th1/Th2 response stimulated by TF immunization of mice with OVA-NPs plus c-di-AMP observed here. Taken together, to stimulate not only strong antibody and Th2 responses following TF immunization, but also efficient Th1 and CD8 $^{+}$ responses vaccination regimes it is required to incorporate adjuvants which further promote cellular responses.

TF immunization of mice with OVA-NPs + c-di-AMP formulation stimulated not only antigen-specific antibody responses, but also CD8⁺ T cell responses. In line with previous reports, CD8⁺ responses were stronger in mice tape stripped prior to vaccination with OVA or OVA-NPs [55]. However, co-administration of c-di-AMP surpassed skin disruption and stimulated the strongest antigen-specific CD8⁺ responses. Furthermore, this formulation also stimulated multifunctional CD8⁺ T cells, which were shown to be more efficient in terms of killing as compared to single producers [110, 111]. More specifically, TF immunization via intact skin with OVA-NPs + c-di-AMP stimulated CD8⁺ T cells that secrete both IFN γ and IL-2, followed by equal levels of those secreting IFN γ and TNF α . While IL-2 is needed in order to expand T cell responses which in turn could enhance CD8⁺ T cell memory, IFN γ and TNF α co-producers have enhanced cytolytic activity [112, 113]. In addition, OVA-NPs co-administered with c-di-AMP via the TF route also stimulated antigen-specific multifunctional CD4⁺ T cells. These cells were shown to be essential, rather than CD8⁺ T cells, in order to protect against Chlamydia infection and tuberculosis [114, 115].

Taken together, the results presented in this study provide the proof-of concept for the potential of NP-based TF vaccination as an approach to deliver antigens across intact skin. Incorporation of an adjuvant in the formulation seems to be essential in order to generate both efficient antigen-specific humoral and cellular responses without breaching the skin barrier as well as to modulate such responses according to the specific clinical needs.

4. Inverse micellar sugar glass nanoparticles as delivery system: adjuvant co-encapsulation, and administration route have a major impact on immunization outcome

Parts of this Chapter will be submitted as a manuscript to a peer reviewed journal:

Mittal, A., Schulze, K., Ebensen, T., Weissmann, S., Hansen, S., Guzmán, C.A., Lehr, C.M. **Inverse micellar sugar glass nanoparticles: Effect of co-encapsulation of adjuvant and administration route on immune response.**

The author of the thesis made the following contribution to the manuscript:

- Planned and designed all experiments.
- Performed experiments related to particle preparation and optimization, characterization of particles, qualitative and quantitative studies related to follicular uptake of particles and *in vivo* formulation application.
- Analysed data from the above mentioned studies and interpreted all experimental data.
- Wrote the manuscript.

4.1. Abstract

The objective of this study was to evaluate the potential of surfactant based inverse micellar sugar glass nanoparticles (IMSG NPs) as a delivery system for vaccination using ovalbumin (OVA) as model antigen. It was also evaluated the effect of co-encapsulating the adjuvant bis-(3',5')-cyclic dimeric adenosine monophosphate (c-di-AMP) on the strength and type of immune response elicited after IMSG NPs administration by intradermal, intranasal or transfollicular route. Thus, encapsulation of antigen in IMSG NPs resulted in enhanced antigen stability and encapsulation efficacy. OVA + c-di-AMP co-encapsulation in IMSG NPs resulted in the stimulation of efficient humoral and cellular responses when administered via intradermal and transfollicular route. However, only marginal immune responses were observed following intranasal administration. The results obtained in this study showed the potential of surfactant based IMSG NPs for the establishment of intradermal and transfollicular vaccination strategies.

4.2. Introduction

Vaccination is considered as the most effective medical intervention introduced in human history. New, safe, efficient, minimal invasive and cheap vaccination strategies are desperately needed to meet the current challenges in vaccine delivery [22]. Among the main vaccination strategies (i.e. live-attenuated, inactivated and subunit vaccines), subunit vaccines are considered the safest. However, subunit vaccines generally suffer from poor immunogenicity [93]. Novel delivery systems and/or alternative routes for administration may be key to address this need.

A common strategy to improve immunogenicity of subunit vaccine is encapsulating antigen into a particulate carrier. Such carriers not only enhance immunogenicity due to mimicking the size of microorganisms, but also help by stabilizing protein antigens, ensuring their consistent release, enhancing antigen uptake by antigen presenting cells (APCs) and allowing co-encapsulation of adjuvants. This results in increased antigen-specific immune responses with reduced amounts of antigen needed at the same time [116].

Polymeric nanoparticles (NPs) such as polylactic-co-glycolic acid (PLGA), polylactic acid (PLA) and Chitosan-PLGA (Chit-PLGA) have been extensively studied as antigen delivery systems [117]. To this end, often emulsion based methods are applied to encapsulate antigens into polymeric NPs. However, these particles still showed some obstacles in terms of antigen loading capacity and incomplete release of encapsulated antigen. Furthermore, during the NP preparation process, protein-based payloads may be exposed to several process- and storage-related stresses (such as liquid/liquid and solid/liquid interfaces), which result in significant degradation, loss of bioactivity and safety concerns [118, 119]. Recently, Giri et al. showed a generic approach for efficient incorporation and stabilization of proteins for tissue engineering and drug delivery using principles from enzyme chemistry and bio-pharmaceutics [120]. In this approach, proteins were protected from nonpolar solvent exposure by dispersing them in organic solution of surfactants, subsequently freeze drying them and finally reintroducing them into polymer solutions and organic solvents for tissue engineering.

In this study, we extended and modified this approach and prepared antigen-loaded NPs by efficient incorporation and stabilization of antigen using an inverse micellar technique and pharmaceutical excipients (surfactants, sugars and oil,

generally regarded as safe (GRAS) listed). These inverse micellar sugar glass (IMSG) NPs were finally dispersed in an oily dispersion and subsequently characterized physico-chemically in terms of size, surface charge and morphology. Prior to their in vivo evaluation as vaccine delivery system, the integrity and biological activity of the encapsulated antigen was monitored. To assess if incorporation of an adjuvant will further enhance the efficacy of the vaccine formulation, bis-(3',5')-cyclic dimeric adenosine monophosphate (c-di-AMP) was co-encapsulated.

Administration of antigenic solutions and particulate carriers by intradermal (ID) and intranasal (IN) route has been widely studied [116, 121]. However, recent attention focuses on non-invasive transcutaneous vaccination strategies. Thus, we previously explored the transfollicular (TF) route as potential immunization route using ovalbumin (OVA) loaded Chit-PLGA NPs co-admixed with c-di-AMP as adjuvant. The obtained results showed the stimulation of efficient immune responses without disrupting the skin barrier [12]. Therefore, in the work presented here antigen-loaded IMSG NPs with and without co-encapsulated adjuvant were evaluated as potential vaccine delivery systems. To this end, mice were immunized via intranasal, intradermal and transfollicular route, as the route of administration also plays a vital role in generating efficient immune responses.

4.3. Materials and methods

4.3.1. Materials

Phospholipon 85G was kindly provided by Lipoid (Lipoid GmbH, Germany), Span 80 and trehalose was obtained from Sigma-Aldrich (St. Louis, MO, USA); EndoGrade® Ovalbumin (OVA) was obtained from Hyglos GmbH (Bernried,

Germany); poly(D,L-lactide-co-glycolide) (PLGA) (Resomer RG 50:50 H; inherent viscosity 0.31 dL/g) was kindly provided by Boehringer Ingelheim (Boehringer Ingelheim GmbH & Co. KG, Ingelheim, Germany); bis-(3',5')-cyclic dimeric adenosine monophosphate c-di-AMP (C₂₀H₂₄N₁₀O₁₂P₂) was synthesized by cyclization, according to established protocols [95]. Polyvinyl alcohol (PVA) Mowiol® 4-88 was obtained from Kuraray Specialties Europe GmbH (Frankfurt, Germany); ultrapure chitosan chloride salt (Protasan® UP CL113) was purchased from FMC BioPolymer AS (Oslo, Norway); fluorescein isothiocyanate conjugated ovalbumin (FITC-OVA) was obtained from Invitrogen (Molecular Probes Inc., Germany). Superglue was kindly provided by Uhu GmbH & Co.KG, (Bühl, Germany). Tesa film was obtained from TESA SE, Hamburg, Germany. The OVA specific ELISA kit was purchased from USCN life science Inc. (Hölzel Diagnostik, Germany). All other solvents and chemicals used were of the highest grade commercially available. Deionized water (Milli Q Plus system, Millipore, Bedford, MA, USA) was used throughout the investigation.

4.3.2. Pig ear skin

Ears from freshly slaughtered pigs were removed before scalding. The ears were washed with water, blotted dry and the hairs were shortened with scissors. The ears were stored at 4-8 °C for a maximum period of 3 days.

4.3.3. Mice

C57BL/6 (H-2b) female mice (6-8 weeks old) were purchased from Harlan (Germany). OVA-TCR transgenic mice C57BL/6-Tg(TcraTcrb)1100Mjb/J (OT-I) and C57BL/6-Tg(TcraTcrb)425Cbn (OT-II) were bred at the animal facility of the Helmholtz Centre for Infection Research (Germany) under specific pathogen-free conditions.

4.3.4. Nanoparticles preparation

IMSG NPs

IMSG NPs were prepared from inverse micelles of lecithin in chloroform by freeze-drying. To this end, 440 mg of lecithin and 60 mg span 80 were dissolved in 1.4 ml of chloroform in a glass vial using continuous stirring. The aqueous phase of 0.15 ml containing OVA (6 mg) and trehalose (6 mg) was added and the mixture was sonicated for 20 s at 8 W. The inverse micelle suspension which formed was flash-frozen in liquid N₂ and subsequently freeze dried for 48 h to remove the organic solvent and water. The resulting IMSG particles were dispersed in medium chain triglycerides (MCT). Antigen/adjuvant (OVA + c-di-AMP) co-encapsulated IMSG NPs were prepared by adding 0.9 mg of c-di-AMP to the aqueous phase for TF route. For ID route, co-encapsulated NPs were prepared in similar manner as described above with different amount of OVA (2 mg) and c-di-AMP (1.5 mg) added to aqueous phase. FITC labelled IMSG NPs were prepared by replacing OVA with FITC-OVA.

Chitosan-PLGA NPs

OVA-loaded Chit-PLGA NPs were prepared by a modified double emulsion method [12]. Briefly, 50 mg of PLGA were dissolved in 2 ml of ethyl acetate at room temperature. Then 400 µl of (1.875% wt/V) OVA solution in PBS was added to form primary water-in-oil (w/o) emulsion. After sonicating at 6 W for 15 s, 4 ml of 2% (wt/V) PVA and Protasan® UP CL113 (0.2% wt/V) solution was added to the primary emulsion which was again sonicated at 8 W for 20 s. Water was added drop-wise to the resulting w/o/w emulsion under constant stirring to allow diffusion and evaporation of the organic solvent. The particles were collected by centrifugation at 10,000 × g for 15 min, washed once with distilled water to remove

excess surfactant and free drug and freeze dried using trehalose (0.2% wt/V) as cryoprotectant. FITC labelled Chit-PLGA NPs were prepared by replacing OVA with OVA-FITC.

4.3.5. Nanoparticle characterization

Size and ζ -potential of the NPs were analyzed by photon correlation spectroscopy (PCS) using a Nano-ZS (Malvern Instruments, Malvern, UK). The morphology of the NPs was characterized using transmission electron microscopy (TEM) (Tecnai 12 G2, FEI Company Hillsboro, Oregon, USA). For TEM, prior to scanning diluted suspensions of freeze dried NPs in cyclohexane were taken and mounted on a copper grid and subsequently dried at room temperature. Then, samples were negatively stained with a 1% solution of phosphor-tungstic acid and further examined.

4.3.6. Integrity and Activity of OVA

The integrity of OVA was determined by SDS PAGE analysis. For IMMSG NPs, briefly, OVA was extracted from freeze-fried NPs and oily dispersion with phosphate buffer (pH 7) under continuous stirring at 100 rpm. The dispersion was then centrifuged for 5 min at 5000 g to sediment the surfactant. A dose of 1 μ g of OVA was loaded onto a 12% (wt/V) polyacrylamide gel under reducing conditions [12]. Detection of protein was performed by staining with colloidal Coomassie blue (Fermentas, St. Leonrot, Germany).

To determine the activity of OVA encapsulated in NPs, OVA was extracted as described above. The active OVA fraction was quantified using an ELISA assay which was performed according to the instructions provided by the manufacturer. The ELISA was calibrated using standards provided by the manufacturer in the

range of 0.156 – 10 ng/ml (lower limit of detection, LLOD = 0.053 ng/ml). Supernatant obtained from blank NPs were used as negative control.

4.3.7. Evaluation and quantification of follicular uptake on excised pig ears:

Influence of encapsulating OVA into particles

Incubation sites of 1.767 cm² were marked on the outer auricle of the pig ears with a permanent marker. A dose of 20 µl of either an aqueous solution of FITC-OVA, an aqueous dispersion of FITC-OVA in Chit-PLGA NPs and FITC-OVA in IMMSG NPs (11.5 µg OVA/cm²) were applied and massaged manually with a gloved forefinger for 3 min. The ears were incubated for 1 h at 32°C under non-occlusive conditions.

After the incubation the skin surface was cleaned from remaining formulation by removing 10 tape strips (Tesa kristallklar, Tesa SE, Germany). A roller was used to enhance the contact between tape strip and skin surface [53]. Subsequently, 2 cyanoacrylate biopsies were performed to collect the amount of OVA penetrated into the hair follicles. The cyanoacrylate biopsies were extracted in acetonitrile: 0.1 N NaOH (50:50) for 3 h on a horizontal shaker and the fluorescence intensity of all samples was measured using a Tecan platereader (Excitation 490 nm, Emission 525 nm). The amount of FITC-OVA extracted from the cyanoacrylate biopsies was calculated with the help of standards prepared from FITC-OVA / FITC-OVA in Chit-PLGA NPs/ FITC-OVA in IMMSG NPs dissolved in acetonitrile: 0.1 N NaOH (50:50) in the range of 0.1-10 µg/ml. The results for the NPs were expressed relatively to FITC-OVA solution.

Blank samples were taken from an incubation site of the same pig ear, where double distilled water/ medium chain triglycerides was applied instead of NPs. The blank values were subtracted from the fluorescence intensity of the samples.

4.3.8. Adoptive transfer model of TCR transgenic CD4 T cells to characterize OVA specific proliferation

For the adoptive transfer experiment naïve CD4⁺ T-cells (CD4⁺ CD62L^{hi} CD44^{lo} CD25⁻) were isolated from pooled lymph nodes and spleens of OTII x Thy1.1 transgenic mice using an ARIA II sorter (purity ≥98%). These cells not only express the OVA-peptide AA323-339 specific T cell receptor (TCR) but also the congenic marker Thy1.1 (CD90.1). The congenic marker CD90.1, which slightly differs in structure but not in function from the wild type receptor Thy1.2 (CD90.2), allows the identification of the transferred cells ex vivo using non-cross-reactive monoclonal antibodies. After the sorting cells were labeled with CFSE, in order to track their proliferative capacity, and finally injected intravenously (1.5 x 10⁶ per mouse) one day prior to immunization into C57BL/6 mice.

Immunization was carried out on the flank part of the mice by either subcutaneous (s.c.) or transfollicular (TF) route. Flanks were shaved (under anesthesia) 2 d before immunization. Shaved areas were carefully inspected for cuts or skin irritation in which case these mice were excluded from the experiment. Animals were assorted to the following treatment groups (3 animals per group): (1) negative control, received blank IMMSG NPs via TF route; (2) received 25 µg LPS-free OVA in Chit-PLGA NPs + 5 µg c-di-AMP as adjuvant via TF application; (3) received 25 µg LPS-free OVA in IMMSG NPs via TF application, (4) received 25 µg LPS-free OVA + 5 µg c-di AMP / 20 µl loaded in IMMSG NPs via TF route; (5) positive control, received 25 µg LPS-free OVA + 5 µg c-di AMP / 20 µl loaded in IMMSG NPs via s.c. route. After another 4 days animals were sacrificed and spleens and draining lymph nodes (iliac and axillary LNs pooled) were isolated separately for each animal. Cells were stained for live/dead, CD3⁺, CD4⁺ and Thy1.1⁺ and analyzed using a LSRII flow cytometer. The proliferative capacity of (CD3⁺ CD4⁺

Thy1.1+ was analyzed using the BD FACSDiva™ Software (BD Biosciences, USA).

4.3.9. Immunization protocols

Female C57BL/6 mice (n = 5) were immunized on day 0, 14 and 28 with different vaccine formulations encompassing either OVA protein alone or admixed with c-di-AMP in an aqueous solution or encapsulated in IMSG NPs via IN, ID or TF route. Antigen dose and application volumes were adjusted to the specific administration route, as depicted in Table 1.

TF vaccination was carried on the flank part of the mice. In brief, 2 days prior the immunization mice were anesthetized and hair was removed using clippers and a depilatory cream. Depilated areas were washed and carefully inspected for cuts or skin irritation in which case these mice were excluded from the experiment.

4.3.10. Sample collection

Blood samples from immunized mice were taken from the retro-orbital complex on day -1, 13, 27 and 48. To separate sera, blood samples were incubated first for 1 h at 37°C followed by 30 min incubation at 4°C. Subsequently, samples were centrifuged at 3000 × g for 10 min and sera were stored at -20°C until further processing. On day 48, mice were sacrificed, lymph nodes and spleens were collected and single cell suspensions were obtained by mechanically homogenization of the organs using a sieve (100 µm). Cell suspensions were generated and analysed for the presence of antigen-specific cells, as previously described [95].

Table 1.
Immunization groups

Group	Route	Dose (OVA ± c-di-AMP)
Blank NPs + c-di-AMP	I.N.	Equivalent to OVA-loaded NPs
OVA	I.N.	10 µg/20 µl
OVA + c-di-AMP	I.N.	10 µg + 7.5 µg/20 µl
OVA NPs	I.N.	10 µg/20 µl
OVA + c-di-AMP NPs	I.N.	10 µg + 7.5 µg/20 µl
Blank NPs + c-di-AMP	I.D.	Equivalent to OVA-loaded NPs
OVA	I.D.	10 µg/20 µl
OVA + c-di-AMP	I.D.	10 µg + 7.5 µg/20 µl
OVA NPs	I.D.	10 µg/ 20 µl
OVA + c-di-AMP NPs	I.D.	10 µg + 7.5 µg/20 µl
Blank NPs + c-di-AMP	T.F.	Equivalent to OVA-loaded NPs
OVA	T.F.	200 µg/60 µl
OVA + c-di-AMP	T.F.	200 µg + 20 µg/60 µl
OVA NPs	T.F.	200 µg/60 µl
OVA + c-di-AMP NPs	T.F.	200 µg + 20 µg/60 µl

IN: intranasal, ID: intradermal, TF: transfollicular, OVA: ovalbumin, NPs: nanoparticles

4.3.11. Detection of antigen-specific IgG and IgG subtypes

OVA-specific antibodies in sera of individual animals were determined by ELISA using microtiter plates coated with 100 µl/well of the antigen (2 µg/ml in 0.05 M carbonate buffer, pH 9.6), as previously described [95]. Briefly, Antigen coated microtiter plates wer incubated overnight incubation at 4 °C, plates were then incubated with 3% bovine serum albumin (BSA) in PBS for 1 h at 37 °C in order to block unspecific binding sites. Before serial 2-fold dilutions of sera in 3% BSA/PBS were added (100µl/well) plates were washed six times with 1% BSA/PBS/0.05% Tween 20. After 1 h of incubation at 37 °C plates were washed six times with 1% BSA/PBS/0.05% Tween 20 and the secondary antibody was added: biotinylated γ chain-specific goat anti-mouse IgG, IgG1 and IgG2c (Sigma, USA), respectively. Subsequently, samples were again incubated at 37 °C for 1 h [see above].

Afterwards, plates were washed six times peroxidase-conjugated streptavidine (BD Pharmingen, USA) was added to each well (100 µl/well) and plates were incubated for 1 h at RT. Finally, after another six washes, reactions were developed using 100 µl of ABTS [2, 20-azino-bis(3-ethylbenzthiazoline-6-sulfonic acid)] in 0.1 M citrate-phosphate buffer (pH 4.35) containing 0.01% H₂O₂. Endpoint titres are expressed as absolute values of the last sample dilution that after a 15 and 30 min incubation gave a 2 times higher optical density at 405 nm compared to the negative control values.

4.3.12. Evaluation of cellular proliferation and cytokine profiles

The proliferative activity of immune cells derived from spleen and lymph nodes of immunized mice was measured as previously described [95]. Briefly, Erythrocytes were lysed from immune cells by incubating them for 1 min with ammonium chloride (ACK) buffer. Lysis was stopped by adding complete medium (RPMI supplemented with 10% fetal calf serum, 100 U/ml penicillin and 100 µg/ml streptomycin). Subsequently, cell suspensions were adjusted to 5×10^6 cells/ml and seeded in quadruplicates at 100 µl/well in flat-bottomed 96-well microtiter plates (Nunc, Roskilde, Denmark). Plates were incubated for 4 days in the presence of different concentrations of EndoGrade® Ovalbumin (Hyglos, Germany), 5 µg/ml Concanavalin A or medium. During the final 18 h of culture, cells were incubated with 1 µCi/well of (³H)thymidine (Amersham International, Freiburg, Germany). Finally, cells were harvested on paper filters (Filtermat A; Wallac, Freiburg, Germany) by using a cell harvester (Inotech, Wohlen, Switzerland) and the relative amount of proliferating cells was determined by measuring the beta radiation of (³H)thymidine incorporated into the DNA of the

cells (Wallac 1450 β -scintillation counter Micro-Trilux). The obtained results are expressed as counts per minute (cpm) and stimulation index (SI), respectively.

To quantify the cytokines and chemokines secreted by antigen-specific immune cells, lymph node derived cells and splenocytes were adjusted to a concentration of 5×10^6 cells/ml, seeded in quadruplicates at 100 μ l/well in flat-bottomed 96-well microtiter plates (Nunc, Roskilde, Denmark) and re-stimulated in vitro for 96 h with different concentrations of EndoGrade® OVA (Hyglos, Germany). Afterwards, supernatants were collected and stored at -80°C until processing. Cytokine amounts (IL-2, IL-4, IL-5, IL-6, IL-10, IL-13, IL-17, TNF α and IFN γ) were determined using the Mouse Th1/Th2 FlowCytomix Multiplex cytokine array, according to the manufacturer's instructions (eBioscience, Bender MedSystems®, USA).

4.3.13. Multifunctional T cells

To evaluate the capacity of different vaccine formulations to stimulate OVA specific multifunctional T cells, splenocytes from immunized mice were isolated and their capacity to produce different cytokines was evaluated by flow cytometry. Splenocytes (2×10^7 cells per well) of immunized mice were incubated (37°C , 5 % CO₂) in 2 ml RPMI containing OVA protein [1 μ g/ml]. After 16-20 hours 5 μ g/ml BrefeldinA and 6 μ g/ml Monensin (Sigma-Chemie, Germany) were added and cells were incubated for additional 6 hours. Subsequently, cells were stained for dead cells (Fixable Dead Cell Stain, Invitrogen, USA) and surface markers (CD3 and CD8, BD, USA; CD4, eBioscience, Germany). Then, cells were fixed with 2 %PFA, permeabilized for 45-60 min with 0.5 % BSA and 0.5 % Saponin in PBS and stained for intracellular cytokines (IL-2 and IFN γ , BD, USA; TNF α , IL-17 and IL-4, eBioscience, Germany). Finally, cells were resuspended in PBS and light emission

measured using BD LSRII. After spectral overlap compensation with the BD FACS Diva Software, the data were analyzed using FlowJo (Tree Star, USA)

4.3.14. Statistical analysis

Statistical significance of the observed differences was analysed using the Graph Pad Prism 5 software for Windows (Version 5.04) by the one-way ANOVA test. Differences were considered significant at $p < 0.05$ (*), $p < 0.01$ (**), $p < 0.001$ (***) and $p < 0.0001$ (****), respectively.

4.4. Results

4.4.1. Characterization of OVA-loaded IMMSG NPs

The characteristics of the NPs are summarized in Table 2. The TEM image in Fig.1 shows smooth, spherical particles. The mean size of OVA-loaded IMMSG NPs (+/- c-di-AMP) for all three routes was approximately 300-350 nm with a mono-disperse size distribution ($PDI < 0.2$). Adjuvant incorporation into NPs does not change the particle characteristics in terms of size and PDI.

Table 2.

Physico-chemical characterization of the optimized IMMSG NPs

S.no.	NPs	Route	Size (nm)	PDI
1	OVA loaded IMMSG NPs	I.D. and I.N.	312.2 ± 14.6	0.146 ± 0.02
2	OVA + c-di-AMP IMMSG NPs	I.D. and I.N.	301.1 ± 14.2	0.146 ± 0.01
3	OVA loaded IMMSG NPs	T.F.	317.4 ± 22.1	0.125 ± 0.04
4	OVA + c-di-AMP IMMSG NPs	T.F.	323.6 ± 9.4	0.132 ± 0.03

Values represent mean \pm standard deviation of $n = 6$ independently prepared batches. I.D.- intra-dermal, I.N.: intra-nasal, T.F.: transfollicular application of NPs. PDI: poly-dispersity index



Fig. 1. TEM image of OVA loaded IMSG NPs

4.4.2. Integrity and bio-availability of OVA are not affected by IMSG NP generation process

To investigate the formation of fragments or aggregates of OVA during NP preparation as well as dispersion in an oily solution, a SDS PAGE was performed. No difference in the migration pattern of OVA extracted from IMSG NPs compared to OVA in aqueous solution was observed (Fig. 2). In addition, OVA integrity is not affected by the NP generation process since no degradation fragments were observed when OVA was extracted from NPs (lanes 5 and 8, Fig. 2). The smear observed after coomassie staining resulted from the lecithin component as evidenced by lanes 3 and 6.

To further validate the proper integrity of the OVA molecules following NP formation, ELISA were performed using the OVA which had been extracted from the NPs. By relating the total amount of protein in the NP sample, the bio-availability of the encapsulated OVA was determined as $85 \pm 5 \%$ in OVA-loaded IMSG NPs.

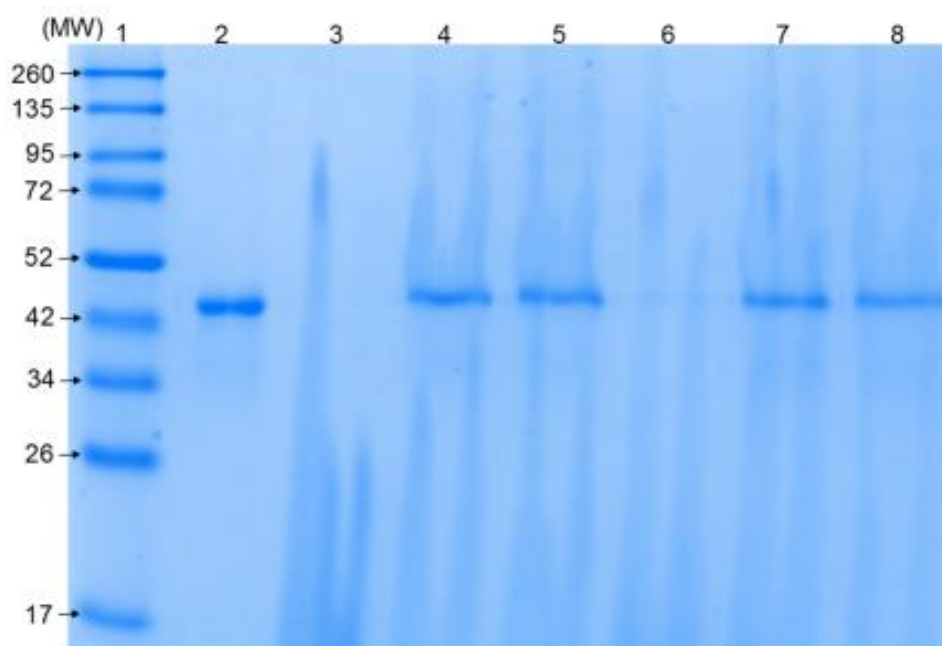
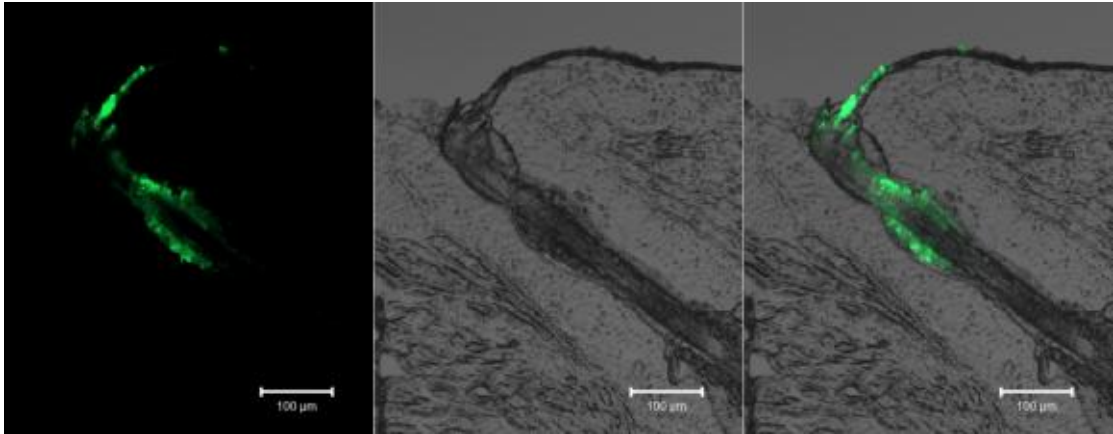


Fig. 2. Integrity of OVA extracted from NPs by water and analysed by SDS PAGE, **Lane1:** Molecular weight Marker, **Lane2:** OVA in solution, **Lane3:** Lecithin + water, **Lane4:** Physical mixture (OVA + lecithin + water), **Lane5:** OVA NPs in water, **Lane6:** Lecithin + oil + water, **Lane7:** Physical mixture (OVA + lecithin + oil + water), **Lane 8:** OVA NPs in oil + water

4.4.3. Follicular uptake of Nanoparticles

Fig. 3A shows representative images illustrating the distribution of fluorescently labeled IMMSG NPs on the skin surface and in the hair follicle after application to excised pig ears. NPs accumulate in the follicle openings, cover the hair and invade the follicular duct. The magnitude of NPs invaded was evaluated by quantifying the fluorescence measured in cyanoacrylate biopsy extracts (Fig. 3B). Thus, encapsulation of OVA into IMMSG NPs significantly enhanced ($p < 0.001$) follicular delivery of OVA by a factor of 4.38 ± 0.81 compared to OVA solution and 1.89 ± 0.35 compared to OVA-loaded Chit-PLGAs.

A



B

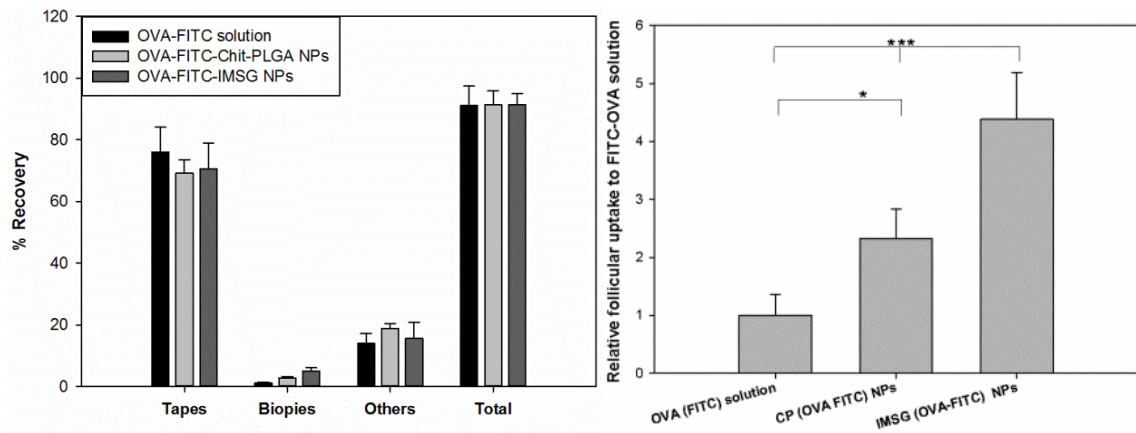


Fig. 3. A) Distribution of fluorescently labelled NPs in hair follicles after application to excised pig ears. (LSM 510 Meta, Carl Zeiss GmbH, Jena Germany; excitation wavelength 458 nm), Transversal cryo section (thickness 12 µm); overlay of fluorescence and transmission light images: NPs are visible on the skin surface and inside the follicle. (B) Quantitative extraction of tapes, superglue biopsy and application device + skin rest allows to quantify the amount of particles that is deposited on the “skin surface” (tapes), inside the “hair follicle” (superglue biopsy) and “others” (application device + skin rest) respectively. Follicular uptake of FITC-labelled OVA encapsulated in IMMSG NPs relative to FITC-OVA solution and FITC-OVA in Chit- PLGA NP (n = 6, mean ± SD; differences were considered significant whenever (* p<0.05, *** p<0.001) compared to OVA-FITC solution.

4.4.4. IMMSG NPs efficiently deliver OVA to immune cells via TF route

In order to verify the overall feasibility of transfollicular delivery of OVA using IMMSG NPs as well as to evaluate their superiority to OVA-loaded Chit-PLGA NPs, an

adoptive transfer model was established. Proliferation of adoptively transferred OVA-specific CD4⁺ T (OT-II) cells was measured by CFSE dilution.

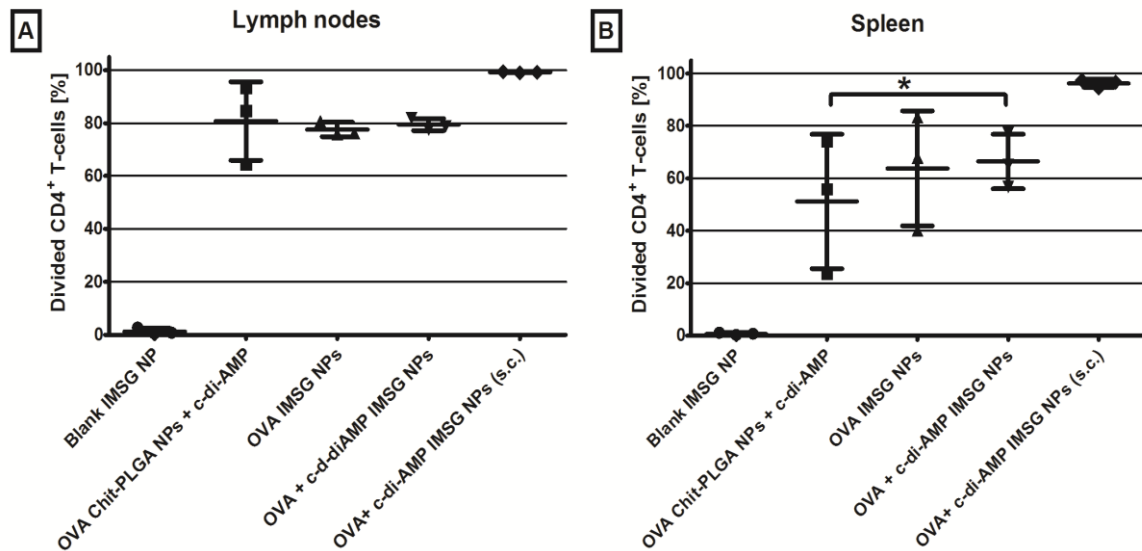


Fig. 4. The percentage of divided transferred cells in the draining lymph nodes (a) and the spleen (b) for each experimental group is shown. The three animals of each group were analyzed separately. While no proliferation was observed in the negative control (Gr. 1.), full proliferation of the transferred cells was observed in animals of the positive control group (Gr. 5.). No differences were seen in the proliferation of lymph nodes cells between different tested groups (Gr. 2. (OVA loaded Chit-PLGA NPs + c-di AMP) and Gr. 3. (OVA-loaded IM SG NPs immunized transfollicularly) & Gr. 4. (OVA + c-di AMP loaded IM SG NPs immunized transfollicularly)). However, spleen cells showed significant differences in the proliferation between Gr. 4 and Gr. 2. Differences were considered significant at $p < 0.05$ (*).

As shown in Fig. 4, all tested vaccine formulations efficiently stimulated proliferation of OT-II cells following TF vaccination except blank NPs. No differences in the proliferative capacity of LN derived cells were detected between groups immunized by TF route (Fig. 4A). In contrast, significant differences ($p < 0.05$) were observed when analyzing the proliferative capacity of spleen derived OT-II cells from mice immunized with OVA + c-di-AMP IM SG NPs in comparison to OVA Chit-PLGA NPs + c-di AMP. Thus, OVA + c-di AMP loaded IM SG NPs

seems to be more efficient in delivering OVA into hair follicles compared to OVA loaded Chit-PLGA NPs + c-di AMP (Fig. 4B).

4.4.5. Adjuvanted IMMSG NPs stimulate efficient humoral immune responses following ID immunization

Vaccine formulations were well tolerated, since no obvious signs of acute toxicity (e.g. weight loss, reduced mobility, hair straightened up) were observed following vaccination. The highest OVA-specific IgG titre was stimulated using OVA + c-di-AMP co-encapsulated IMMSG NPs (Fig. 5A). The differences were significant as compared to all tested formulations ($p < 0.001$). Interestingly, high titres were observed even after a single boost, whereas for all other formulations a second boost was needed in order to stimulate antibody production (Fig. 5B).

Interestingly, OVA-loaded IMMSG NPs generated similar IgG titres compared to OVA protein co-administered with c-di-AMP indicating the beneficial effect of IMMSG NPs. OVA protein alone generated lowest IgG titres when injected ID.

As expected, incorporation of c-di-AMP as adjuvant resulted in the stimulation of mixed Th1/Th2 responses, as indicated by increased levels of IgG2c antibodies in sera of immunized mice (Fig. 5C). In contrast, OVA protein alone or encapsulated in IMMSG NPs stimulated predominant production of IgG1, indicating a Th2 biased response. However, the strongest IgG2c titres ($p < 0.05$) were stimulated in mice receiving OVA + c-di-AMP co-encapsulated in IMMSG NPs (Fig. 5C).

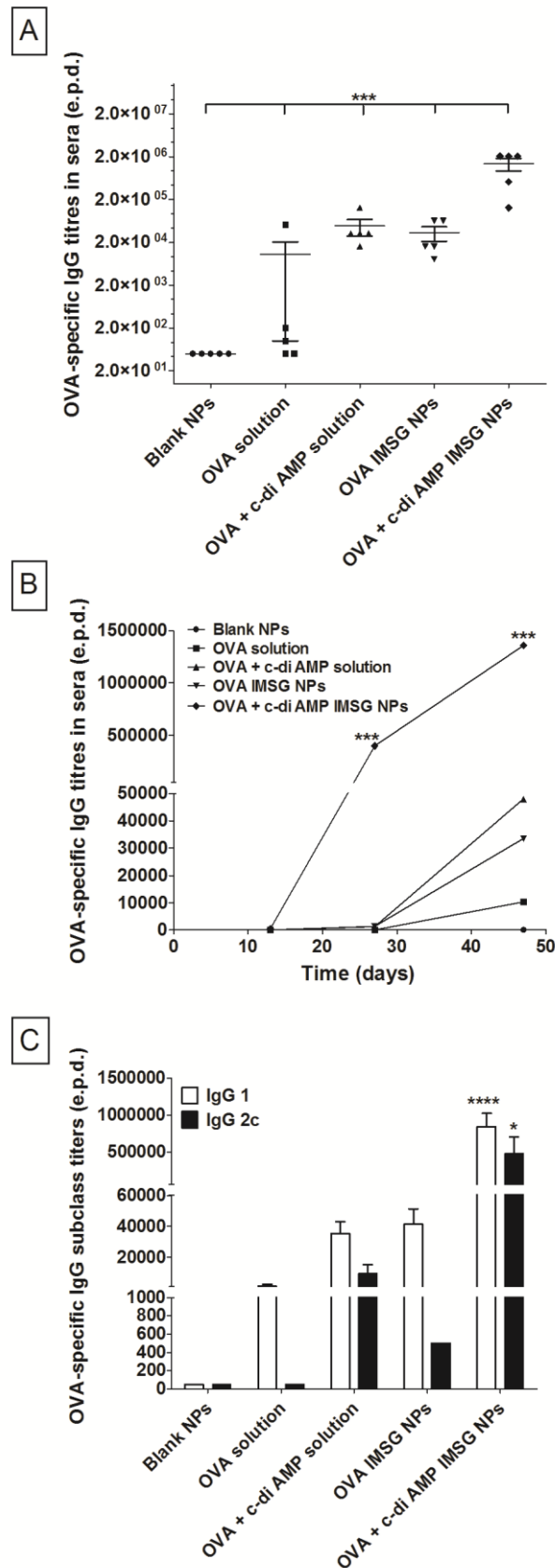


Fig. 5. Systemic humoral immune responses stimulated in C57BL/6 mice ($n = 5$) after three immunizations with different OVA containing formulations via ID route. (A) OVA-specific IgG titres in sera of mice 20 d after the last immunization. (B) Kinetics of OVA-specific IgG production in sera

of immunized mice on day 0, 13, 27 and 48. (C) OVA-specific IgG subclasses in sera of immunized mice. Results are expressed as the last dilution giving the double value (OD_{450 nm}) of the background value (negative control). Standard error of mean (SEM) is indicated by vertical lines. Differences were considered significant at $p < 0.05$ (*), $p < 0.001$ (***) and $p < 0.0001$ (****), respectively

4.4.6. Adjuvanted IMMSG NPs stimulate efficient cellular immune responses following ID immunization

ID immunization of mice using OVA + c-di-AMP co-encapsulated in IMMSG NPs stimulated the strongest cellular response, whereas OVA protein alone or encapsulated in IMMSG NPs was less efficient (Fig. 6A). The absolute numbers of proliferating cells were higher at local level with respect to systemic responses. To further characterize the stimulated responses we analysed the cytokine secretion profiles of splenocytes and LN derived cells from vaccinated mice by cytometric bead arrays (Fig. 6B). The strongest cytokine production was stimulated in mice immunized with OVA co-administered with c-di-AMP, followed by those receiving OVA + c-di-AMP co-encapsulated IMMSG NPs (Fig. 6B).

Only vaccine formulations including c-di-AMP stimulated strong production of IFN γ . OVA alone or OVA encapsulated in IMMSG NPs stimulated predominantly IL-13, followed by IL-5 and IL-10 (Fig. 6B). Only mice receiving OVA + c-di-AMP co-encapsulated in IMMSG NPs showed significantly increased levels of TNF- α , IL-17 and IL-6. No significant differences were observed in the cytokine profiles of groups receiving OVA protein or OVA loaded IMMSG NPs, besides from the fact that the absolute numbers of different cytokines (IL-5, IL-13 and IFN γ) being higher in mice receiving OVA loaded IMMSG NPs. In line with the obtained IgG subclass patterns, vaccine formulations containing c-di-AMP stimulated a mixed Th1/Th2

response, whereas those without adjuvant promoted a Th2-dominated response (Fig. 6B).

Recent findings support the assumption that vaccine efficacy not only depends on the strength but also, to a large extent, on the quality of the stimulated T cell response. In this regard, stimulation of multifunctional T cells which possess a broader functional spectrum results in enhanced protective immunity, as compared to mono-functional cells [98].

Therefore, we investigated the quality of the T cell responses stimulated by IMSG NPs. Immunization with OVA encapsulated IMSG NPs already increases the proportion of OVA-specific bi- ($\text{IFN}\gamma$ +/ $\text{TNF}\alpha$ +, $\text{IFN}\gamma$ +/ IL-2 +) and tri-functional ($\text{IFN}\gamma$ +/ $\text{TNF}\alpha$ / IL-2 +) CD4^+ T cells, as compared to OVA alone. This effect was further strengthened using OVA + c-di-AMP co-encapsulated IMSG NPs (Fig. 6C). A similar pattern was observed following vaccination with OVA protein add-mixed with c-di-AMP. Nevertheless, the highest number of $\text{IFN}\gamma$ producing CD4^+ T cells was stimulated by combining IMSG NPs with c-di-AMP (Fig. 6C). None of the vaccine formulations was able to stimulate antigen-specific CD8^+ T cells.

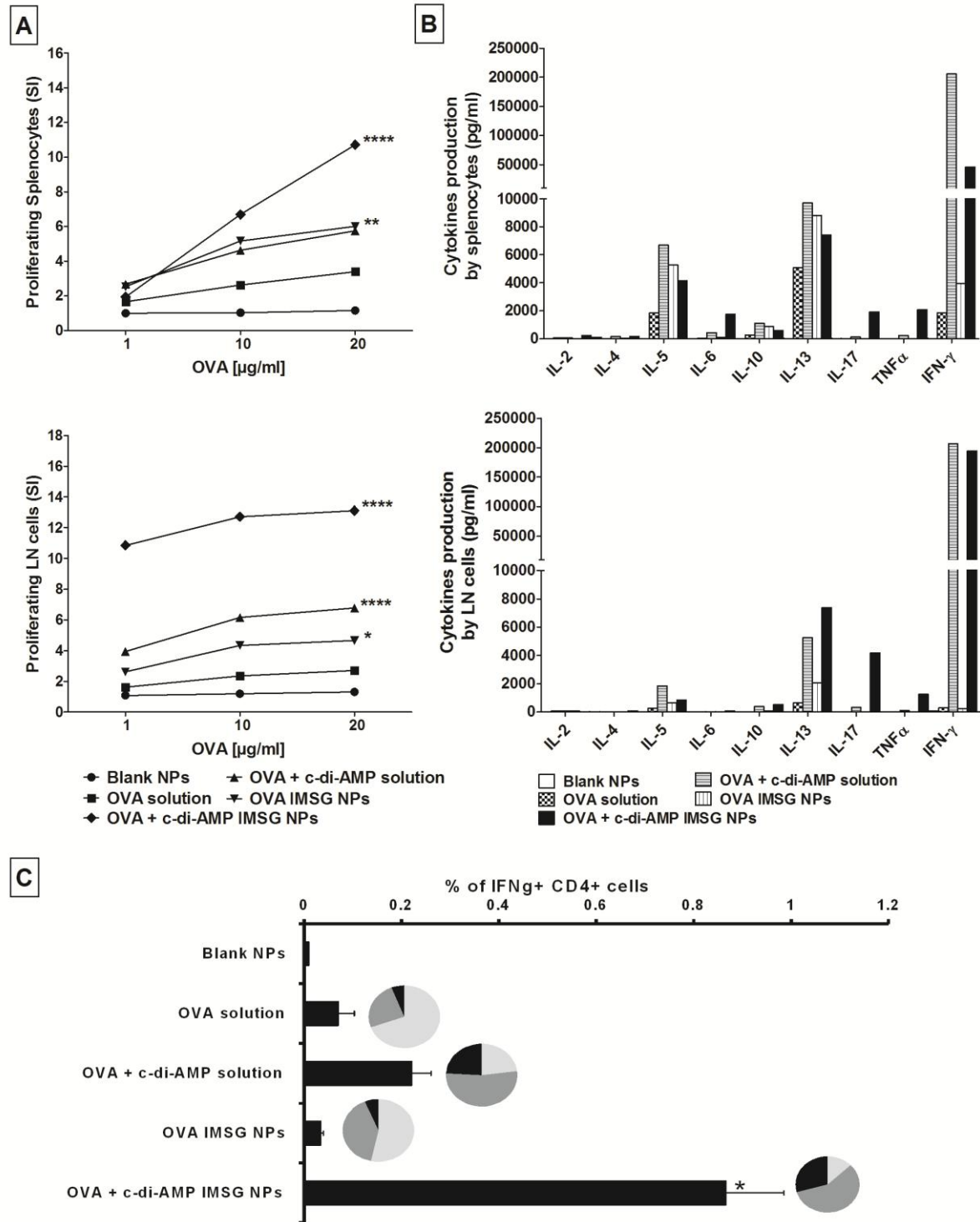


Fig. 6. Cellular responses stimulated following ID immunization. Splenocytes (upper panel) and LN cells (lower panel) from vaccinated animals were restimulated with different concentrations of OVA for 96 h. (A) Cellular proliferation was assessed by determination of the [3 H] thymidine incorporated into the DNA of replicating cells. Results are averages of quadruplicates and expressed as stimulation index (SI). (B) Cytokine profiles stimulated by the different vaccine formulations were evaluated by cytometric bead array. Results are expressed in pg/ml. (C) Quality of the T cell responses stimulated following vaccination via ID route. Cells were collected at day 20 after the last

immunization and subsequently incubated for 24 h in the presence and absence, respectively, of OVA. Results are expressed as difference between re- and non-restimulated % of all CD4⁺ cells expressing IFN γ . Living cells were gated for CD3⁺ CD4⁺ double positive cells. These subpopulation was further divided into monofunctional expressing only IFN γ , bifunctional expressing two cytokines (IFN γ / IL-2 or IFN γ / TNF α) and trifunctional expressing IFN γ , IL-2 and TNF α . Pie charts represent the proportion of tri- (black), bi- (dark gray) and mono-functional (light gray) cells. The differences were considered significant compared to OVA alone at $p < 0.05$ (*), $p < 0.01$ (**) and $p < 0.0001$ (****), respectively.

4.4.7. Adjuvanted IMSG NPs fail to stimulate efficient humoral immune responses following IN immunization

Serum anti-OVA IgG antibody titres obtained after IN vaccination with OVA and OVA-loaded NPs with or without introduction of c-di-AMP as adjuvant are shown in Fig. 7A. OVA co-administered with c-di-AMP stimulated the highest OVA-specific IgG titres as compared to all tested formulations ($p < 0.001$). Surprisingly, in contrast to ID vaccination, immunization of mice with OVA-encapsulated NPs and OVA + c-di-AMP co-encapsulated NPs via the IN route stimulated only very low IgG titres. Furthermore, mice need to receive three immunizations in order to stimulate efficient antibody titres (Fig. 7B), suggesting problems related to NPs delivery across the mucosal barrier. As described for ID immunization, co-administration of c-di-AMP results in a significantly increased production of IgG2c compared to all tested formulations ($p < 0.01$, Fig. 7C).

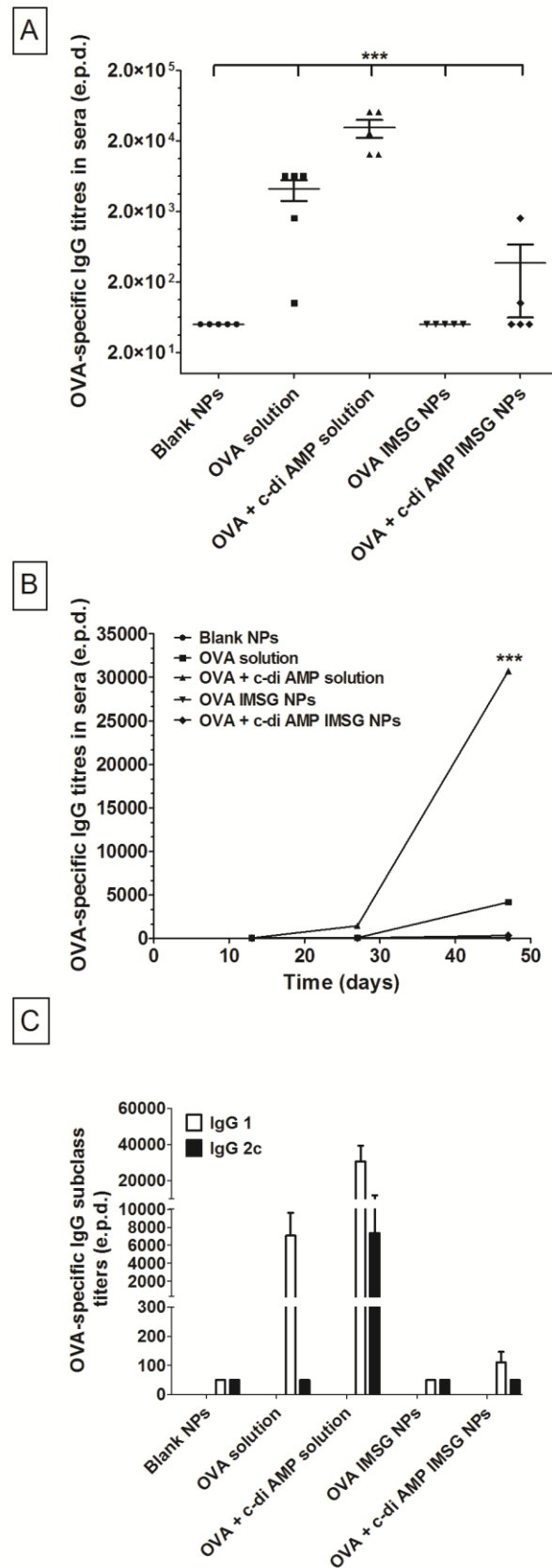


Fig. 7. Systemic humoral immune responses stimulated in C57BL/6 mice ($n = 5$) after three immunizations with different OVA containing formulations via IN route. (A) OVA-specific IgG titres in sera of mice 20 d after the last immunization. (B) Kinetics of OVA-specific IgG production in sera

of immunized mice on day 0, 13, 27 and 48. (C) OVA-specific IgG subclasses in sera of immunized mice. Results are expressed as the last dilution giving the double value (OD_{450 nm}) of the background value (negative control). Standard error of mean (SEM) is indicated by vertical lines. Differences were considered significant at $p < 0.05$ (*) and $p < 0.001$ (***), respectively.

4.4.8. Adjuvanted IMMSG NPs fail to stimulate efficient cellular immune responses following IN immunization

In contrast to the ID vaccination strategy, IN immunization of mice with IMMSG NPs did not result in the stimulation of strong cellular responses. Thus, only marginal proliferation was observed of re-stimulated splenocytes and LN cells derived from mice vaccinated with OVA + c-di-AMP co-encapsulated IMMSG NPs (Fig. 8A). As expected, strong proliferative and cytokine responses were obtained when cells from control mice receiving OVA co-administered with c-di-AMP by IN route were tested (Fig. 8A and 8B). Similarly to the profiles stimulated by ID immunization, IFN γ was the dominant cytokine induced by adjuvantation with c-di-AMP. However, IN vaccination with OVA co-administered with c-di-AMP also induced strong IL-17 and IL-13 production. Interestingly, IL-5 production was considerably decreased with respect to what observed after ID immunization (Fig. 8B). No or only very low amounts of cytokines were detected in mice receiving OVA loaded IMMSG NPs.

Similar to what observed after immunization via the ID route, none of the vaccine formulations was able to stimulate antigen-specific CD8 $^{+}$ T cells when applied by IN route. However, CD4 $^{+}$ cellular responses were slightly increased in mice vaccinated with OVA + c-di-AMP co-encapsulated IMMSG NPs (Fig. 8C). As shown for ID immunization, incorporation of c-di-AMP results in higher numbers of OVA-specific bi- (IFN γ $^{+}$ /TNF α $^{+}$, IFN γ $^{+}$ /IL-2 $^{+}$) and tri-functional (IFN γ $^{+}$ /TNF α /IL-2 $^{+}$) CD4 $^{+}$ T cells, as compared to values in animals receiving OVA alone and OVA

encapsulated IMSG NPs (Fig. 8C). Control mice receiving OVA co-administered with c-di-AMP showed the highest number of IFN γ producing CD4 $^{+}$ T cells and slightly better proportion of bi- and tri-functional cells (Fig. 8C).

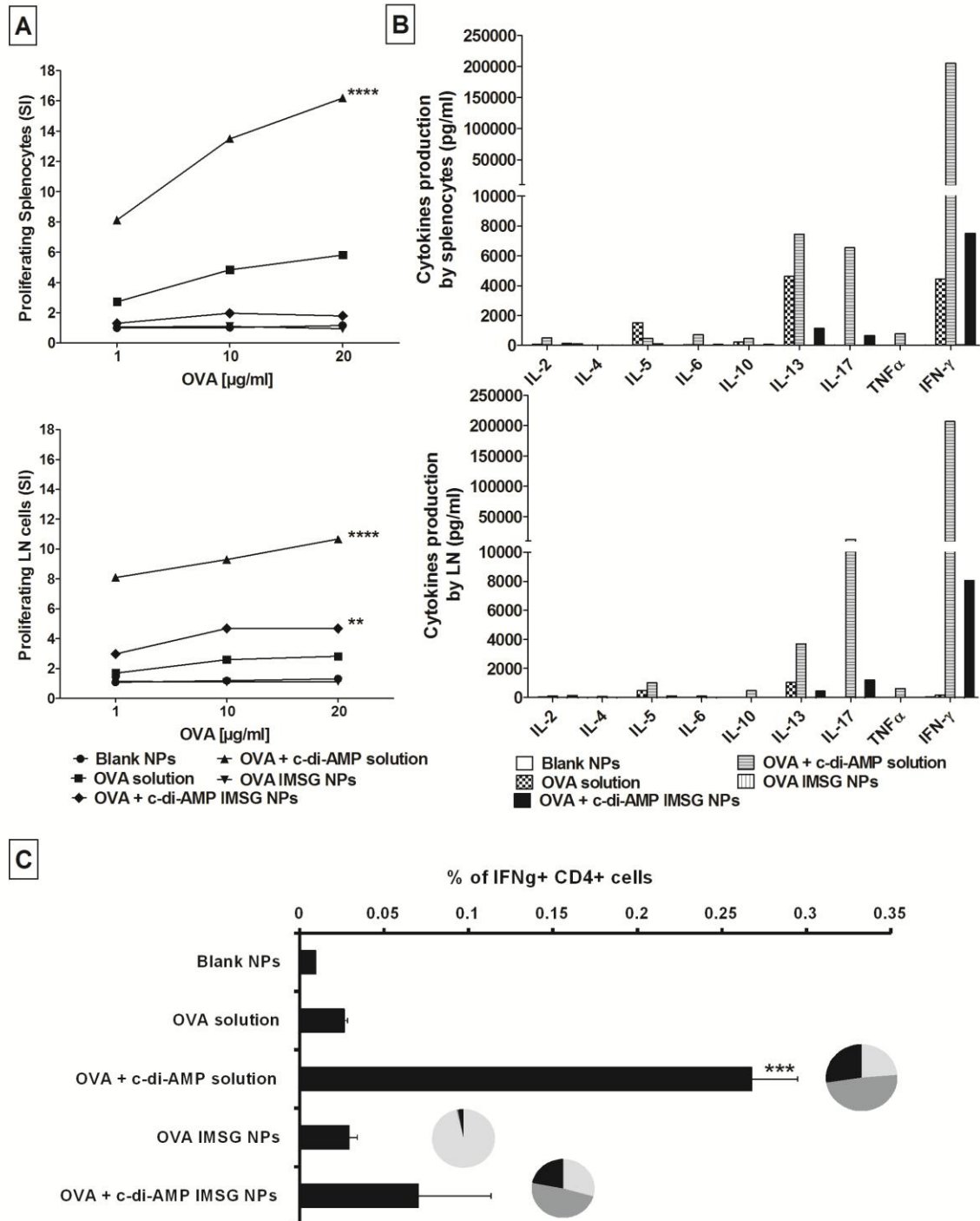


Fig. 8. Cellular responses stimulated following IN immunization. Splenocytes (upper panel) and LN cells (lower panel) from vaccinated animals were restimulated with different concentrations of OVA for 96 h. (A) Cellular proliferation was assessed by determination of the [3 H] thymidine incorporated

into the DNA of replicating cells. Results are averages of quadruplicates and expressed as stimulation index (SI). (B) Cytokine profiles stimulated by the different vaccine formulations were evaluated by cytometric bead array. Results are expressed in pg/ml. (C) Quality of the T cell responses stimulated following vaccination via IN route. Cells were collected at day 20 after the last immunization and subsequently incubated for 24 h in the presence and absence, respectively, of OVA. Results are expressed as difference between re- and non-restimulated % of all CD4⁺ cells expressing IFN γ . Living cells were gated for CD3⁺ CD4⁺ double positive cells. These subpopulation was further divided into monofunctional expressing only IFN γ , bifunctional expressing two cytokines (IFN γ / IL-2 or IFN γ / TNF α) and trifunctional expressing IFN γ , IL-2 and TNF α . Pie charts represent the proportion of tri- (black), bi- (dark gray) and mono-functional (light gray) cells. The differences were considered significant compared to OVA alone at p<0.01 (**), p<0.001 (***), and p<0.0001 (****), respectively.

4.4.9. Adjuvanted IMMSG NPs stimulate efficient humoral immune responses following TF vaccination

When mice were vaccinated by TF route, the highest serum anti-OVA IgG titres (p<0.001) were observed in mice receiving OVA + c-di-AMP co-encapsulated IMMSG NPs (Fig. 9A). Differences in titres were significant already after the 1st boost (p<0.001). However, also IMMSG NPs loaded with OVA alone stimulated significantly stronger IgG production than OVA alone or co-administered with c-di-AMP. This shows the beneficial effect of antigen encapsulation within IMMSG NPs for TF vaccination. In contrast, similar IgG titres were stimulated when OVA was applied via ID route encapsulated in IMMSG NPs or co-administered with c-di-AMP (Fig. 9A). However, while ID immunization with OVA + c-di-AMP co-encapsulated IMMSG NPs stimulated strong humoral responses already after a single boost, TF vaccination needed a 2nd boost in order to stimulate efficient OVA-specific IgG titres (Fig. 9B). As expected, the overall IgG titres stimulated after immunization via TF route were lower than those obtained after ID vaccination. Unlike the IgG subclass pattern observed after ID and IN vaccination, TF immunization of mice stimulated only poor IgG2c responses (Fig.9C).

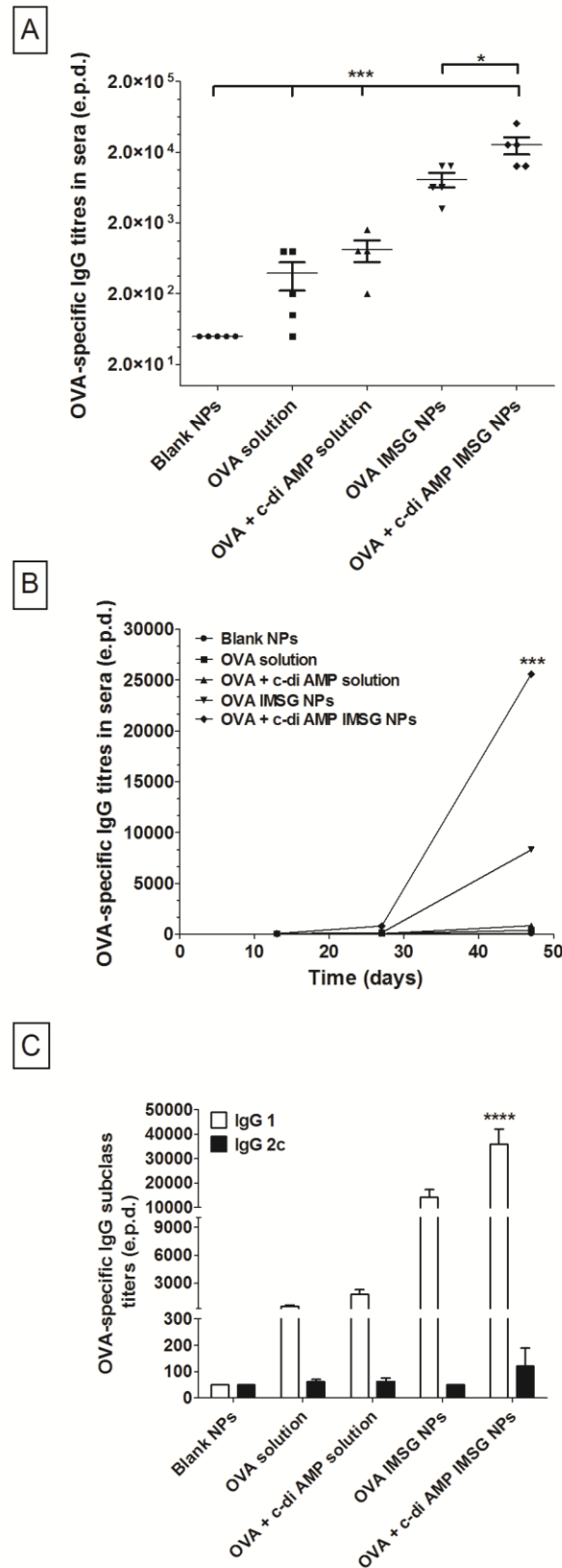


Fig. 9. Systemic humoral immune responses stimulated in C57BL/6 mice after three vaccinations with different OVA containing formulations TF. (A) Total OVA specific IgG titres in sera after immunization (n = 5). (B) Kinetics analysis of OVA specific IgG titres in sera of immunized mice on day 0, 14, 28 with (n = 5). (C) Analysis of OVA specific IgG subclasses in sera of immunized mice

(n = 5). Differences in outcome between different tested groups were assessed using One way ANOVA. Differences were considered significant at $p < 0.05$ (*), $p < 0.001$ (***) and $p < 0.0001$ (****), respectively.

4.4.10. Adjuvanted IMMSG NPs stimulate efficient cellular immune responses following TF vaccination

The strongest cellular response at local and systemic level was stimulated by OVA + c-di-AMP co-encapsulated IMMSG NPs, as indicated by strong proliferative responses (Fig. 10A upper panel; $p < 0.0001$). However, also NPs encapsulated OVA and OVA co-administered with c-di-AMP stimulated significantly increased ($p < 0.01$) proliferative responses of LN derived cells, as compared to cells derived from OVA and Blank NPs immunized mice (Fig. 10A, lower panel).

When analysing the cytokine profiles stimulated following TF vaccination, it turned out that application of IMMSG NPs on intact skin stimulated similar profiles, as compared to IN immunization, namely, high titres of $\text{IFN}\gamma$, IL-13 and IL-17 (Fig. 10B). However, while at local level $\text{IFN}\gamma$ was strongest induced cytokine followed by IL-13 and IL-17, at systemic level this pattern was only observed after restimulation of splenocytes from mice receiving OVA + c-di-AMP co-encapsulated IMMSG NPs (Fig. 10B). Splenocytes from mice receiving all other formulations produce predominantly IL-13, followed by $\text{IFN}\gamma$ and IL-17. Interestingly, while OVA encapsulated IMMSG NPs were less efficient at stimulating cellular responses compared to OVA + c-di-AMP co-encapsulated IMMSG NPs when administered by IN or ID route, only small differences were observed after TF vaccination (Fig. 10B). In agreement with the stimulated IgG subclasses observed after TF immunization, the observed cytokine profiles indicate a Th2-dominated immune

response. Only OVA + c-di-AMP co-encapsulated IMMSG NPs seem to be able to stimulate a mixed Th1/Th2 response.

Compared to IN or ID vaccination, TF immunization stimulated only weak induction of multifunctional CD4⁺ T cells (Fig. 10C). Furthermore, immunization with either OVA alone, OVA co-administered with c-di-AMP or OVA encapsulated IMMSG NPs resulted in the generation of mainly (~70%) mono-functional (IFN γ ⁺ CD4⁺ T cells, followed by bi- (IFN γ ⁺/TNF α ⁺, IFN γ ⁺/IL-2⁺, ~23%) and tri-functional (IFN γ ⁺/TNF α /IL-2⁺, ~6%) CD4⁺ T cells (Fig. 10C). No significant differences were observed between these groups. In contrast, mice immunized with OVA + c-di-AMP co-encapsulated IMMSG NPs showed an improved quality of CD4⁺ responses, as indicated by increased proportions of bi- and tri-functional CD4⁺ cells (Fig. 10C). As shown for IN and ID immunization, incorporation of c-di-AMP results in increased quality of the stimulated cellular responses after TF immunization (Fig. 10C). However, no OVA-specific CD8⁺ cells were detected.

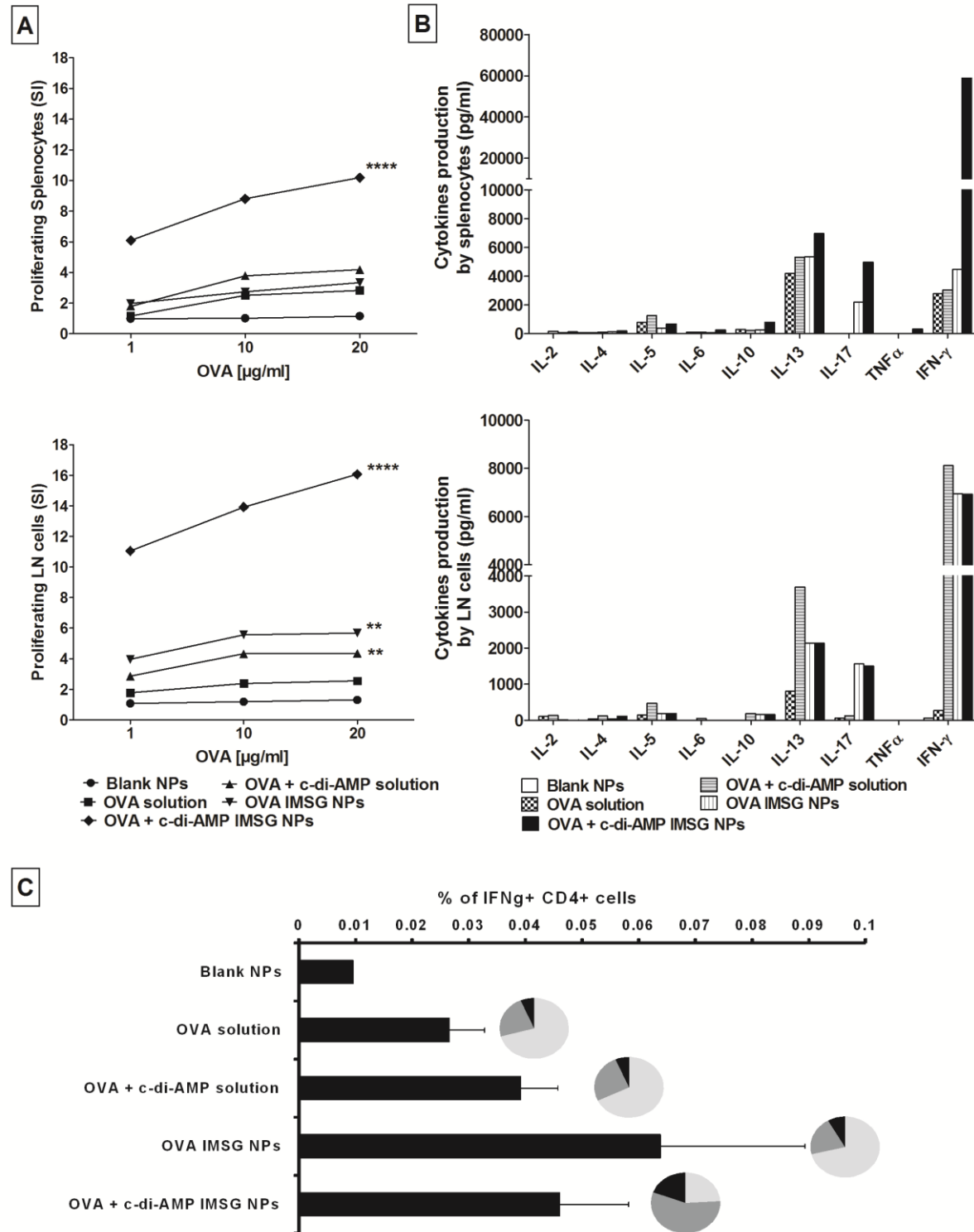


Fig. 10. Cellular responses stimulated following TF immunization. Splenocytes (upper panel) and LN cells (lower panel) from vaccinated animals were restimulated with different concentrations of OVA for 96 h. (A) Cellular proliferation was assessed by determination of the [3 H] thymidine incorporated into the DNA of replicating cells. Results are averages of quadruplicates and expressed as stimulation index (SI). (B) Cytokine profiles stimulated by the different vaccine formulations were evaluated by cytometric bead array. Results are expressed in pg/ml. (C) Quality of the T cell responses stimulated following vaccination via TF route. Cells were collected at day 20

after the last immunization and subsequently incubated for 24 h in the presence and absence, respectively, of OVA. Results are expressed as difference between re- and non-restimulated % of all CD4⁺ cells expressing IFN γ . Living cells were gated for CD3⁺ CD4⁺ double positive cells. These subpopulation was further divided into monofunctional expressing only IFN γ , bifunctional expressing two cytokines (IFN γ / IL-2 or IFN γ / TNF α) and trifunctional expressing IFN γ , IL-2 and TNF α . Pie charts represent the proportion of tri- (black), bi- (dark gray) and mono-functional (light gray) cells. The differences were considered significant compared to OVA alone at $p < 0.01$ (**) and $p < 0.0001$ (****), respectively.

4.5. Discussion

Micro- and nanoparticle based delivery systems offer unique possibilities to create safe and effective vaccines [122]. However, the route of vaccination is also an important parameter to define the immune response triggered by particulate carriers. This is not only due to differences in physic-chemical properties (e.g. size, surface charge) or the carrier, but also due to targeted antigen delivery to APCs located at the inductive site [123]. Among the various potential routes of immunization, the transcutaneous and nasal routes aroused considerable interest, particularly due to their amenability for non-invasive delivery of vaccines.

Most of the currently studied polymeric NPs, such as PLGA and PLA, suffer from multiple limitations. Among them can be mentioned the use of chemical solvents and physical stresses during the production process, which negatively affect antigen stability, and the involvement of complex multistep processes to generate them [118]. In the present work we overcome some of the problems described above, by using a simple approach based on inverse micelles. IMMSG NPs were prepared using pharmaceutical excipients which are GRAS (generally regarded as safe) listed, and possess biocompatible and biodegradable properties. Furthermore, antigen encapsulated in IMMSG NPs turned out to be much more

biological active ($85 \pm 5\%$) using ELISA in comparison to previously described antigen-loaded Chitosan-PLGA NPs ($65 \pm 5\%$) [12].

We evaluated the antigen delivery efficacy of our novel particulate system (IMSG NPs) by immunizing mice via three different routes (IN, ID and TF). To this end, we firstly evaluated the performance of OVA encapsulated IMSG NPs over OVA solution and the previously evaluated OVA-loaded Chit-PLGA NPs for TF delivery. We observed a significantly ($p < 0.001$) higher follicular uptake of OVA encapsulated IMSG NPs compared to OVA solution and OVA-loaded Chit-PLGA NPs (Fig. 3). This is in line with previous results obtained by Raber et al. who showed that penetration of nanoparticles into hair follicles is material dependent [124]. Moreover, we observed strong induction of OVA-specific T cells proliferation by IMSG NPs in comparison to the previously evaluated OVA-loaded Chit-PLGA NPs [12] using an adoptive T cell transfer mouse model (Fig. 4).

In case of the ID route, recent studies showed that ID delivery of antigen is more efficient in stimulating antigen-specific immune responses compared to intramuscular injection, even using low antigenic doses [125]. This is further supported by data from Bal et al. showing the beneficial effect of delivering antigen using nanoparticles via ID route [65]. Our data demonstrated that similar results can be obtained using IMSG NPs. Furthermore, immunization with OVA and c-di-AMP co-encapsulated IMSG NPs significantly increased OVA-specific IgG titers. The enhanced humoral response most likely is based on the combination of the strong adjuvant activity of c-di-AMP and the depot effect created by the oily character of the IMSG NPs-based system, which in turn ensures antigen and adjuvant release in a sustained manner. Furthermore, co-encapsulation of adjuvant in the NPs significantly boosted the production of the IgG2c subclass, thereby indicating an enhanced Th1 response. In contrast, administration of OVA-

encapsulated NPs or soluble OVA admixed with c-di-AMP does not significantly affect the polarization of the antigen-stimulated Th response. This is in line with previous observations demonstrating that co-encapsulation of antigen and adjuvant in the same NPs is crucial for a potent immune response due to concomitant delivery of antigen and adjuvant to the same APC [42, 123, 126]. Interestingly, although TF vaccination with OVA + c-di-AMP co-encapsulated in IMMSG NPs also promoted strong OVA-specific IgG responses, no shift towards a more balanced Th1/Th2 response was observed. This might be explained by the interaction of IMMSG NPs with different APCs at the different anatomic niches. In the epidermal area of the hair follicle canal mainly langerhans cells (LCs) are resident, whereas the dermal area is populated by dermal DCs [127]. Both DC subsets were shown to be able to stimulate different, if not opposing, adaptive immune responses. This is not only based on the cytokines produced by these cells following interaction with the antigen and/or adjuvant, but also due to differences in their intrinsic properties, such as cross-presentation [128]. Further studies are needed to elucidate the underlying mechanisms, but several aspects such as miscibility of oil components with sebum and pH gradient might play a significant role. However, IN delivery of OVA-loaded IMMSG NPs with or without co-encapsulation of c-di-AMP generated only poor antibody responses, if any at all. Presumably, oil viscosity hindered the delivery of antigen and adjuvants through the nasal epithelium. Interestingly, in contrast to what was observed following ID and TF immunization, only mice receiving OVA + c-di-AMP solution via IN route showed increased levels of IgG2c. These results are in line with previous studies showing that co-administration of antigens (OVA as well as vaccine antigens) c-di-AMP by IN route triggers an efficient and balanced Th1/Th2/Th17 response [95].

T cell-mediated immunity is a central element of the adaptive immune system, which is needed to eliminate pathogens or malignant cells. Thus, we evaluated cellular immune responses following immunization with IMMSG NP-based formulations by different routes. Consistent with the humoral responses stimulated after vaccination via ID and TF route, OVA and c-di-AMP co-encapsulated within IMMSG NPs stimulated the strongest cellular responses, both at local and systemic level. In contrast, when mice were immunized via IN route using this formulation, increased proliferative capacity of antigen-specific cells was only observed at local level. However, this cellular response was significantly weaker compared to that stimulated by soluble OVA admixed with c-di-AMP. Nevertheless, when the cytokine profiles of antigen-restimulated cells were analyzed, increased levels of cytokines (e.g. IFN γ) were detected in the group receiving OVA and c-di-AMP co-encapsulated IMMSG NPs and OVA + c-di-AMP solution. This suggests that despite the fact that the overall immunogenicity of the IMMSG NP-based formulation was rather modest, it was sufficient for priming. Furthermore, adjuvantation with c-di-AMP seems to be essential to stimulate IFN γ production. Nevertheless, the concurrent expression of the Th1 associated cytokine IFN γ and the Th2 associated cytokines IL-5 and IL-13 indicate a balanced Th1/Th2 response, which is in line with the observed IgG subclass profiles. Interestingly, TF immunization also resulted in enhanced expression of IL-17, whereas vaccination via ID route did not. This is consistent with observations by Igyártó et al. showing that epidermis resident LCs promote the stimulation of Th17 cells, whereas dermis resident DCs rather stimulate Th1 responses and inhibit Th17 differentiation [128]. While Th17 responses were shown to play an important role in host protection against extracellular pathogens (e.g. bacteria and fungi), Th1 responses are needed to

efficiently protect against intracellular bacterial and viral infections (reviewed in [129, 130].

Vaccination using IMMSG NPs seems to stimulate only strong CD4⁺ T helper responses, since only marginal activation of antigen-specific CD8⁺ T cells could be observed. Most likely this failure is based on the oily nature of the formulations, as similar observations were made with Freund's incomplete adjuvant (IFA, a water-in-oil emulsion), as well as with oil-in-water emulsions (e.g. MF59 and AS03) [131]. IFA is one of the most commonly used adjuvants in research and is prepared from non-metabolizable oils (paraffin oil and mannide monooleate), whereas MF59 and AS03 adjuvants encompass squalene, one of the most common lipids produced by human skin cells, forming oil-in-water nano-emulsions made up of <250 nm droplets [131, 132]. Both types of adjuvants preferentially polarize the T cell response towards a functional Th2 phenotype by a yet unknown mechanism [133]. Possible explanations can be (i) a depot effect, (ii) enhanced antigen uptake by DCs and (iii) altered cellular lipid metabolism [134-136]. In case of IFA, it has been suggested that NOD2, an intracellular pattern recognition receptor recognizing bacterial component, modulates the adjuvanticity of IFA [137]. Incorporation of a potent CD8⁺ stimulating adjuvant might favor stimulation of IFN γ producing CD8⁺ by IMMSG NPs-based formulations. Antigen concentration could be also optimized, since Ebensen et al. showed efficient stimulation of cytotoxic T cells after IN immunization by increasing the OVA dosage [95].

There is a consensus that efficient protection against infection not only depends on the number of antigen-specific T cells but also on their functional properties. T cells which produce several cytokines at the time are more potent as compared to single producers [98]. In this regard, the quality of the T helper response stimulated using OVA and c-di-AMP co-encapsulated IMMSG NPs was significantly

improved. OVA and c-di-AMP co-encapsulated in IMMSG NPs stimulated the highest values of bi- and tri-functional CD4⁺ T cells following ID and TF immunization. Interestingly, also IN vaccination resulted in the stimulation of multifunctional CD4⁺ cells, although to a lesser extent compared to the adjuvanted OVA solution. This is particularly important considering that in some infections stimulation of multifunctional CD4⁺ T cells seems to be even more critical than activation of CD8⁺ T cells to confer protection [114, 115].

4.6. Conclusion

The results presented in this study showed IMMSG NPs as a unique delivery system with enhance protein encapsulating efficacy and stability. Moreover, co-encapsulation of an adjuvant inside the particles resulted in enhanced humoral and cellular immune responses both at local and systemic level when mice were immunized by ID or TF route. Immunization of mice with OVA + c-di-AMP co-encapsulated in IMMSG NPs also stimulated strong antigen-specific multifunctional CD4⁺ T helper responses with bi- and tri-functional capacity. Thus, IMMSG NPs constitute a promising delivery system for the establishment of ID and TF vaccination strategies.

5. Overall Conclusion and Outlook

The major aim of this thesis was to highlight the potential of transfollicular delivery of a model antigen (ovalbumin) using nanoparticles based delivery systems without pre-treating the skin for non-invasive transcutaneous vaccination. Nanoparticles (NPs) are the ideal vehicles for transfollicular delivery as they accumulate in hair follicles and skin folds and penetrate deeper into hair follicles than molecules in solution. In literature, vaccination via the transfollicular pathway using NPs has been shown to generate effective immune responses, however much of this work was conducted after pretreating the skin area in various ways such as by plucking the hairs, waxing, or cyanoacrylate (superglue) stripping. As a result of pre-treatment, the stratum corneum is (at least partially) removed, meaning that it is not clear to which extent the antigen penetrates via the hair follicles or across the permeabilized stratum corneum. In contrast, the results reported here have demonstrated the potential of NPs to deliver antigen and adjuvant via the transfollicular route without pre-treating the skin. Furthermore, we have demonstrated the significance of nanoparticulate delivery systems in influencing the immune response generated via this vaccination pathway, thus providing a platform to support rational design of vaccines combining antigen and adjuvants in a particulate system in order to generate efficient immune responses and create safe vaccines.

- As was shown in the first section of this thesis, immune responses can be generated via the transfollicular route without disrupting the stratum corneum barrier by using polymeric NPs. This was demonstrated by *in vitro* and *in vivo* experiments. Firstly, the efficacy of polymeric NPs (polylactic-

co-glycolide (PLGA) and Chitosan-PLGA NPs) in enhancing follicular uptake of ovalbumin (OVA) in comparison to OVA solution was tested using an *in vitro* pig ear model. A 2-3 fold enhancement in follicular uptake was observed when antigen was encapsulated into NPs. Moreover, in a cell culture assay, the ability of NPs to stimulate proliferation of OVA-specific T cells in comparison to OVA in solution was evaluated. An enhanced proliferation of OVA-specific T cells (CD4⁺ T cells) was observed when antigen was encapsulated into NPs. However, only OVA-loaded Chitosan-PLGA NPs were able to stimulate proliferation of CD8⁺ T cells to a large extent in comparison to OVA in solution. Secondly, by *in vivo* experiments using an adoptive transfer model, we could show generation of immune responses by the transfollicular route using OVA-loaded Chitosan-PLGA NPs. Moreover, the immune response generated by OVA-loaded NPs following transfollicular administration was able to elicit the same proliferation of OVA-specific CD4⁺ T cells as an intramuscular injection of OVA.

- As the adoptive transfer experiment showed the viability of the transfollicular route, an extensive characterization of the immune responses generated by this route was further required. Therefore, in the second section of this thesis, *in vivo* mouse studies were extended to a normal vaccination setting (conventional mice) to confirm the viability of the transfollicular route, as well as to obtain deeper insights into the immune responses generated using antigen-loaded Chitosan-PLGA NPs without skin pre-treatment. Additionally, we tested the integrity of skin using

transepidermal water loss (TEWL) measurements before and after depilation and for the following 2 days to ensure skin integrity before applying formulations on skin. Interestingly, we found that TEWL measurements 30 min after depilation were double those of the normal untreated skin; a return to baseline levels, as recorded before depilation, was however seen within 2 days, indicating a full recovery. Moreover, immune responses generated by applying different formulations (OVA loaded Chitosan-PLGA NPs and OVA solution) on tape stripped and intact skin were also compared. Furthermore, immune responses generated by applying antigen-loaded NPs on untreated skin in the presence (co-admixed) or absence of an adjuvant (bis-(3',5')-cyclic dimeric adenosine monophosphate (c-di-AMP)) were characterized. We could show from our *in vivo* studies that inclusion of an adjuvant is necessary in the formulation along with nanoparticulate system in order to generate both efficient antigen-specific humoral as well as cellular immune responses based on multifunctional CD4⁺ and CD8⁺ T cells when no pre-treatment was applied on skin.

- Preparation of Chitosan-PLGA NPs by the emulsion-diffusion-evaporation method involves multiple steps with use of chemical solvents and physical stresses during the production process that may negatively affect antigen stability. Therefore, we planned to fabricate a new particulate system with (i) enhanced stability of the encapsulated protein; (ii) simplified preparation method; (iii) co-encapsulation of adjuvant and antigen in the same system (as in literature, co-encapsulation of antigen and adjuvant in the same NPs has been shown to generate better immune response due to concomitant delivery of antigen and adjuvant to the same dendritic cells (DCs)); (iv)

enhanced follicular uptake; and (v) ease of formulation applicability on skin. These points motivated us to perform the studies described in the third section of this thesis. Inverse micellar sugar glass NPs were prepared using an inverse micellar technique and pharmaceutically accepted excipients (surfactants, sugars and oil, GRAS (generally regarded as safe) listed) and characterized for efficient incorporation and stabilization of antigen. At first, we tested the integrity and stability of the encapsulated antigen, OVA, using SDS PAGE and ELISA and compared these results with previously prepared Chitosan-PLGA NPs. Moreover, we compared follicular uptake efficacy and immune responses generated by inverse micellar sugar glass NPs with Chitosan-PLGA NPs *in vitro* using a pig ear model, and *in vivo* using an adoptive transfer mouse model. We observed superiority of inverse micellar sugar glass NPs in terms of stabilization of the encapsulated antigen, delivery of antigen into hair follicles and proliferation of antigen-specific T cells in comparison to antigen loaded Chitosan-PLGA NPs. Next, we evaluated the immune response generated by inverse micellar sugar glass NPs with or without adjuvant in a conventional mouse model after transfollicular application. Moreover, we tested inverse micellar sugar glass NPs delivered intranasally and intradermally, in order to study the effectiveness of this formulation when administered via other routes. In the case of intranasal delivery, no or low immune response was generated, presumably due to the viscosity of the oil component of the formulation, which hindered the delivery of antigen and adjuvants through the nasal epithelium. This showed that such a delivery system is not suitable for application via the nasal route. Interestingly, in case of the intradermal route, OVA-loaded sugar glass NPs generated similar humoral response

compared to OVA protein co-administered with c-di-AMP indicating the beneficial effect of NPs. Moreover, enhanced humoral and cellular responses both at local and systemic level were observed when OVA + c-di AMP loaded NPs were administered. In case of transfollicular route, enhanced humoral and cellular response were also observed in mice immunized with OVA + c-di AMP loaded NPs. However, immune responses generated by transfollicular vaccination were less strong in comparison to intradermal vaccination. These data further support the inherent potential of transfollicular vaccination in conjunction with nanotechnology, but also showed the need to further optimize the carrier technology to achieve a robust immune response. In summary, inverse micellar sugar glass NPs constitute a promising delivery system for the establishment of intradermal and transfollicular vaccination strategies.

Suggestions for Future work:

Based on our studies so far, vaccination via the transfollicular route holds the potential to generate effective immune responses for the development of patient-compliant, needle-free, safe vaccines. However, the major challenge is to deliver antigen to peri-follicular antigen presenting cells in order to generate an efficient immune response. Results from this thesis have shown the potential of nanoparticulate systems to deliver antigen to the peri-follicular region; at the same time however, it has been demonstrated that it is necessary to include an adjuvant in such nanoparticulate formulations to modulate the immune response via transfollicular route. Future work should focus on i) mechanistic studies for better understanding the translocation as well as uptake mechanism of the antigen and/or adjuvant by antigen presenting cells after transfollicular application, ii)

validation studies using disease relevant antigens (e.g. influenza virus antigens, hepatitis C virus) in mouse as well as other pre-clinical models, and iii) further development in terms of fabrication of particulate systems for transfollicular delivery. Although the particulate systems studied in this thesis showed improved transfollicular delivery and enhanced immune responses in comparison to OVA solution, further modifications of the studied systems or in fact new particulate system could enhance the effectiveness of this approach. These efforts should focus on i) improving the targeting efficacy of NPs to the hair follicle as large amount of NPs (~90%) were lost on the skin surface or during application, and ii) optimizing nanoparticulate systems with a special focus on studies of the impact of adjuvant type and degree of NP association (co-mixed, NP surface decorated or co-encapsulated). Such studies would lead to the development of a more robust delivery system.

6. List of Abbreviations

APCs	Antigen presenting cells
BSA	Bovine serum albumin
CD 4 or CD 8	Clusters of differentiation (4 or 8)
CFSE	Carboxyfluoresceine succinimidyl ester
Chit-PLGA	Chitosan-PLGA
CPM	Counts per minute
DCs	Dendritic cells
ELISA	Enzyme linked Immuno assay
FACS	Fluorescence activated cell sorting
FITC	Fluorescein isothiocyanate
GRAS	Generally regarded as safe
I.D.	Intradermal
I.N.	Intranasal
IFN γ	Interferon gamma
IL	Interleukin
IMSG NPs	Inverse micellar sugar glass nanoparticles
LCs	Langerhans cells
LPS	Lipopolysaccharide
MCT	Medium chain triglycerides
MPs	Microparticles
NALT	Nasal associated lymphoid tissue
NPs	Nanoparticles

OVA	Ovalbumin
PBS	Phosphate buffer saline
PDI	Polydispersity index
PLGA	Poly lactide-co-glicolide
PVA	Polyvinyl alcohol
RPMI	Roswell Park Memorial Medium
SC	Stratum corneum
SD	Standard deviation
SDS PAGE	Sodium dodecyl sulfate polyacrylamide gel electrophoresis
SEM	Scanning electron microscopy
SEM	Standard error mean
SI	Stimulation Index
T.F.	Transfollicular
TCI	Transcutaneous Immunization
TCV	Transcutaneous vaccination
TEM	Transmission electron microscopy
TEWL	Transepidermal water loss
Th1 / Th2	T helper cells (1 or 2)
TNF α	Tumor necrosis factor-alpha

References

- [1] G. Cevc, G. Blume, Lipid Vesicles Penetrate into Intact Skin Owing to the Transdermal Osmotic Gradients and Hydration Force, *Biochim Biophys Acta*, 1104 (1992) 226-232.
- [2] T. Gratieri, U.F. Schaefer, L.H. Jing, M.Y. Gao, K.H. Kostka, R.F.V. Lopez, M. Schneider, Penetration of Quantum Dot Particles Through Human Skin, *J Biomed Nanotechnol*, 6 (2010) 586-595.
- [3] P.N. Gupta, V. Mishra, A. Rawat, P. Dubey, S. Mahor, S. Jain, D.P. Chatterji, S.P. Vyas, Non-invasive vaccine delivery in transfersomes, niosomes and liposomes: a comparative study, *Int J Pharm*, 293 (2005) 73-82.
- [4] A. Paul, G. Cevc, B.K. Bachhawat, Transdermal immunisation with an integral membrane component, gap junction protein, by means of ultradeformable drug carriers, transfersomes, *Vaccine*, 16 (1998) 188-195.
- [5] B. Geusens, M. Van Gele, S. Braat, S.C. De Smedt, M.C.A. Stuart, T.W. Prow, W. Sanchez, M.S. Roberts, N.N. Sanders, J. Lambert, Flexible Nanosomes (SECosomes) Enable Efficient siRNA Delivery in Cultured Primary Skin Cells and in the Viable Epidermis of Ex Vivo Human Skin, *Adv Funct Mater*, 20 (2010) 4077-4090.
- [6] D. Mishra, P.K. Mishra, V. Dubey, M. Nahar, S. Dabadghao, N.K. Jain, Systemic and mucosal immune response induced by transcutaneous immunization using Hepatitis B surface antigen-loaded modified liposomes, *Eur J Pharm Sci*, 33 (2008) 424-433.
- [7] J. Wang, J.H. Hu, F.Q. Li, G.Z. Liu, Q.G. Zhu, J.Y. Liu, H.J. Ma, C. Peng, F.G. Si, Strong cellular and humoral immune responses induced by

- transcutaneous immunization with HBsAg DNA-cationic deformable liposome complex, *Exp Dermatol*, 16 (2007) 724-729.
- [8] S. Hansen, C.M. Lehr, Nanoparticles for transcutaneous vaccination, *Microb Biotechnol*, 5 (2012) 156-167.
- [9] E.L. Romero, M.J. Morilla, Topical and mucosal liposomes for vaccine delivery, *Wires Nanomed Nanobi*, 3 (2011) 356-375.
- [10] J.P. Ryman-Rasmussen, J.E. Riviere, N.A. Monteiro-Riviere, Penetration of intact skin by quantum dots with diverse physicochemical properties, *Toxicol Sci*, 91 (2006) 159-165.
- [11] A. Patzelt, H. Richter, F. Knorr, U. Schafer, C.M. Lehr, L. Dahne, W. Sterry, J. Lademann, Selective follicular targeting by modification of the particle sizes, *J Control Release*, 150 (2011) 45-48.
- [12] A. Mittal, A.S. Raber, U.F. Schaefer, S. Weissmann, T. Ebensen, K. Schulze, C.A. Guzman, C.M. Lehr, S. Hansen, Non-invasive delivery of nanoparticles to hair follicles: A perspective for transcutaneous immunization, *Vaccine*, 31 (2013) 3442-3451.
- [13] U. Jacobi, K. Engel, A. Patzelt, M. Worm, W. Sterry, J. Lademann, Penetration of pollen proteins into the skin, *Skin Pharmacol Phys*, 20 (2007) 297-304.
- [14] H.R. Fan, Q. Lin, G.R. Morrissey, P.A. Khavari, Immunization via hair follicles by topical application of naked DNA to normal skin, *Nat Biotechnol*, 17 (1999) 870-872.
- [15] D.S. Shaker, B.R. Sloat, U.M. Le, C.V. Lohr, N. Yanasarn, K.A. Fischer, Z. Cui, Immunization by application of DNA vaccine onto a skin area wherein the hair follicles have been induced into anagen-onset stage, *Mol Ther*, 15 (2007) 2037-2043.

- [16] R.B. Baleeiro, K.H. Wiesmuller, Y. Reiter, B. Baude, L. Dahne, A. Patzelt, J. Lademann, J.A. Barbuto, P. Walden, Topical Vaccination with Functionalized Particles Targeting Dendritic Cells, *J Invest Dermatol*, 133 (2013) 1933-1941.
- [17] B. Combadiere, A. Vogt, B. Mahe, D. Costagliola, S. Hadam, O. Bonduelle, W. Sterry, S. Staszewski, H. Schaefer, S. van der Werf, C. Katlama, B. Autran, U. Blume-Peytavi, Preferential Amplification of CD8 Effector-T Cells after Transcutaneous Application of an Inactivated Influenza Vaccine: A Randomized Phase I Trial, *Plos One*, 5 (2010).
- [18] N. Otberg, A. Patzelt, U. Rasulev, T. Hagemeister, M. Linscheid, R. Sinkgraven, W. Sterry, J. Lademann, The role of hair follicles in the percutaneous absorption of caffeine, *Brit J Clin Pharmacol*, 65 (2008) 488-492.
- [19] J. Lademann, H. Richter, A. Teichmann, N. Otberg, U. Blume-Peytavi, J. Luengo, B. Weiss, U.F. Schaefer, C.M. Lehr, R. Wepf, W. Sterry, Nanoparticles - An efficient carrier for drug delivery into the hair follicles, *Eur J Pharm Biopharm*, 66 (2007) 159-164.
- [20] S. Mitragotri, Mechanical Disruption of Skin Barrier for Vaccine Delivery, *Drug Delivery System*, 27 (2012) 202-212
- [21] R.F.V. Lopez, J.E. Seto, D. Blankschtein, R. Langer, Enhancing the transdermal delivery of rigid nanoparticles using the simultaneous application of ultrasound and sodium lauryl sulfate, *Biomaterials*, 32 (2011) 933-941.
- [22] P. Karande, S. Mitragotri, Transcutaneous Immunization: An Overview of Advantages, Disease Targets, Vaccines, and Delivery Technologies, *Annu Rev Chem Biomol*, 1 (2010) 175-201.

- [23] J. Lisziewicz, E. Rosenberg, J. Lieberman, H. Jessen, L. Lopalco, R. Siliciano, B. Walker, F. Lori, Control of HIV despite the discontinuation of antiretroviral therapy, *New Engl J Med*, 340 (1999) 1683-1684.
- [24] L. Gudmundsdotter, B. Wahren, B.K. Haller, A. Boberg, U. Edback, D. Bernasconi, S. Butto, H. Gaines, N. Imami, F. Gotch, F. Lori, J. Lisziewicz, E. Sandstrom, B. Hejdeman, Amplified antigen-specific immune responses in HIV-1 infected individuals in a double blind DNA immunization and therapy interruption trial, *Vaccine*, 29 (2011) 5558-5566.
- [25] J. Lisziewicz, N. Bakare, S.A. Calarota, D. Banhegyi, J. Szlavik, E. Ujhelyi, E.R. Toke, L. Molnar, Z. Lisziewicz, B. Autran, F. Lori, Single DermaVir Immunization: Dose-Dependent Expansion of Precursor/Memory T Cells against All HIV Antigens in HIV-1 Infected Individuals, *Plos One*, 7 (2012).
- [26] J. Williams, L. Fox-Leyva, C. Christensen, D. Fisher, E. Schlichting, M. Snowball, S. Negus, J. Mayers, R. Koller, R. Stout, Hepatitis A vaccine administration: comparison between jet-injector and needle injection, *Vaccine*, 18 (2000) 1939-1943.
- [27] C. Mathei, P. VanDamme, A. Meheus, Hepatitis B vaccine administration: Comparison between jet-gun and syringe and needle, *Vaccine*, 15 (1997) 402-404.
- [28] J.D. Millar, L. Morris, A. Macedo Filho, T.M. Mack, W. Dyal, A.A. Medeiros, The introduction of jet injection mass vaccination into the national smallpox eradication program of Brazil, *Trop Geogr Med*, 23 (1971) 89-101.
- [29] J. Abb, F. Deinhardt, J. Eisenburg, The Risk of Transmission of Hepatitis-B Virus Using Jet Injection in Inoculation, *J Infect Dis*, 144 (1981) 179-179.
- [30] P.C. DeMuth, W.F. Garcia-Beltran, M.L. Ai-Ling, P.T. Hammond, D.J. Irvine, Composite Dissolving Microneedles for Coordinated Control of Antigen and

- Adjuvant Delivery Kinetics in Transcutaneous Vaccination, *Adv Funct Mater*, 23 (2013) 161-172.
- [31] M. Singh, A. Chakrapani, D. O'Hagon, Nanoparticles and microparticles as vaccine-delivery systems, *Expert Rev Vaccines*, 6 (2007) 797-808.
- [32] P.L. Mottram, D. Leong, B. Crimeen-Irwin, S. Gloster, S.D. Xiang, J. Meanger, R. Ghildyal, N. Vardaxis, M. Plebanski, Type 1 and 2 immunity following vaccination is influenced by nanoparticle size: Formulation of a model vaccine for respiratory syncytial virus, *Mol Pharmaceut*, 4 (2007) 73-84.
- [33] F. Rancan, Q. Gao, C. Graf, S. Troppens, S. Hadam, S. Hackbarth, C. Kembuan, U. Blume-Peytavi, E. Ruhl, J. Lademann, A. Vogt, Skin Penetration and Cellular Uptake of Amorphous Silica Nanoparticles with Variable Size, Surface Functionalization, and Colloidal Stability, *Acs Nano*, 6 (2012) 6829-6842.
- [34] Y.F. Ma, Y. Zhuang, X.F. Xie, C. Wang, F. Wang, D.M. Zhou, J.Q. Zeng, L.T. Cai, The role of surface charge density in cationic liposome-promoted dendritic cell maturation and vaccine-induced immune responses, *Nanoscale*, 3 (2011) 2307-2314.
- [35] L.H. Higa, P. Schilrreff, A.P. Perez, M.A. Iriarte, D.I. Roncaglia, M.J. Morilla, E.L. Romero, Ultradeformable archaeosomes as new topical adjuvants, *Nanomed-Nanotechnol*, 8 (2012) 1319-1328.
- [36] T. Uto, T. Akagi, T. Hamasaki, M. Akashi, M. Baba, Modulation of innate and adaptive immunity by biodegradable nanoparticles, *Immunol Lett*, 125 (2009) 46-52.
- [37] S.A. Frech, H.L. DuPont, A.L. Bourgeois, R. McKenzie, J. Belkind-Gerson, J.F. Figueroa, P.C. Okhuysen, N.H. Guerrero, F.G. Martinez-Sandoval, J.H.M. Melendez-Romero, Z.D. Jiang, E.J. Asturias, J. Halpern, O.R. Torres,

- A.S. Hoffman, C.P. Villar, R.N. Kassem, D.C. Flyer, B.H. Andersen, K. Kazempour, S.A. Breisch, G.M. Glenn, Use of a patch containing heat-labile toxin from *Escherichia coli* against travellers' diarrhoea: a phase II, randomised, double-blind, placebo-controlled field trial, *Lancet*, 371 (2008) 2019-2025.
- [38] R.K. Gupta, E.H. Relyveld, E.B. Lindblad, B. Bizzini, S. Benefraim, C.K. Gupta, Adjuvants - a Balance between Toxicity and Adjuvanticity, *Vaccine*, 11 (1993) 293-306.
- [39] M. Diwan, P. Elamanchili, M. Cao, J. Samuel, Dose sparing of CpG oligodeoxynucleotide vaccine adjuvants by nanoparticle delivery, *Curr Drug Deliv*, 1 (2004) 405-412.
- [40] K.D. Wilson, S.D. de Jong, Y.K. Tam, Lipid-based delivery of CpG oligonucleotides enhances immunotherapeutic efficacy, *Adv Drug Deliver Rev*, 61 (2009) 233-242.
- [41] A. Bershteyn, M.C. Hanson, M.P. Crespo, J.J. Moon, A.V. Li, H. Suh, D.J. Irvine, Robust IgG responses to nanograms of antigen using a biomimetic lipid-coated particle vaccine, *J Control Release*, 157 (2012) 354-365.
- [42] S. Fischer, E. Schlosser, M. Mueller, N. Csaba, H.P. Merkle, M. Groettrup, B. Gander, Concomitant delivery of a CTL-restricted peptide antigen and CpG ODN by PLGA microparticles induces cellular immune response, *J Drug Target*, 17 (2009) 652-661.
- [43] E. Schlosser, M. Mueller, S. Fischer, S. Basta, D.H. Busch, B. Gander, M. Groettrup, TLR ligands and antigen need to be coencapsulated into the same biodegradable microsphere for the generation of potent cytotoxic T lymphocyte responses, *Vaccine*, 26 (2008) 1626-1637.

- [44] S.M. Bal, S. Hortensius, Z. Ding, W. Jiskoot, J.A. Bouwstra, Co-encapsulation of antigen and Toll-like receptor ligand in cationic liposomes affects the quality of the immune response in mice after intradermal vaccination, *Vaccine*, 29 (2011) 1045-1052.
- [45] G.M. Glenn, D.N. Taylor, X.R. Li, S. Frankel, A. Montemarano, C.R. Alving, Transcutaneous immunization: A human vaccine delivery strategy using a patch, *Nat Med*, 6 (2000) 1403-1406.
- [46] B. Combadiere, B. Mahe, Particle-based vaccines for transcutaneous vaccination, *Comp Immunol Microb*, 31 (2008) 293-315.
- [47] G.M. Glenn, R.T. Kenney, Mass vaccination: Solutions in the skin, *Curr Top Microbiol*, 304 (2006) 247-268.
- [48] A. Domashenko, S. Gupta, G. Cotsarelis, Efficient delivery of transgenes to human hair follicle progenitor cells using topical lipoplex, *Nat Biotechnol*, 18 (2000) 420-423.
- [49] Z. Yu, W.G. Chung, B.R. Sloat, C.V. Lohr, R. Weiss, B.L. Rodriguez, X.R. Li, Z.R. Cui, The extent of the uptake of plasmid into the skin determines the immune responses induced by a DNA vaccine applied topically onto the skin, *J Pharm Pharmacol*, 63 (2011) 199-205.
- [50] H.J. Weigmann, J. Lademann, H. Meffert, H. Schaefer, W. Sterry, Determination of the horny layer profile by tape stripping in combination with optical spectroscopy in the visible range as a prerequisite to quantify percutaneous absorption, *Skin Pharmacol Appl*, 12 (1999) 34-45.
- [51] M.D. Blanco, M.J. Alonso, Development and characterization of protein-loaded poly(lactide-co-glycolide) nanospheres, *Eur J Pharm Biopharm*, 43 (1997) 287-294.

- [52] C. Schulze, U.F. Schaefer, C.A. Ruge, W. Wohlleben, C.M. Lehr, Interaction of metal oxide nanoparticles with lung surfactant protein A, *Eur J Pharm Biopharm*, 77 (2011) 376-383.
- [53] J. Lademann, H.J. Weigmann, S. Schanzer, H. Richter, H. Audring, C. Antoniou, G. Tsikrikas, H. Gers-Barlag, W. Sterry, Optical investigations to avoid the disturbing influences of furrows and wrinkles quantifying penetration of drugs and cosmetics into the skin by tape stripping, *J Biomed Opt*, 10 (2005).
- [54] B. Weiss, U.F. Schaefer, J. Zapp, A. Lamprecht, A. Stallmach, C.M. Lehr, Nanoparticles made of fluorescence-labelled poly(L-lactide-co-glycolide): Preparation, stability, and biocompatibility, *J Nanosci Nanotechnol*, 6 (2006) 3048-3056.
- [55] C. Liard, S. Munier, M. Arias, A. Joulin-Giet, O. Bonduelle, D. Duffy, R.J. Shattock, B. Verrier, B. Combadiere, Targeting of HIV-p24 particle-based vaccine into differential skin layers induces distinct arms of the immune responses, *Vaccine*, 29 (2011) 6379-6391.
- [56] B. Mahe, A. Vogt, C. Liard, D. Duffy, V. Abadie, O. Bonduelle, A. Boissonnas, W. Sterry, B. Verrier, U. Blume-Peytavi, B. Combadiere, Nanoparticle-Based Targeting of Vaccine Compounds to Skin Antigen-Presenting Cells By Hair Follicles and their Transport in Mice, *J Invest Dermatol*, 129 (2009) 1156-1164.
- [57] P.E. Taylor, K.W. Jacobson, J.M. House, M.M. Glovsky, Links between pollen, atopy and the asthma epidemic, *Int Arch Allergy Imm*, 144 (2007) 162-170.
- [58] A.C. Gilliam, I.B. Kremer, Y. Yoshida, S.R. Stevens, E. Tootell, M.B.M. Teunissen, C. Hammerberg, K.D. Cooper, The human hair follicle: A

- reservoir of CD40(+) B7-deficient Langerhans cells that repopulate epidermis after UVB exposure, *J Invest Dermatol*, 110 (1998) 422-427.
- [59] J.W. Streilein, L.W. Lonsberry, P.R. Bergstresser, Depletion of Epidermal Langerhans Cells and Ia Immunogenicity from Tape-Stripped Mouse Skin, *J Exp Med*, 155 (1982) 863-871.
- [60] M. Amidi, E. Mastrobattista, W. Jiskoot, W.E. Hennink, Chitosan-based delivery systems for protein therapeutics and antigens, *Adv Drug Deliver Rev*, 62 (2010) 59-82.
- [61] D.T. O'Hagan, M. Singh, R.K. Gupta, Poly(lactide-co-glycolide) microparticles for the development of single-dose controlled-release vaccines, *Adv Drug Deliver Rev*, 32 (1998) 225-246.
- [62] S.S. Pai, R.D. Tilton, T.M. Przybycien, Poly(ethylene glycol)-Modified Proteins: Implications for Poly(lactide-co-glycolide)-Based Microsphere Delivery, *Aaps J*, 11 (2009) 88-98.
- [63] S.R. Mao, W. Sun, T. Kissel, Chitosan-based formulations for delivery of DNA and siRNA, *Adv Drug Deliver Rev*, 62 (2010) 12-27.
- [64] S. Taetz, N. Nafee, J. Beisner, K. Piotrowska, C. Baldes, T.E. Murdter, H. Huwer, M. Schneider, U.F. Schaefer, U. Klotz, C.M. Lehr, The influence of chitosan content in cationic chitosan/PLGA nanoparticles on the delivery efficiency of antisense 2'-O-methyl-RNA directed against telomerase in lung cancer cells, *Eur J Pharm Biopharm*, 72 (2009) 358-369.
- [65] S.M. Bal, B. Slutter, E. van Riet, A.C. Kruithof, Z. Ding, G.F.A. Kersten, W. Jiskoot, J.A. Bouwstra, Efficient induction of immune responses through intradermal vaccination with N-trimethyl chitosan containing antigen formulations, *J Control Release*, 142 (2010) 374-383.

- [66] C.M. Lehr, J.A. Bouwstra, E.H. Schacht, H.E. Junginger, *In vitro* Evaluation of Mucoadhesive Properties of Chitosan and Some Other Natural Polymers, *Int J Pharm*, 78 (1992) 43-48.
- [67] M. Friede, M.T. Aguado, Need for new vaccine formulations and potential of particulate antigen and DNA delivery systems, *Adv Drug Deliver Rev*, 57 (2005) 325-331.
- [68] Y. Men, C. Thomasin, H.P. Merkle, B. Gander, G. Corradin, A Single Administration of Tetanus Toxoid in Biodegradable Microspheres Elicits T-Cell and Antibody-Responses Similar or Superior to Those Obtained with Aluminum Hydroxide, *Vaccine*, 13 (1995) 683-689.
- [69] Y. Ogawa, H. Okada, T. Heya, T. Shimamoto, Controlled Release of Lhrh Agonist, Leuprolide Acetate, from Microcapsules - Serum Drug Level Profiles and Pharmacological Effects in Animals, *J Pharm Pharmacol*, 41 (1989) 439-444.
- [70] P. Riesz, T. Kondo, Free-Radical Formation Induced by Ultrasound and Its Biological Implications, *Free Radical Bio Med*, 13 (1992) 247-270.
- [71] A.S. Determan, J.H. Wilson, M.J. Kipper, M.J. Wannemuehler, B. Narasimhan, Protein stability in the presence of polymer degradation products: Consequences for controlled release formulations, *Biomaterials*, 27 (2006) 3312-3320.
- [72] M.L. Ye, S. Kim, K. Park, Issues in long-term protein delivery using biodegradable microparticles, *J Control Release*, 146 (2010) 241-260.
- [73] G. Crotts, T.G. Park, Stability and release of bovine serum albumin encapsulated within poly(D,L-lactide-co-glycolide) microparticles, *J Control Release*, 44 (1997) 123-134.

- [74] J. Banchereau, R.M. Steinman, Dendritic cells and the control of immunity, *Nature*, 392 (1998) 245-252.
- [75] B. Ludewig, T. Junt, H. Hengartner, R.M. Zinkernagel, Dendritic cells in autoimmune diseases, *Curr Opin Immunol*, 13 (2001) 657-662.
- [76] Y.Y. Lan, Z.L. Wang, G. Raimondi, W.H. Wu, B.L. Colvin, A. De Creus, A.W. Thomson, "Alternatively activated" dendritic cells preferentially secrete IL-10, expand Foxp3(+)CD4(+) T cells, and induce long-term organ allograft survival in combination with CTLA4-Ig, *J Immunol*, 177 (2006) 5868-5877.
- [77] S.S. Iyer, A.A. Ghaffari, G. Cheng, Lipopolysaccharide-Mediated IL-10 Transcriptional Regulation Requires Sequential Induction of Type I IFNs and IL-27 in Macrophages, *J Immunol*, 185 (2010) 6599-6607.
- [78] O. Harush-Frenkel, N. Debotton, S. Benita, Y. Altschuler, Targeting of nanoparticles to the clathrin-mediated endocytic pathway, *Biochem Bioph Res Co*, 353 (2007) 26-32.
- [79] C. Keijzer, B. Slutter, R. van der Zee, W. Jiskoot, W. van Eden, F. Broere, PLGA, PLGA-TMC and TMC-TPP Nanoparticles Differentially Modulate the Outcome of Nasal Vaccination by Inducing Tolerance or Enhancing Humoral Immunity, *Plos One*, 6 (2011).
- [80] B. Slutter, L. Plapied, V. Fievez, M.A. Sande, A. des Rieux, Y.J. Schneider, E. Van Riet, W. Jiskoot, V. Preat, Mechanistic study of the adjuvant effect of biodegradable nanoparticles in mucosal vaccination, *J Control Release*, 138 (2009) 113-121.
- [81] M. Yoshida, J.E. Babensee, Molecular aspects of microparticle phagocytosis by dendritic cells, *J Biomat Sci-Polym E*, 17 (2006) 893-907.
- [82] S. Fischer, E. Uetz-von Allmen, Y. Waeckerle-Men, M. Groettrup, H.P. Merkle, B. Gander, The preservation of phenotype and functionality of dendritic cells

- upon phagocytosis of polyelectrolyte-coated PLGA microparticles, *Biomaterials*, 28 (2007) 994-1004.
- [83] K.A. Pape, E.R. Kearney, A. Khoruts, A. Mondino, R. Merica, Z.M. Chen, E. Ingulli, J. White, J.G. Johnson, M.K. Jenkins, Use of adoptive transfer of T-cell-antigen-receptor-transgenic T cells for the study of T-cell activation in vivo, *Immunol Rev*, 156 (1997) 67-78.
- [84] E. Proksch, J. Brasch, W. Sterry, Integrity of the permeability barrier regulates epidermal Langerhans cell density, *Brit J Dermatol*, 134 (1996) 630-638.
- [85] G. Mattheolabakis, G. Lagoumintzis, Z. Panagi, E. Papadimitriou, C.D. Partidos, K. Avgoustakis, Transcutaneous delivery of a nanoencapsulated antigen: Induction of immune responses, *Int J Pharm*, 385 (2010) 187-193.
- [86] OECD, Guidance document for the conduct of skin absorption studies, OECD Series on Testing and Assessment. No 28. Paris: Environment Directorate, (2004).
- [87] S. Mangelsdorf, N. Otberg, H.I. Maibach, R. Sinkgraven, W. Sterry, Ethnic variation in vellus hair follicle size and distribution, *Skin Pharmacol Phys*, 19 (2006) 159-167.
- [88] M. S., Comparative evaluation of skin physiological parameters which influence percutaneous penetration in different animal species, (2006).
- [89] R.L. Bronaugh, R.F. Stewart, E.R. Congdon, Methods for in vitro percutaneous absorption studies. II. Animal models for human skin, *Toxicol Appl Pharmacol*, 62 (1982) 481-488.
- [90] A. Patzelt, H. Richter, R. Buettmeyer, H.J. Huber, U. Blume-Peytavi, W. Sterry, J. Lademann, Differential stripping demonstrates a significant reduction of the hair follicle reservoir in vitro compared to in vivo, *European journal of pharmaceutics and biopharmaceutics : official journal of*

- Arbeitsgemeinschaft für Pharmazeutische Verfahrenstechnik e.V, 70 (2008) 234-238.
- [91] R. Toll, U. Jacobi, H. Richter, J. Lademann, H. Schaefer, U. Blume-Peytavi, Penetration profile of microspheres in follicular targeting of terminal hair follicles, *J Invest Dermatol*, 123 (2004) 168-176.
- [92] V.M. Meidan, M.C. Bonner, B.B. Michniak, Transfollicular drug delivery - Is it a reality?, *Int J Pharm*, 306 (2005) 1-14.
- [93] S.M. Bal, Z. Ding, E. van Riet, W. Jiskoot, J.A. Bouwstra, Advances in transcutaneous vaccine delivery: Do all ways lead to Rome?, *J Control Release*, 148 (2010) 266-282.
- [94] G. Xiao, X.R. Li, A. Kumar, Z.R. Cui, Transcutaneous DNA immunization following waxing-based hair depilation elicits both humoral and cellular immune responses, *Eur J Pharm Biopharm*, 82 (2012) 212-217.
- [95] T. Ebensen, R. Libanova, K. Schulze, T. Yevsa, M. Morr, C.A. Guzman, Bis-(3',5')-cyclic dimeric adenosine monophosphate: Strong Th1/Th2/Th17 promoting mucosal adjuvant, *Vaccine*, 29 (2011) 5210-5220.
- [96] F. Netzlauff, K.H. Kostka, C.M. Lehr, U.F. Schaefer, TEWL measurements as a routine method for evaluating the integrity of epidermis sheets in static Franz type diffusion cells in vitro. Limitations shown by transport data testing, *Eur J Pharm Biopharm*, 63 (2006) 44-50.
- [97] R. Paus, T. Christoph, S. Muller-Rover, Immunology of the hair follicle: A short journey into terra incognita, *J Invest Derm Symp P*, 4 (1999) 226-234.
- [98] R.A. Seder, P.A. Darrah, M. Roederer, T-cell quality in memory and protection: implications for vaccine design, *Nat Rev Immunol*, 8 (2008) 247-258.

- [99] N. Li, L.H. Peng, X. Chen, T.Y. Zhang, G.F. Shao, W.Q. Liang, J.Q. Gao, Antigen-loaded nanocarriers enhance the migration of stimulated Langerhans cells to draining lymph nodes and induce effective transcutaneous immunization, *Nanomedicine*, (2013).
- [100] F. Rancan, S. Amselgruber, S. Hadam, S. Munier, V. Pavot, B. Verrier, S. Hackbarth, B. Combadiere, U. Blume-Peytavi, A. Vogt, Particle-based transcutaneous administration of HIV-1 p24 protein to human skin explants and targeting of epidermal antigen presenting cells, *Journal of controlled release : official journal of the Controlled Release Society*, 176C (2013) 115-122.
- [101] N. Li, L.H. Peng, X. Chen, S. Nakagawa, J.Q. Gao, Effective transcutaneous immunization by antigen-loaded flexible liposome in vivo, *Int J Nanomedicine*, 6 (2011) 3241-3250.
- [102] D. Sen, L. Forrest, T.B. Kepler, I. Parker, M.D. Cahalan, Selective and site-specific mobilization of dermal dendritic cells and Langerhans cells by Th1- and Th2-polarizing adjuvants, *P Natl Acad Sci USA*, 107 (2010) 8334-8339.
- [103] J. Inoue, S. Yotsumoto, T. Sakamoto, S. Tsuchiya, Y. Aramaki, Changes in immune responses to antigen applied to tape-stripped skin with CpG-oligodeoxynucleotide in mice, *Journal of controlled release : official journal of the Controlled Release Society*, 108 (2005) 294-305.
- [104] R. Kahlon, Y. Hu, C.H. Orteu, A. Kifayet, J.D. Trudeau, R. Tan, J.P. Dutz, Optimization of epicutaneous immunization for the induction of CTL, *Vaccine*, 21 (2003) 2890-2899.
- [105] H. Kita, Eosinophils: multifunctional and distinctive properties, *Int Arch Allergy Imm*, 161 Suppl 2 (2013) 3-9.

- [106] J.R. MacKenzie, J. Mattes, L.A. Dent, P.S. Foster, Eosinophils promote allergic disease of the lung by regulating CD4(+) Th2 lymphocyte function, *J Immunol*, 167 (2001) 3146-3155.
- [107] H.Z. Shi, Eosinophils function as antigen-presenting cells, *J Leukocyte Biol*, 76 (2004) 520-527.
- [108] L.A. Spencer, P.F. Weller, Eosinophils and Th2 immunity: contemporary insights, *Immunol Cell Biol*, 88 (2010) 250-256.
- [109] N. Roth, S. Stadler, M. Lemann, S. Hosli, H.U. Simon, D. Simon, Distinct eosinophil cytokine expression patterns in skin diseases - the possible existence of functionally different eosinophil subpopulations, *Allergy*, 66 (2011) 1477-1486.
- [110] M.J. Boaz, A. Waters, S. Murad, P.J. Easterbrook, A. Vyakarnam, Presence of HIV-1 gag-specific IFN-gamma+IL-2(+) and CD28(+)IL-2(+) CD4 T cell responses is associated with nonprogression in HIV-1 infection, *J Immunol*, 169 (2002) 6376-6385.
- [111] S.C. Zimmerli, A. Harari, C. Cellera, F. Vallelian, P.A. Bart, G. Pantaleo, HIV-1-specific IFN-gamma/IL-2-secreting CD8 T cells support CD4-independent proliferation of HIV-1-specific CD8 T cells, *P Natl Acad Sci USA*, 102 (2005) 7239-7244.
- [112] M.R. Betts, M.C. Nason, S.M. West, S.C. De Rosa, S.A. Migueles, J. Abraham, M.M. Lederman, J.M. Benito, P.A. Goepfert, M. Connors, M. Roederer, R.A. Koup, HIV nonprogressors preferentially maintain highly functional HIV-specific CD8(+) T cells, *Blood*, 107 (2006) 4781-4789.
- [113] M.A. Williams, A.J. Tynnik, M.J. Bevan, Interleukin-2 signals during priming are required for secondary expansion of CD8(+) memory T cells, *Nature*, 441 (2006) 890-893.

- [114] D.A. Kaveh, V.S. Bachy, R.G. Hewinson, P.J. Hogarth, Systemic BCG Immunization Induces Persistent Lung Mucosal Multifunctional CD4 T-EM Cells which Expand Following Virulent Mycobacterial Challenge, *Plos One*, 6 (2011).
- [115] S.G. Morrison, H. Su, H.D. Caldwell, R.P. Morrison, Immunity to murine *Chlamydia trachomatis* genital tract reinfection involves B cells and CD4(+) T cells but not CD8(+) T cells, *Infect Immun*, 68 (2000) 6979-6987.
- [116] A. Mittal, A.S. Raber, C.M. Lehr, S. Hansen, Particle based vaccine formulations for transcutaneous immunization, *Hum Vaccin Immunother*, 9 (2013) 1950-1955.
- [117] A. des Rieux, V. Fievez, M. Garinot, Y.J. Schneider, V. Preat, Nanoparticles as potential oral delivery systems of proteins and vaccines: A mechanistic approach, *J Control Release*, 116 (2006) 1-27.
- [118] B.G. De Geest, M.A. Willart, B.N. Lambrecht, C. Pollard, C. Vervaet, J.P. Remon, J. Grooten, S. De Koker, Surface-Engineered Polyelectrolyte Multilayer Capsules: Synthetic Vaccines Mimicking Microbial Structure and Function, *Angew Chem Int Edit*, 51 (2012) 3862-3866.
- [119] D.J. Irvine, M.A. Swartz, G.L. Szeto, Engineering synthetic vaccines using cues from natural immunity, *Nat Mater*, 12 (2013) 978-990.
- [120] J. Giri, W.J. Li, R.S. Tuan, M.T. Cicerone, Stabilization of Proteins by Nanoencapsulation in Sugar-Glass for Tissue Engineering and Drug Delivery Applications, *Adv Mater*, 23 (2011) 4861-4867.
- [121] J.F. Correia-Pinto, N. Csaba, M.J. Alonso, Vaccine delivery carriers: Insights and future perspectives, *Int J Pharm*, 440 (2013) 27-38.
- [122] L. Zhao, A. Seth, N. Wibowo, C.X. Zhao, N. Mitter, C.Z. Yu, A.P.J. Middelberg, Nanoparticle vaccines, *Vaccine*, 32 (2014) 327-337.

- [123] B. Slutter, S.M. Bal, Z. Ding, W. Jiskoot, J.A. Bouwstra, Adjuvant effect of cationic liposomes and CpG depends on administration route, *J Control Release*, 154 (2011) 123-130.
- [124] A.S. Raber, A. Mittal, J. Schafer, U. Bakowsky, J. Reichrath, T. Vogt, U.F. Schaefer, S. Hansen, C.M. Lehr, Quantification of nanoparticle uptake into hair follicles in pig ear and human forearm, *J Control Release*, 179C (2014) 25-32.
- [125] F. Rahman, A. Dahmen, S. Herzog-Hauff, W.O. Bocher, P.R. Galle, H.F. Lohr, Cellular and humoral immune responses induced by intradermal or intramuscular vaccination with the major hepatitis B surface antigen, *Hepatology*, 31 (2000) 521-527.
- [126] J.M. Blander, R. Medzhitov, Toll-dependent selection of microbial antigens for presentation by dendritic cells, *Nature*, 440 (2006) 808-812.
- [127] J.M. Moresi, T.D. Horn, Distribution of Langerhans cells in human hair follicle, *J Cutan Pathol*, 24 (1997) 636-640.
- [128] B.Z. Igyarto, K. Haley, D. Ortner, A. Bobr, M. Gerami-Nejad, B.T. Edelson, S.M. Zurawski, B. Malissen, G. Zurawski, J. Berman, D.H. Kaplan, Skin-Resident Murine Dendritic Cell Subsets Promote Distinct and Opposing Antigen-Specific T Helper Cell Responses, *Immunity*, 35 (2011) 260-272.
- [129] S.A. Khader, S.L. Gaffen, J.K. Kolls, Th17 cells at the crossroads of innate and adaptive immunity against infectious diseases at the mucosa, *Mucosal Immunol*, 2 (2009) 403-411.
- [130] F. Broere, S. Apasov, M. Sitkovsky, W. Eden, A2 T cell subsets and T cell-mediated immunity, in: F.P. Nijkamp, M.J. Parnham (Eds.) *Principles of Immunopharmacology*, Birkhäuser Basel, 2011, pp. 15-27.

- [131] A. Podda, The adjuvanted influenza vaccines with novel adjuvants: experience with the MF59-adjuvanted vaccine, *Vaccine*, 19 (2001) 2673-2680.
- [132] E. Lindblad, Freund's Adjuvants, in: D. O'Hagan (Ed.) *Vaccine Adjuvants*, Springer New York, 2000, pp. 49-63.
- [133] G. Galli, D. Medini, E. Borgogni, L. Zedda, M. Bardelli, C. Malzone, S. Nuti, S. Tavarini, C. Sammiceli, A.K. Hilbert, V. Brauer, A. Banzhoff, R. Rappuoli, G. Del Giudice, F. Castellino, Adjuvanted H5N1 vaccine induces early CD4(+) T cell response that predicts long-term persistence of protective antibody levels, *P Natl Acad Sci USA*, 106 (2009) 3877-3882.
- [134] A. Seubert, E. Monaci, M. Pizza, D.T. O'Hagan, A. Wack, The adjuvants aluminum hydroxide and MF59 induce monocyte and granulocyte chemoattractants and enhance monocyte differentiation toward dendritic cells, *J Immunol*, 180 (2008) 5402-5412.
- [135] S. Calabro, M. Tortoli, B.C. Baudner, A. Pacitto, M. Cortese, D.T. O'Hagan, E. De Gregorio, A. Seubert, A. Wack, Vaccine adjuvants alum and MF59 induce rapid recruitment of neutrophils and monocytes that participate in antigen transport to draining lymph nodes, *Vaccine*, 29 (2011) 1812-1823.
- [136] L. Kalvodova, Squalene-based oil-in-water emulsion adjuvants perturb metabolism of neutral lipids and enhance lipid droplet formation, *Biochem Bioph Res Co*, 393 (2010) 350-355.
- [137] L.O. Moreira, A.M. Smith, A.A. DeFreitas, J.E. Qualls, K.C. El Kasmi, P.J. Murray, Modulation of adaptive immunity by different adjuvant-antigen combinations in mice lacking Nod2, *Vaccine*, 26 (2008) 5808-5813.

Curriculum vitae

Personal Information

Name	Ankit Mittal
Address	Waldhausweg 21, Saarbruecken, Germany
Date of birth	22-07-01984
Nationality	Indian

Educational Qualification:

PhD (2010-present)	Department of Biopharmaceutics and Pharmaceutical Technology Saarland University, Saarbruecken
M.S. (Pharm.) (2007-09)	NIPER, Mohali, India (Pharmaceutics) CGPA: 9.38 /10 (1 st rank)
B. Pharm. (2003- 2007)	Dr. H. S. Gour University, Sagar, India 71.92%
GATE (2007)	Entrance exam to qualify for Master's degree, organized by IIT (Kanpur) 23 rd (rank)-All India rank
Intermediate (2002)	Central Board of Secondary Education (CBSE) Board, Academic board in India for education 76.2%
Matriculation (2000)	CBSE Board 74%
General Course on IPR (2007)	Conducted by World Intellectual Property Organization (WIPO) PASS (80)

Awards:

- CRS 2013 travel grant: To attend CRS conference in Hawaii, USA
- Best Poster presentation: A. Raber, A. Mittal, S. Hansen, C.-M. Lehr: Trans-follicular vaccination with nanoparticles - Is it possible? Biological barriers 2012, Feb. 28, Saarbrücken, Germany
- DAAD scholarship 2010: Scholarship to pursue PhD in Germany
- FCS scholarship 2010 (Declined position): Scholarship to pursue PhD in Switzerland

List of Publication

Mittal A., Schulze K., Ebensen T., Weissmann S., Hansen S., Guzmán C.A., Lehr C.-M., Inverse micellar sugar glass NPs: Effect of co-encapsulation of adjuvant and administration route on immune response. (To be submitted)

Mittal A., Schulze K., Ebensen T., Weissmann S., Hansen S., Lehr C.-M., Guzmán C.A., Needle-Free transcutaneous vaccination via hair follicles using nanoparticles: Necessity of Adjuvant. *Submitted*

Raber A.S., **Mittal A.**, Schäfer J., Bakowsky U., Reichrath J., Vogt T., Schaefer U.F., Hansen S., Lehr C.-M., Quantification of nanoparticle uptake into hair follicles in pig ear and human forearm. *Journal of Controlled Release*, 2014; 179, 25-32.

Mittal A., Raber A.S., Lehr C.M., Hansen S., Particle based vaccine formulations for transcutaneous immunization, *Human Vaccine and Immunotherapy*, 2013; 9, 44-43.

Mittal A., Raber A.S., Schaefer U.F., Weissmann S., Ebensen T., Schulze K., Guzmán C.A., Lehr C.-M., Hansen S., Non-invasive delivery of nanoparticles to hair follicles - a perspective for transcutaneous immunization, *Vaccine*, 2013; 31, 3442-3451.

Jain S., **Mittal A.**, Jain, A.K., Enhanced Topical Delivery of Cyclosporin-A Using PLGA Nanoparticles as Carrier. *Current Nanoscience*, 2011; 7, 524-530.

Jain S., **Mittal A.** et al., Cyclosporin A Loaded PLGA Nanoparticle: Preparation, Optimization, In-Vitro Characterization and Stability Studies. *Current Nanoscience*, 2010, 6, 422-43.

Oral Presentation:

A. Mittal: Transfollicular vaccination, Biological barriers 2014, February 18, Saarbruecken, Germany

A. Mittal: Needle free vaccination using nanoparticles via transfollicular route – a perspective for transcutaneous vaccination, CRS 2013, July 22, Hawaii, USA

A. Mittal: Trans-follicular vaccination with nanoparticles - Is it possible? CRS 2012, March 29, Wurzburg, Germany.

S. Hansen, **A. Mittal:** Nanoparticles for transcutaneous vaccination. Skin Vaccination Summit 2011, October 12-14, Washington D.C., USA.

Poster Presentation:

A.S. Raber, **A. Mittal**, J. Schäfer, U. Bakowsky, J. Reichrath, T. Vogt, U.F. Schäfer, C.M. Lehr, S. Hansen: Quantification of nanoparticle uptake into hair follicles- in vitro in vivo correlation, CRS 2013, July 21, Hawaii, USA

S. Hansen, **A. Mittal**, A.S. Raber, U.F. Schaefer, T. Ebensen, K. Schulze, C.A. Guzmán, C.M. Lehr: Non-invasive delivery of nanoparticles to hair follicles for transcutaneous vaccination. HIPS symposium 2013, July 18, Saarbrücken, Germany.

S. Hansen, **A. Mittal**, A. Raber, C.A. Guzman, C.-M. Lehr: Nanoparticles for transcutaneous vaccination. HIPS Symposium 2012, June 28, Saarbrücken, Germany.

A. Raber, **A. Mittal**, S. Hansen, C.-M. Lehr: Trans-follicular vaccination with nanoparticles - Is it possible? Biological barriers 2012, Feb. 28, Saarbrücken, Germany.

S. Hansen, **A. Mittal**, A. Paulus, C.A. Guzman, C.-M. Lehr: Nanoparticles for transcutaneous vaccination. HIPS Symposium 2011, June 16, Saarbrücken, Germany.

A. Mittal, S. Hansen, C.-M. Lehr: Preparation and characterization of ovalbumin loaded PLGA and Chitosan-PLGA nanoparticles for transcutaneous vaccination. Nanomedicine 2011, 3rd European Science Foundation (ESF), June 19-24, Halle-Wittenberg, Germany.

S. Hansen, **A. Mittal**, A. Paulus, C.A. Guzman, C.-M. Lehr: Nanoparticles for transcutaneous vaccination. HIPS Symposium 2011, June 16, Saarbrücken, Germany.

A. Mittal, S. Jain: Preparation and Characterization of cyclosporine loaded nanoparticles. National conference on Nanomaterials: synthesis & Application 2009, Jalandhar, India.

Acknowledgements

This thesis would not be possible without the effort of so many people. Although it is hard to express what support, help and encouragement I got from them, I would like to convey my gratitude to all of them

First and foremost, I would like to thank my supervisor (Doktorvater) Prof. Dr. Claus-Michael Lehr for not only giving me the chance to join his working group to build my scientific skills but also for making me a better individual. In addition, I would like to thank him for being understanding and easy-going in many times not only in professional life but also in personal circumstances. I learned a lot from him and thankful to him for everything.

I feel deeply grateful to my co-supervisor Dr. Steffi Hansen for her support, encouragement and mentorship. I would like to thank her for investing significant time and effort in this project, for providing me freedom to try new ideas and trust she has put into me. Also I would like to thank her for all her personal dedication to find collaborators for our projects and solutions to my problems.

I would like to thank Prof. Carlos Guzman and his team for their effort to make this work running smoothly and being such nice collaboration partners. I would like to personally thank Dr. Thomas Ebensen and Dr. Sebastian Weissmann for their scientific inputs and contributions for manuscript presented in this work. To Dr. Kai Schulze, "thank you" word will not be enough for the help you provided not only in making me understand minute details of immunology but also setting up experiments and endless phone calls and conversation to make this work where it stands today. I feel deeply grateful to him for taking care of various things during my trips to Braunschweig whether it is picking me and dropping me up every day from hotel and dropping me to the station or planning and preparing everything in

advance to run the experiments smoothly. I learned from him not only in scientific perspective but how to remain humble and calm in our life.

To German academic exchange service (DAAD) for providing me financial support for my stay in Germany.

To Prof. Marc Schneider, for his scientific discussions during my PhD and learning from him, how to remain calm and happy whatever be the situation you are going through. Also I learned from him how to take practical classes and taking care of student's queries and make them understand in depth of certain topics. Thanks are extended to Prof. Ulrich Schäfer for sharing his guidance and valuable suggestions.

To my group meeting members (Christina, Anne, Veronica, Salem and Chrissi) where we discussed our scientific problems and solution in friendly ways, encouraged and helped each other in one way or another. Special thanks to Chrissi for helping me out with sectioning of the skin and her friendly attitude. To Anne for showing me pig ear model. I would also like to thank Protein Group (Rene and Nico) for discussing issues related to proteins and delivery. Special thanks to Nico for endless discussion during late working hours in our office.

Thanks to our expert technician team which helped me in learning and providing support for not only handling the instruments but also providing tricks and tactics to use them. Special thanks to Chiara for providing help regarding dispatching of samples to co-operation partners whether it is finding a right box or ordering stuff which I need for my experiments.

To all my labmates: for their encouragements, support, discussions; for their inspiration, abilities and their never give up attitude which made my stay wonderful and less stressful. Special thanks to Hiroe, Salem, Florian, Emad, JD, Clemens, Marius, Arianna, Sarah, Nicole, Steffi, Daniel, Simon, Lutz, Ali, Saeed, Sarah, Dr.

Brigitta, Dr. Noha, for wonderful time. I enjoyed sharing each moment with you all whether it is sports activities, parties, and different countries evenings with movies. Special thanks to Christina, Christiane, Dr. Sarah for the language assistance in this thesis.

My sincere thanks to my new friends Navas and Panch whom I got to know during my earlier days of DAAD language course in Mannheim, Germany; Tariq, Annie, Ashutosh, Mittul, Nupur, Ashish, Kavita, Niket, Anjali during my stay in Saarbrücken. Thanks all for nice moments and memories. Special thanks to Anita and Leon, Salem for being part of our extended family in Saarbrücken.

To my parents, my sister and Anjali (my Wife): I don't have word to express how much I owe you. I hope my thesis could be a way to express my gratitude towards you. From bottom of my heart, I really thank you for believing in me, sharing my sorrows and happiness, teaching me believing in myself and all the sacrifices you did for me. Everything that I have done would not be possible without your support and nor it would have meant anything without sharing it with you.